

Republic of Iraq  
Ministry of Higher Education  
and Scientific Research  
University of Baghdad  
College of Education for Pure Science  
Ibn- Al Haitham  
Department of (Chemistry)



# **Synthesis, Characterization and Biological Activity Study of New Schiff Bases Ligands and their Complexes with some Metal Ions**

A Thesis

Submitted to The College of Education for Pure Sciences Ibn AlHaitham, University of Baghdad in Partial Fulfillment of the Requirements for the Master degree of Science in Chemistry

*By*

*Salam Kareem Sahib*

B.Sc. in Chemistry 2002, University of Baghdad

*Supervised by*

*Asst. Prof. Dr.*

**Lekaa Khalid Abdul Kareem**

*1440 AH*

*2019 AD*

بِسْمِ اللَّهِ الرَّحْمَنِ الرَّحِيمِ

{ الرَّحْمَنُ (1) عَلَّمَ الْقُرْآنَ (2)

خَلَقَ الْإِنْسَانَ (3) عَلَّمَهُ الْبَيَانَ (4) }

صدق الله العظيم

سورة الرحمن الآيات (1 - 4)

## *Supervisor's certification*

We certify that this (thesis) was prepared under my supervision at the department of chemistry, college of Education for Pure Science Ibn Al Haitham, University of Baghdad as a partial fulfillment of the completion for the degree of (Master) of science in chemistry, and this work has never been submitted or published anywhere else.

Signature: 


Supervisor: **Dr. Lekaa Khalid Abdul Karem**

Title: Assistant professor

Address: Department of Chemistry, College of Education for Pure Science, Ibn Al Haitham , University of Baghdad

Data: 6 / 11 / 2019

In view of the available recommendations, I forward this thesis for debate by the examining committee.

Signature: 

Name: **Dr. Mohamad Jaber Al Jeboori**


Titles: prof.

Address: Head of the Chemistry Department, College of Education for Pure Science Ibn Al Haitham , University of Baghdad

Data: 6 / 11 / 2019

## Examination Committee Certificate

We chairman and members of the examination committee, certify that we have studied this thesis presented by the student **Salam Kareem Sahib** and examined him in its contents and that, we have found its worthy to be accepted for the degree of the of Master of Science in Chemistry with (Excellent)

Signature: 

Name: Dr.Amer Jabar Jarad

Title: Professor

Date: / / 2019

(Chairman)

Signature: 

Name: Dr. Fawzi Yahya Waddai

Title: Assistant professor

Date: 6 / 11 / 2019

(Member)

Signature: 

Name: Dr. waleed khalid mahdi

Title: Assistant professor

Date: 6 / 11 / 2019

(Member)

Signature: 

Name: Dr. Lekaa Khalid Abdul Karem

Title: Assistant professor

Date: 6 / 11 / 2019

(Supervisor)

I have certified upon the discussion of the examination committee

Signature: 

**Prof. Dr. Hasan Ahmed Hasan**

The Dean of Collage of Education For Pure Science / Ibn Al Haitham

Data : 7 / 11 / 2019

## Acknowledgment

I would like to thank my supervisor Dr. Lekaa K. Karem for her guidance and encouragement. I would also to thank my family who supported me to finish my thesis.

*Salam* 



***DEDICATION***

*'To those who have given me  
time of distress and prosperity to  
my wife*

## Abstract

This study deals with Schiff base ligands derivative from (3-Amino-1-phenyl-2-pyrazoline-5-one) with 4-Hydroxy-3-methoxybenzaldehyde to create ligand (SB1) and 4-(Dimethylamino)benzaldehyde to create ligand (SB2).

The two ligands were characterized by spectroscopic techniques such as infrared, ultraviolet, <sup>1</sup>H NMR and element analysis, mass spectrometry.

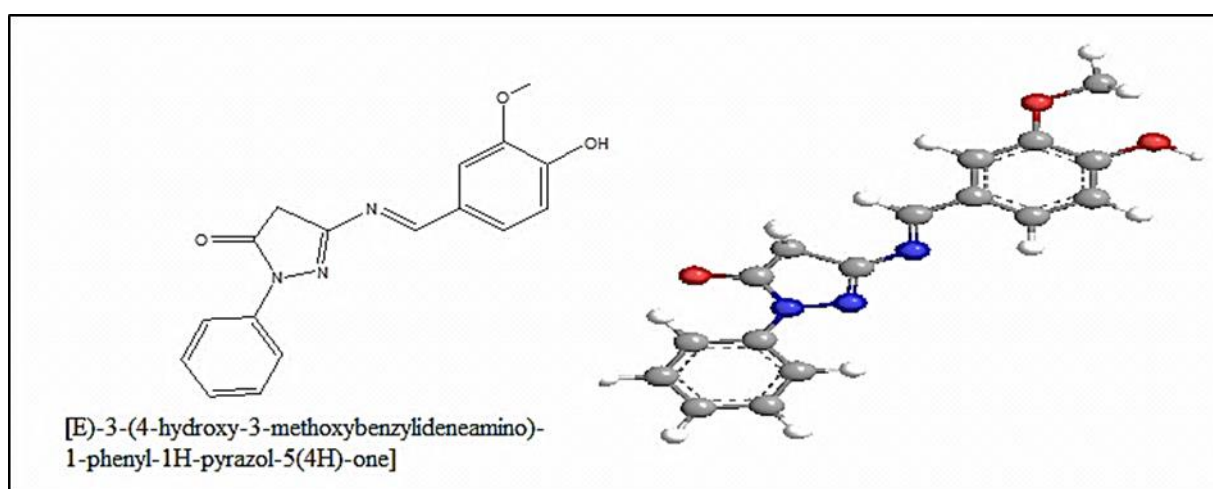


**Figure (1): Structure and 3D shape of ligand SB1**

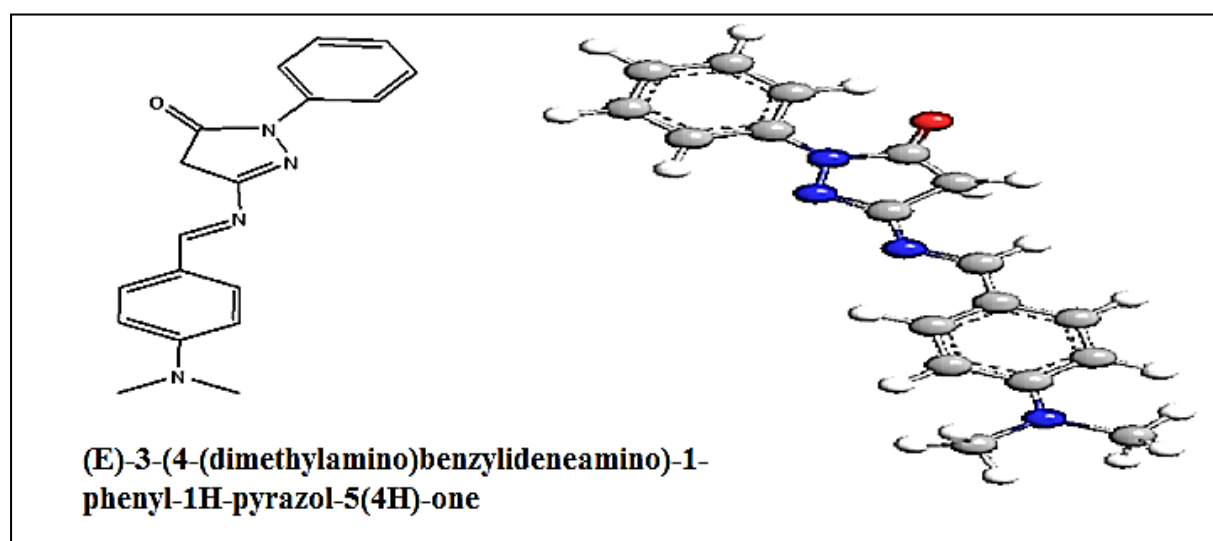


**Figure (2): Structure and 3D shape of ligand SB2**

Mixed ligands complexes were composed of Schiff bases and Anthranillic acid with some transition elements ions M (II) such as: Co, Ni, Cu, Cd and Hg. These complexes were identified by elemental micro-analysis, molar conductivity, infrared, ultraviolet-visible, atomic absorption, and magnetic susceptibility measurement.

The spectral data showed that the ligands SB1 and SB2 as a neutral bidentate and consistent with metal ions through the N atom of the azomethine group and the N atom for pyrazole ring. The expected geometric shape is the octahedral for all complexes.

Finally, the biological antibacterial efficiency of the ligands and their complexes was tested from *Staphylococcus aureus* and *Escherichia coli* by the measurement of the inhibition zone (ZI).



## List of Contents

No.	Content	Page
	Abstract	
	List of Contents	I
	List of Tables	V
	List of Figures	VI
	List of Scheme	VIII
	List of Charts	IX
	List of Abbreviation	IX
<b><i>Chapter One: Introduction</i></b>		
1	Introduction	1
1.1	Schiff Base	1
1.2	Schiff base compounds	3
1.3	Heterocyclic Compounds	3
1.4	Starting Materials Chemicals	4
1.4.1	3-Amino-1-phenyl-2-pyrazoline-5-one (3-APO)	4
1.4.2	Vanillin (VA)	5
1.4.3	4-(Dimethylamino) benzaldehyde (4-DMAB)	5
1.4.4	Anthranilic Acid (A)	6
1.5	Literature Survey	8
1.5.1	Complexes of Schiff bases from Vanillin	8
1.5.2	Complexes of Schiff bases from 4-(Dimethylamino)benzaldehyde (4-DMAB)	13
1.5.3	Complexes related to the Schiff bass from 3-aino-1-phenyl-2-pyrazolin-5-one	17
1.6	Mixed Ligands Complexes of Anthranilic Acid (A)	19
1.7	Aim of the work	23
<b><i>Chapter two: Experimental section</i></b>		
2.	Experimental section	24
2.1	Initial compounds	24

No.	Content	Page
2.2	Instrumental analysis	25
2.2.1	Melting points measurement	25
2.2.2	Fourier Transform Infrared FT-IR	25
2.2.3	Electronic spectra	25
2.2.4	Conductivity devices	25
2.2.5	Elemental micro analysis (CHNO)	25
2.2.6	Atomic Absorption Spectrometry A.A.S.	26
2.2.7	Proton nuclear magnetic resonance ( <sup>1</sup> HNMR)	26
2.2.8	GC-mass Spectra	26
2.2.9	Measurements of the Magnetic Susceptibility	26
2.2.10	Proposal of the molecular structure	26
2.2.11	Biological Activity	26
2.2.12	The materials and instrumental in Biological laboratory	27
2.3	Preparation of the SB1 and SB2 ligands	28
2.3.1	3-(4-hydroxy-3-methoxybenzylideneamino)-1-phenyl-1H-pyrazol-5(4H)-one SB1	28
2.3.2	3-(4-(dimethylamino)benzylideneamino)-1-phenyl-1H-pyrazol-5(4H)-one SB2	29
2.4	Preparation of new complexes	30
2.4.1	Preparation of SB1 complexes	30
2.4.1.1	Preparation of [CoA2SB1] complex	30
2.4.1.2	Preparation of mixed complexes	30
2.4.2	Preparation of SB2 complexes	31
2.4.2.1	Preparation of [CoA2SB2] complex	31
2.4.2.2	Preparation of mixed complexes	31
<b><i>Chapter Three : Results and Discussion</i></b>		
3	Result and discussion	33
3.1	Part one: Characterization of ligands SB1 and SB2	33
3.1.1	Solubility	33

No.	Content	Page
3.1.2	Physical properties of new ligands	33
3.1.3	FTIR spectral data of starting material and new ligands	33
3.1.4	<sup>1</sup> H-NMR Spectral Data	37
3.1.4.1	<sup>1</sup> H-NMR of ligand SB1	37
3.1.4.2	<sup>1</sup> H-NMR spectrum of the ligand SB2	38
3.1.5	The Electronic Transfers for SB1 and SB2	39
3.1.5.1	The spectrum of ligand SB1	39
3.1.5.2	The spectrum of ligand SB1	40
3.1.6	The GC-mass spectral for ligands SB1 and SB2	41
3.1.6.1	Mass spectrum of SB1	41
3.1.6.2	Mass spectrum of SB2	43
3.2	Part two: Characterization of complexes with SB1 and SB2	44
3.2.1	Solubility	44
3.2.2	The Physical properties and CHNO and M for SB1 and SB2 complexes	45
3.2.3	Molar conductivity	47
3.2.4	FT-IR spectral data for complexes	48
3.2.4.1	FT-IR spectral for SB1 complexes	48
3.2.4.2	FT-IR Spectral Data for SB2 Complexes	54
3.2.5	Electronic spectra	58
3.2.5.1	Electronic spectra of SB1 complexes	58
3.2.5.2	[CoA2SB1] Complex	58
3.2.5.3	[NiA2SB1] Complex	59
3.2.5.4	[CuA2SB1] Complex	59
3.2.5.5	[CdA2SB1] Complex	59
3.2.5.6	[HgA2SB1] complex	59
3.2.6	Electronic spectra for SB2 Complexes	62
3.2.3.1	[CoA2SB2] Complex	62

No.	Content	Page
3.2.6.2	[NiA <sub>2</sub> SB <sub>2</sub> ] Complex	63
3.2.6.3	[CuA <sub>2</sub> SB <sub>2</sub> ] Complex	63
3.2.6.4	[CdA <sub>2</sub> SB <sub>2</sub> ] Complex	63
3.2.6.5	[HgA <sub>2</sub> SB <sub>2</sub> ] Complex	63
3.3	Magnetic susceptibility of SB1, SB2 complexes	67
3.4	The Proposed molecular structures	68
<b><i>Chapter Four: Biological activity</i></b>		
4	Biological activity	70
4.1	Bacterial Activity of Ligands Complexes	70
4.1.1	SB1 Complexes	70
4.1.2	SB2 Complexes	71
4.2	Prospective studies	76
	Reference	77
	الخلاصة	

## List of Tables

No.	Table	Page
1-1	The Physical Characteristics of Starting Materials	7
2-1	The initial materials	24
2-2	Weights of materials involved in the preparation of complexes[MA <sub>2</sub> SB <sub>1</sub> ]	31
2-3	Weights of materials involved in the preparation of complexes[MA <sub>2</sub> SB <sub>2</sub> ]	32
3-1	Solubility of SB1&SB2 in several solvents	33
3-2	Some physical properties for SB1&SB2	33
3-3	Distinguish the frequencies of the ligands and compare them with the initial materials	34
3-4	<sup>1</sup> HNMR Data for SB1	37
3-5	The <sup>1</sup> HNMR for SB2	38
3-6	Type of transition of SB1	39
3-7	Type of transition of SB2	40
3-8	Solubility of SB1 and SB2 Complexes	45
3-9	The Physical Properties and Elemental Microanalysis for SB1 and SB2 Complexes	46
3-11	Molar conductivity for SB1 and SB2 Complexes	47
3-12	The FTIR Spectra for the SB1 Complexes	50
3-13	The FTIR Spectra for the SB2 Complexes	55
3-14	Electronic spectral data of SB1 complexes	60
3-15	Electronic spectral data of SB2 complexes	64
3-16	Measurements of the magnetic of prepared complexes	68
4-1	Biological activity of SB1 complexes	70
4-2	The Biological Activity of SB2 Complexes	72

## List of Figures

No.	Figure	Page
<b>Chapter one</b>		
1-1	Geometrical Schiff base isomers	1
1-2	The structure of (3-APO)	4
1-3	The structure of Vanillin	5
1-4	The structure of 4-(Dimethylamino) benzaldehyde	6
1-5	The chemical structure of Anthranilic Acid	7
1-6	The Chemical composition of L complexes	8
1-7	Schiff base ligand salt KL Structure	9
1-8	(a)Tetrahedral geometry complexes and (b) Square planar complex	9
1-9	Structure of stable complexes	10
1-10	Proposed structure of complexes	10
1-11	Structure of the Ni (II) compounds	11
1-12	The cobalt compounds structure	12
1-13	The geometry of Ni complex	13
1-14	Tetrahedral Ni (II) complex	13
1-15	Synthesis of Cu(II) complex	14
1-16	The structures of the Cu (II) complex	15
1-17	The structures of the Zn (II) complex	16
1-18	The structural formulas related to mixed HL metal complexes	20
1-19	The composition of mixed ligands complexes	21
1-20	Structures of new complexes	22
<b>Chapter two</b>		
2-1	Some of instruments in biological laboratory	27
<b>Chapter three</b>		
3-1	The FTIR spectrum of vanillin	35
3-2	The FTIR spectrum of [4-(Dimethylamino)benzaldehyde]	35
3-3	The FTIR spectrum of 3APO	36

No.	Figure	Page
3-4	The FTIR spectrum of SB1 Ligand	36
3-5	The FTIR spectrum of SB2 Ligand	37
3-6	The <sup>1</sup> HNMR spectrum of the Ligand SB1	38
3-7	The <sup>1</sup> HNMR spectrum of SB2	39
3-8	Electronic spectrum of SB1ligand	40
3-9	Electronic spectrum of SB2 ligand	41
3-10	The Mass Spectrum of SB1	42
3-11	The Mass Spectrum of SB2	43
3-12	FTIR spectrum of (Anthranilic acid)	51
3-13	FTIR spectrum of [CoA2SB1]	51
3-14	FTIR spectrum of [NiA2SB1]	52
3-15	FTIR spectrum of [CuA2SB1]	52
3-16	FTIR spectrum of [CdA2SB1]	53
3-17	FTIR spectrum of [HgA2SB1]	53
3-18	FTIR spectrum of [CoA2SB2]	56
3-19	FTIR spectrum of [NiA2SB2]	56
3-20	FT-IR Spectrum of [CuA2SB2]	57
3-21	FTIR spectrum of [CdA2SB2]	57
3-22	FTIR spectrum of [HgA2SB2]	58
3-23	Electronic spectrum of [CoA2SB1] complex	61
3-24	Electronic spectrum of [NiA2SB1] complex	61
3-25	Electronic spectrum of [CuA2SB1] complex	61
3-26	Electronic spectrum of [CdA2SB1] complex	62
3-27	Electronic spectrum of [HgA2SB1] complex	62
3-28	Electronic spectrum of [CoA2SB2] complex	65
3-29	Electronic spectrum of [NiA2SB2] complex	65
3-30	Electronic spectrum of [CuA2SB2] complex	66
3-31	Electronic spectrum of [CdA2SB2] complex	66
3-32	Electronic spectrum of [HgA2SB2] complex	67

No.	Figure	Page
3-33	The suggested geometry for metal complexes of SB1	69
3-34	The suggested geometry for metal complexes of SB2	69
<b>Chapter four</b>		
4-1	Inhibition zone of ligands and their complexes towards <i>Staphylococcus aureus</i> bacteria	73
4-2	Inhibition zone of ligands and their complexes towards <i>E.coli</i> bacteria	74

### List of Scheme

No.	Scheme	Page
1-1	General mechanical Schiff base preparation	2
1-2	General structure of metal complexes	12
1-3	Synthesis route regarding complexes	15
1-4	The synthesis route of Fe <sup>+3</sup> -complexes	16
1-5	Synthesis route of L1-5 ligands	17
1-6	The prepared of the three ligands	18
1-7	Synthesis of new mixed ligand complexes	19
1-8	Preparation route of the Complexes	21
2-1	Synthesis of SB1 ligand	28
2-2	Synthesis of SB2 ligand	29
2-3	Preparation of [MA <sub>2</sub> SB1] complexes	30
2-4	Preparation of [MA <sub>2</sub> SB2] complexes	32
3-1	The fragmentation pattern of the ligand SB1	42
3-2	Fragmentation pattern of the ligand SB2	44



## List of Charts

No	Chart	Page
Chart 1	Biological activity for prepared compounds [MA <sub>2</sub> SB1]	70
Chart 2	Biological activity for prepared compounds [MA <sub>2</sub> SB2]	72

## List of Abbreviation

Abbreviation	Details
AAS	Atomic absorption spectroscopy
Abs	Absorbance
b.p	Boiling point
m.p	Melting point
4-DMAB	4-(Dimethylamino) benzaldehyde
C	Concentration
°C	Celsius
BM	Bohr Magneton
Dec.	Decomposition
M.Wt	Molecular weight
Ppm	Parts per million
$\lambda_{\max}$	Wave length of maximum absorbance
<i>o</i> -	Ortho
<i>m</i> -	Meta
<i>p</i> -	Para
J	Coupling constant
MHz	Mega Hertz
$\epsilon_{\max}$	Molar absorptivity
3-APO	3-Amino-1-phenyl-2-pyrazoline-5-one
Nm	Nanometer
°A	Angstrom
TLC	Thin layer chromatography
VA	Vanillin
TGA	Thermal gravimetric analysis
DTG	Differential Thermal gravimetric
CT-DNA	Circulating tumor DNA
$\delta$	chemical shift

## 1. Introduction

### 1.1 Schiff Base

Schiff base preparation having azomethine as a functional group consisting of primary amines and the carbonyl group were prepared by Hugo Schiff. These Schiff bases compounds have a light yellow color<sup>[1,2]</sup>. The product includes the active group referred to as the imine group. When amine has a reaction with a ketone or an aldehyde, the generic formulas become  $(R_1R_2C=N-R_3)$  and  $(R_1HC=N-R_2)$ , respectively<sup>[3,4]</sup>. Their colored crystals have weak base properties and degrade with water and solid acids to form ammonia and carbonate and they have two types of geometric isomers Figure (1-1)<sup>[5, 6]</sup>

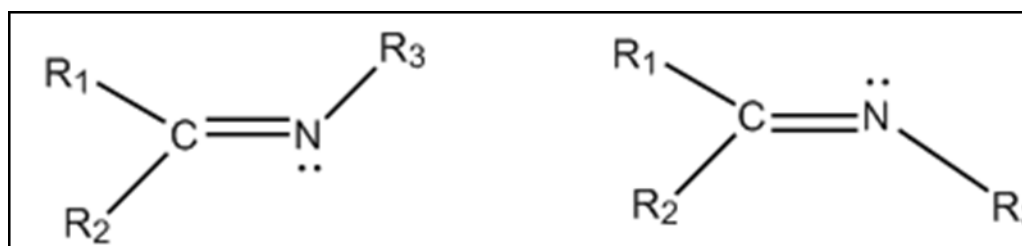
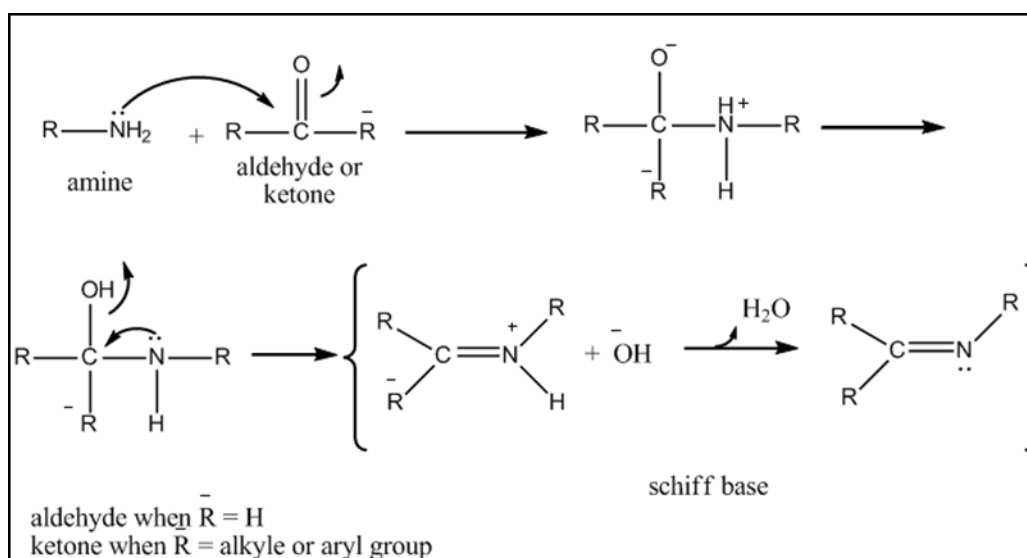


**Figure (1-1): Geometrical Schiff base isomers**

Schiff bases ligands ketimines and secondary aldimines are reversible and happens when there is a base or acid present, as catalysts, with heat<sup>[7]</sup>. The inability of separating isomers is a result of the free rotation between atoms of carbon and nitrogen around their double bond. The above mentioned inability happens as a result of considerable difference in the electro-negativity between nitrogen and that decreases the feature of double bond between those two atoms due to polarization<sup>[8,9]</sup>

The mechanism of Schiff bases was achieved by nucleophilic addition to  $(C=O)$  group that forms a hemiaminal, followed by dehydration to configure imines<sup>[5]</sup> according to the following scheme (1-1):



**Scheme (1-1): General mechanical Schiff base preparation**

Ligands of Schiff base are important complexes for coordinating medicine and chemistry due to the existence of  $\text{HC}=\text{N}$  group as catalysis and has anti-oxidative activity, anti-bacterial activity, anti-fungal activity, magnetism, enzymatic reaction, and bio-inorganic. In industrial areas, they are applied in many different applications such as dyes, starting materials and in a wide variety of compounds of synthesis, such as plastics and pigments<sup>[10]</sup>. Through the years, Schiff bases have drawn a great deal of interest due to the fact that they have synthetic flexibility, sensitivity, as well as the selectivity concerning central atom of metal<sup>[11]</sup>.

Schiff base complexes were utilized as a dye of photo stabilizer for the solar filters and assemblers due to photochromic characteristics. In addition to that, they were used in the technology of optic sound recording<sup>[12]</sup>. Schiff base is a compound that has thermal stability which is utilized as a stationary phase in the gas chromatography<sup>[13]</sup>. As a result of optic non-linearity of those complexes, they were utilized as photonic components and electronic materials<sup>[14]</sup>. The double bond of carbon-nitrogen ( $\text{C}=\text{N}$ ) of the Schiff base is readily reduced with metal transition. Compounds of Schiff base metals are the optimal coordination-organometallic complexes for forming supra-molecular<sup>[15]</sup>.

## 1.2 Schiff base compounds

Schiff bases, as well as their metal compounds were synthesized due to the interesting and significant characteristics they have, such as the capability of binding heavy metal and toxic atoms, undergo tautomerism, show catalytic reductions and photochromic <sup>[16]</sup>. The Schiff base metal complexes chemistry is interesting due to the fact that those species show different modes of reactivity, besides they have biological and catalytic activities <sup>[17]</sup>. Schiff bases are capable of accommodating a variety of metal centers which involve a variety of modes of coordination, and as a result they successfully allow synthesizing hetero-metallic and homo-metallic compounds with different stereo-chemistry <sup>[18]</sup>. Compounds of Schiff base which contain various atoms of central metals like copper, nickel, and cobalt were researched in thorough details due to their different crystallographic characteristics, steric effects, enzymatic reactions, mesogenic properties, structure redox relationships, magnetic characteristics, catalysis. In addition their significant role in understanding transition metal ions' coordination chemistry <sup>[19]</sup>.

The transition metal complexes of Schiff base ligand with donor groups as N, O and S gained importance for more than two decades because of their using as models of biological systems<sup>[20,21]</sup>, including antibacterial<sup>[22]</sup>, antifungal, antitumor, and anti-inflammatory activities<sup>[23]</sup>.

## 1.3 Heterocyclic Compounds

Different type of atoms can found in compounds that have acyclic structure like S, N, and O atoms <sup>[24]</sup>. The heterocyclic compounds have much important physiological functions in plants and animals, as well as they have important biological feature. For example in drug of penicillin as antibiotic, painkillers like phenobarbital and saccharin <sup>[25]</sup>. Heterocyclic system was speared in many natural products, such as nucleic acid, chlorophyll, and plants alkaloids <sup>[26]</sup>. Further, these

complexes are very significant in chelates chemistry due to the stability with metal ions. However, these complexes could be applied in areas of biology, analytics, clinical and pharmacology <sup>[27, 28]</sup>. The 3-Amino-1-phenyl-2-pyrazoline-5-one derivatives are one of the heterocyclic compounds, which are used in the field of medicinal chemistry because of their pharmacological, photographic and catalytic applications <sup>[29-31]</sup>.

## 1.4 Starting Materials Chemicals

Table (1-1) shows the physical characteristics of starting materials.

### 1.4.1 3-Amino-1-phenyl-2-pyrazoline-5-one (3-APO)

The formula of 3-Amino-1-phenyl-2-pyrazoline-5-one (3-APO) is shown in Figure (1-2). It is hetero electric defined with a 5-membered ring of 3 carbonates and 2 neighboring atoms of Nitrogen are also considered as a weak base <sup>[32-34]</sup>. Prominent medications which contain loop of pyrazole are silicoxib (Celebrex), and activated steroids. New compounds of pyrazolone are of outstanding co-polymerization and undergo on rinse in organic solvents in the case of using them for eyes <sup>[35,36]</sup>.

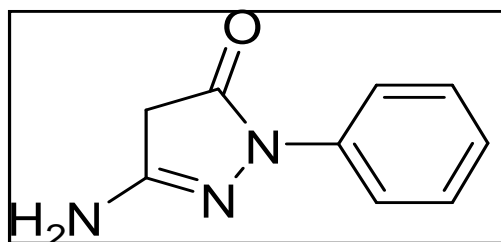


**Figure (1-2): The structure of (3-APO)**

### 1.4.2 Vanillin (VA)

Vanillin (VA) can be considered as the main chemical element of vanilla bean extract<sup>[37]</sup>, Figure (1-3). The (VA) is prepared in two steps process from the petrochemical precursors: ethyl VA, guaiacol and, glyoxylic acid<sup>[38,39]</sup>. The vanillin is a mild aromatic complex, which is naturally occurring in vanilla beans. It is widely used as a flavor additive in drinks, cooking, as an aromatic addition to incense, candles, perfumes, perfume, air fresheners, and fragrances. Can be separated from vanilla beans, and are usually extracted as a pulp and paper industry by-product via oxidative lignin refraction<sup>[40,41]</sup>.

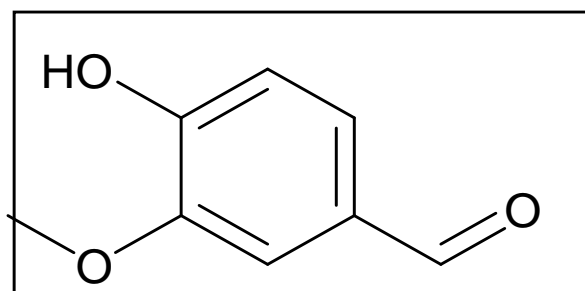


**Figure (1-3): The structure of Vanillin**

### 1.4.3 4-(Dimethylamino) benzaldehyde (4-DMAB)

The 4-DMAB is a paramount intermediate of dyes. It is an organic composite contains amine an aldehydes moieties which is used in Ehrlich's reagent for limitation of hydrazine<sup>[42]</sup>, Figure (1-4). Interaction output was azo-dye. Therefore it is used to determine the spectral of hydrazine in (aqueous) solutions at (457 nm)<sup>[43]</sup>.

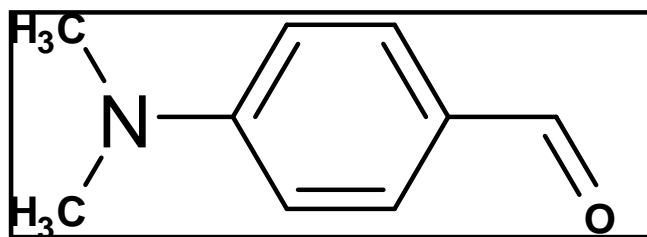


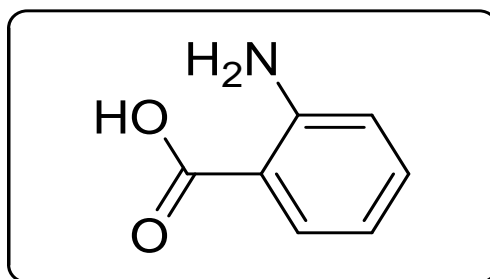
**Figure (1-4): The structure of  
4-(Dimethylamino) benzaldehyde**

It belongs to the same family as 4-DMAB which exhibits dual fluorescence and was a subject of extensive investigations. A tin complex in which 4-DMAB serves as a ligand coordinating through its O atom and of a 1:1 crystal of 4-DMAB and 6-phenyl-1,3,5-triazine-2,4-diamine have been reported <sup>[44-46]</sup>.

#### **1.4.4 Anthranilic Acid (A)**

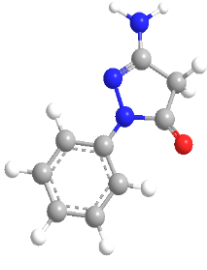
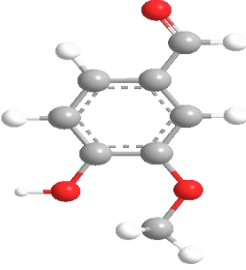
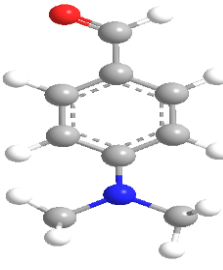

Anthranilic acid is an aromatic acid Figure (1-5), the molecule is made up of an adapted ring of gasoline <sup>[47,48]</sup>, and categorized as aromatic, with two adjacent functional ortho or groups, amine and carboxylic acid. The assembler is, therefore, an oscillator. In appearance, anthranilic acid is a solid white matter when it is pure; however, commercial samples might look yellow. Industrially, anthranilic acid is an intermediary in the production of azo and saccharin dyes <sup>[49]</sup>.

Anthranilic acid may be included in the organic synthesis for the generation of gasoline <sup>[50]</sup>. It can interact with phosgene for giving an isotonic anhydride, a versatile detector <sup>[51]</sup>.



**Figure (1-5): The chemical structure of Anthranilic Acid**

**Table (1-1): The Physical Characteristics of Starting Materials**

	3-Amino-1-phenyl-2-pyrazoline-5-one	vanillin	4-(dimethyl amino) benzaldehyde	Anthranillic acid
Molecular formula	$C_9H_9N_3O$	$C_8H_8O_3$	$C_9H_{11}NO$	$C_7H_7NO_2$
Crystal formula				
M.wt (g/ mol)	175.187	152.15	149.19	137.14
Appearance	White pale powder	White crystals	yellow-white powder	White or yellow powder
M. p °C	210-215	81-83	176 -177	146-148



## 1.5 Literature Survey

### 1.5.1 Complexes of Schiff bases from Vanillin

Rakitskaya *et.al.*, in (2006)<sup>[52]</sup> have synthesis Mn (II), Co(II) and Cu(II) complexes with Schiff bases L = 4-hydroxy-3-methoxybenzaliminopropyl) immobilized on Aerosil. The formation of pseudo octahedral complexes  $M(L_2)_2$  on the modified surface of Aerosil was confirmed by FTIR and ESR spectroscopy and by diffuse reflectance spectroscopy (DSR). The catalytic activity of iso structural complexes in ozone decomposition varies in the order  $Mn > Co > Cu$ , and  $M(L_2)_2$  complexes.

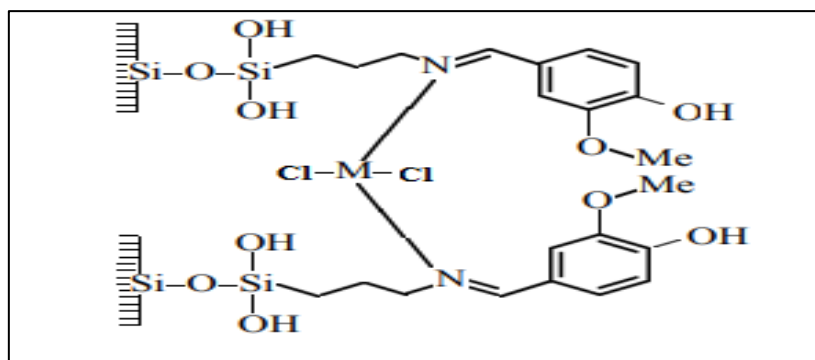


**Figure (1-6): The Chemical composition of L complexes**

Sivasankaran *et al.*, in (2008)<sup>[53]</sup> have synthesis Schiff base (L) Figure (1-7). It has been utilized for the synthesis of compounds of Ni(II), Co(II), Zn(II), and Cu(II) Figure (1-7) and defined by CHN, FT-IR, conductivity measurements, electronic spectral, XRD, magnetic measurements, spectroscopic studies which have shown that the L from behave as complexes of tridentate ligand and metal(II) purposed tetrahedral geometry for compounds of Ni(II), Zn(II), and Co(II), whereas the compound of Cu(II) was square planar where the ratio of metal to ligand was (1:2). The antimicrobial activity from all compounds were tested against *S. aureus*, *K. pneumoniae*, *E. coli*, *P. aeruginosa*, *P.*

*vulgaris*, and *C. albicans* and all complexes were active than the L ligand.

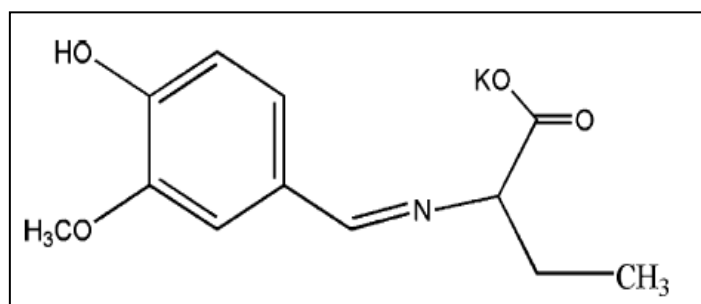


**Figure (1-7): Schiff base ligand salt KL Structure**

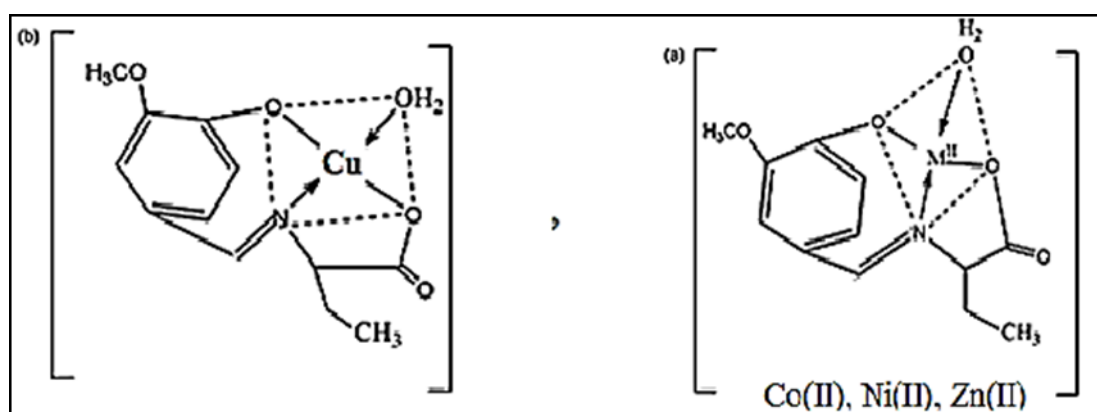


**Figure (1-8): (a) Tetrahedral geometry complexes and  
(b) Square planar complex**

Suresh *et al.*, in (2010) <sup>[54]</sup> have reported A novel bidentate Schiff base, synthesized from 1-phenyl 2, 3-dimethyl-4-aminopyrazol-5-one (4-aminoantipyrine) and vanillin forms stable complexes with transition metal ions such as Cr (III), Mn (II), Co (II), Ni (II), Cu (II), Zn (II) and Cd (II) Figure (1-9). Their structures were investigated by elemental analysis, infrared Spectroscopy, electronic spectroscopy, NMR spectroscopy; thermo gravimetric analysis and electron spin resonance spectroscopy. On the basis of the studies the coordination sites were proven to be through oxygen of the ring C = O and Nitrogen of the azomethine CH = N group. The microbiological studies revealed the antibacterial nature of the complexes

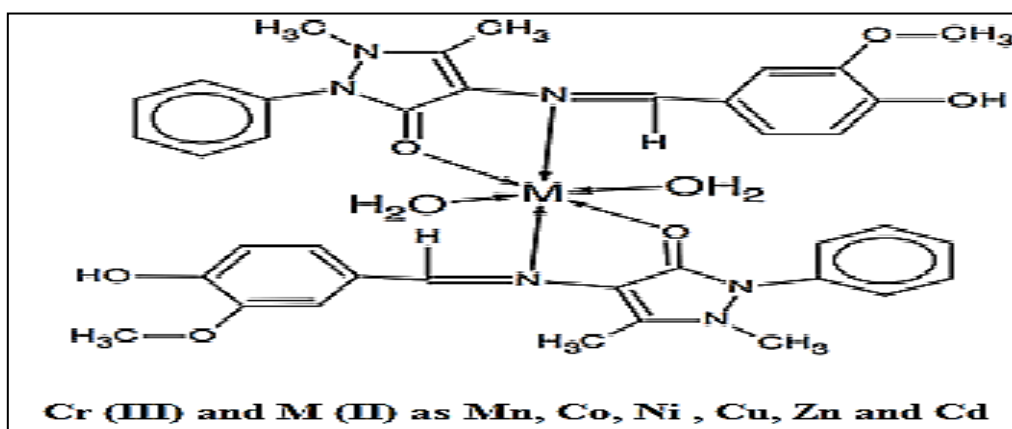


**Figure (1-9): Structure of stable complexes**

Fugu *et al.*, in (2013)<sup>[55]</sup> have synthesized five new complexes of  $Zn^{+2}$ ,  $Cu^{+2}$ ,  $Ni^{+2}$  and  $Co^{+2}$  with (L) ligand derived from reaction of (VA) and (2-Hydroxyaniline) Figure (1-10). The new ligand and their complexes were diagnosed by the spectroscopic methods. The proposed geometric shape of the complex was the octahedral. All complexes were checked by using different type of bacteria.

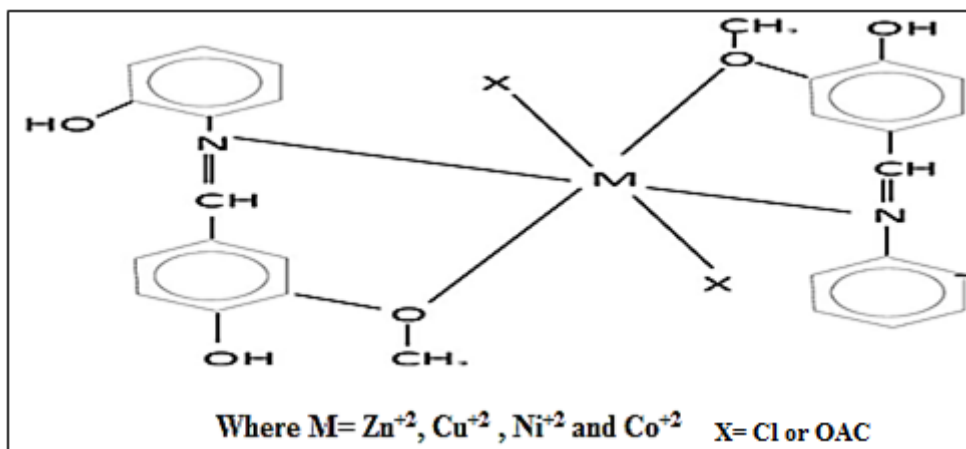


**Figure (1-10): Proposed structure of complexes**

Roji *et.al*, in (2015)<sup>[56]</sup> have reported the preparation of Ni(II) chelate of vanillin SB Figure (1-11). New complex was diagnosed by magnetic moment, FT-IR spectral, microanalysis CHNO, and UV-visible. Octahedral structure composition has been assigned. The ligand and its

Ni-compounds were tested for biological activity against various types of bacteria.

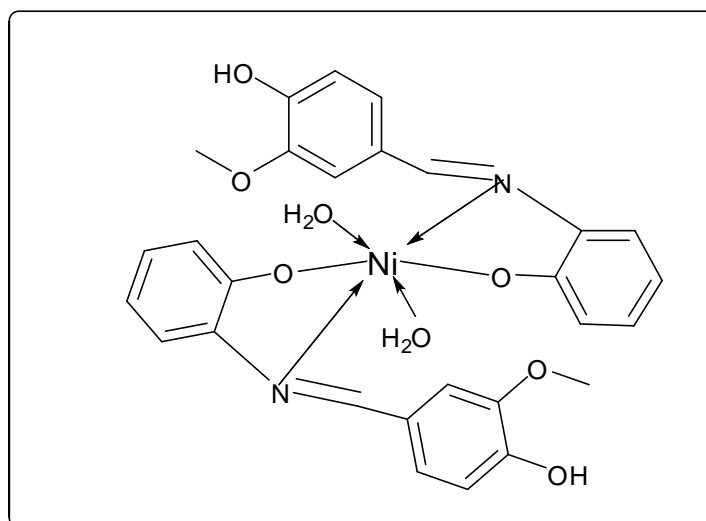
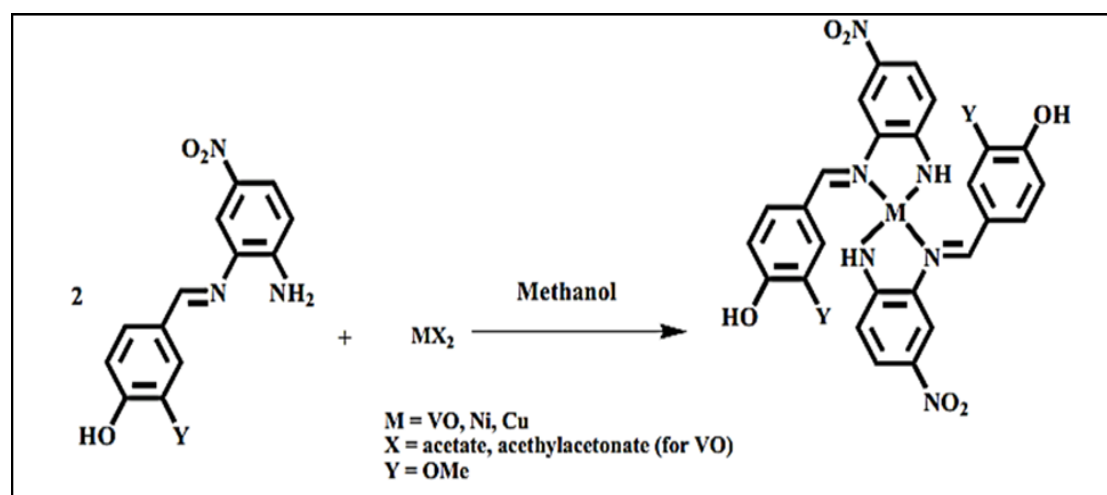


**Figure (1-11): Structure of the Ni (II) compound**

Dostani *et al.*, in (2017) <sup>[57]</sup> have synthesized a new bidentate NN-Schiff base ligand of vanillin, (E)-4-(((2-amino-5-nitrophenyl)imino)methyl)-2-methoxyphenol, was synthesized and characterized by different spectroscopic techniques. In addition, mononuclear complexes were synthesized by treating the corresponding metal salts of Ni<sub>2</sub>, Cu<sub>2</sub> and VO<sub>2</sub> and Schiff base ligand in methanol. The resulting complexes were characterized by FT-IR, UV-Vis and <sup>1</sup>H NMR techniques. The hybrids of complex-TiO<sub>2</sub> nanoparticles were prepared and their structure and morphology were characterized by FT-IR, XRD, TEM, SEM and solid state UV-Vis absorption. The photocatalytic activities of the prepared modified semiconductors were tested under visible radiation for the degradation of methylene blue in the aqueous solution. The results indicated that the incorporation of these complexes improved the activation of TiO<sub>2</sub> with visible light. See in scheme (1-3).



**Scheme (1-2): General structure of metal complexes**

Abduljeel *et al.*, in (2018)<sup>[58]</sup>, have synthesized Schiff base ligand L1-L3 complexes derived from di amine compounds and (VA) with Co(II) ion Figure (1-12), the prepared complexes have been diagnosed by different techniques as NMR, UV visible, atomic absorption, FT-IR, magnetic sensitivity and molar conductance. Data have shown that ligands behave as bi dentate and linked from N azomethine sites. The compounds are proposed as electrolytes para-magnetic complexes and the coordination number = 4. All prepared compounds were tested for their anti-bacterial activity against gram (+ and -) bacteria, these compounds have shown a good biological activities.

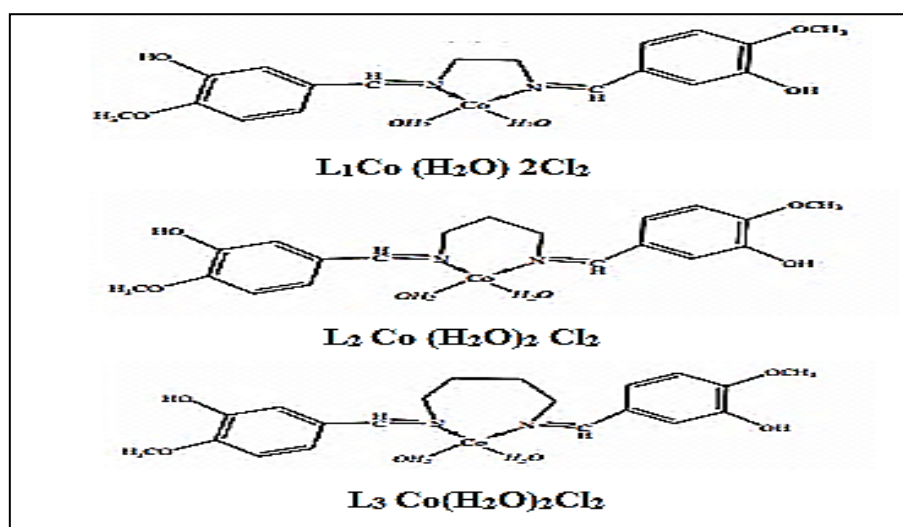


**Figure (1-12): The cobalt complexes structure**

### 1.5.2 Complexes of Schiff bases from (4-dimethylamino)

#### benzaldehyde (4-DMAB))

El-Ajaily *et al.*, in (2006)<sup>[59]</sup> have reported that Ni (II) complexes of L ligand derived from cysteine and 4-DMAB has been synthesis and diagnosed by physicochemical methods such as molar conductance, FTIR, CHN, mass and H-NMR spectra. Spectral studies have shown that  $[\text{Ni L}(\text{OH})(\text{H}_2\text{O})].2\text{H}_2\text{O}$  complex has a square planar Figure (1-13).

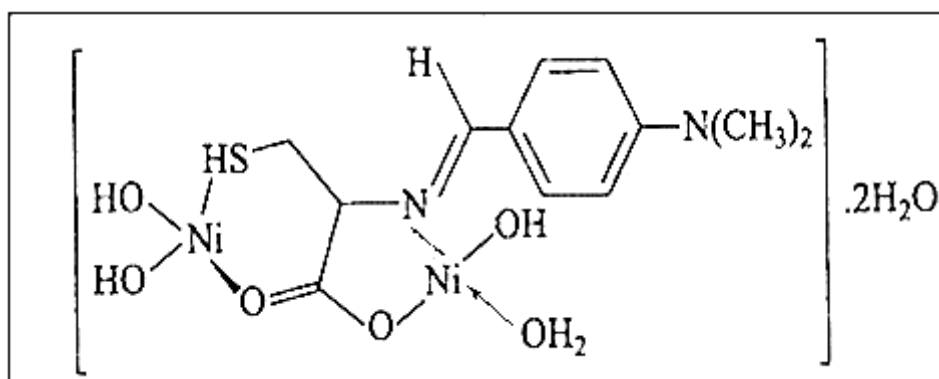


**Figure (1-13): The geometry of Ni complex**

Devendra *et al.*, in (2011)<sup>[60]</sup> were prepared complexes of Ni (II) containing Schiff base Figure (1-14), which has been derived from the o-amino benzoic acid and 4-DMAB, and diagnosed by different methods such as the magnetic susceptibility, UV- visible, X- ray diffraction, FTIR, molar conductivity, NMR, and CHN. Spectroscopic studies have supported that the ligand behave as tetra dentate ligand type ( $\text{N}_2\text{O}_2$ ) donor.

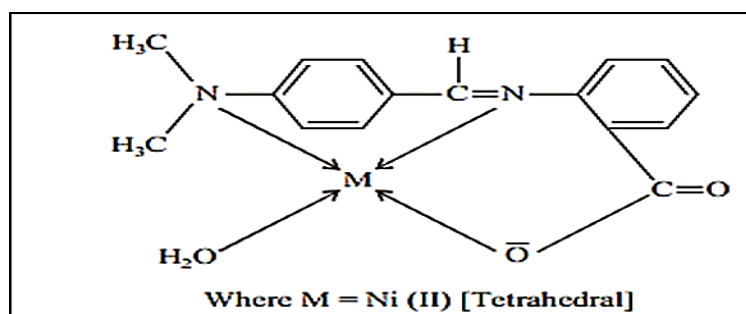


**Figure (1-14): Tetrahedral Ni (II) complex**

Anu *et al.*, in (2013)<sup>[61]</sup> reported synthesize Cu (II) complexes with isatin Figure (1-15) , were prepared and characterized by analytical and spectroscopic techniques. Schiff base complex of Cu (II) from the ligands like 2-aminophenol and para dimethyl amino benzaldehyde have been synthesised. The molar conductance, IR, <sup>1</sup>H-NMR, <sup>13</sup>C NMR, UV-Visible spectroscopy have been carried out to suggest tentative structure of the complex.

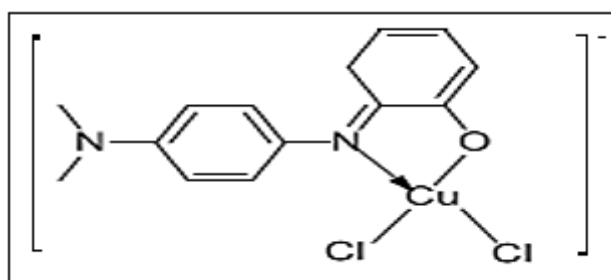
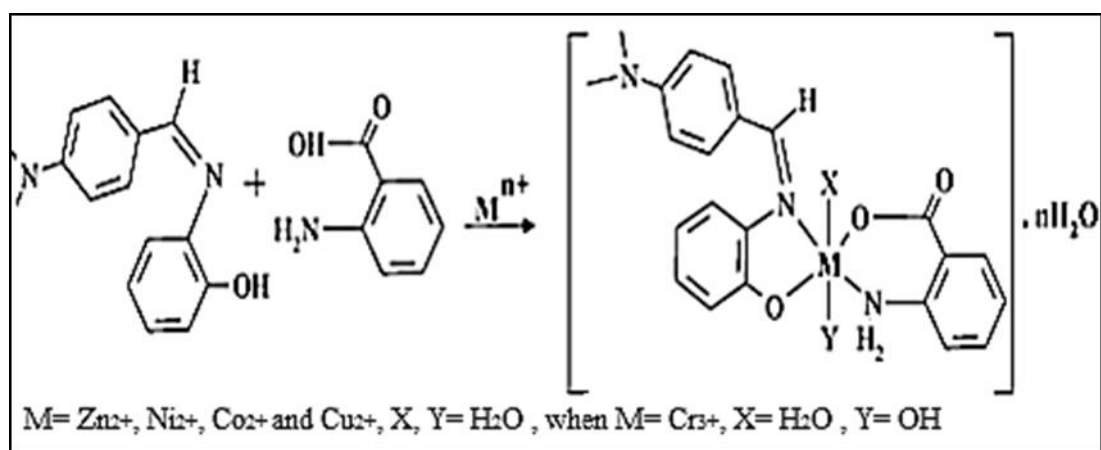


**Figure (1-15): Synthesis of Cu (II) complex**

Alassbaly *et al.*, in (2016)<sup>[62]</sup> reported about synthesis and characterization of five complexes of mixed ligands consists of amino acid (anthranillic acid) as a secondary ligand and Schiff base resulted from 4-AMAB & 2-amiophenol as a primary were studied. All compounds were measured using various methods such as mass, FTIR, CHN, electronic spectroscopies, magnetic moment, and molar conductivity. The Synthetic studies suggested the octahedral geometry of all these complexes. The anti-bacterial activity that is related to Schiff bases, Histidine, and mixed complexes were tested. It has been found that mixed ligands have more biological activity compared to free ligand. Scheme (1-3)



**Scheme (1-3):** Synthesis route regarding complexes

Abubakar et al., in (2017)<sup>[63]</sup> were prepared a bi dentate Schiff base ligand (DBAP) derived from 2-amino phenol and (4-DMAB) have been prepared. This new ligand has been treated with Cu (II) and Zn(II) salt with a ratio of metal: ligand equal to (1:2) to produce the two new ligand compounds  $[\text{Cu}(\text{DBAP})_2]8\text{H}_2\text{O}$  and  $[\text{Zn}(\text{DBAP})_2]3\text{H}_2\text{O}$ , Figure (1-16) and Figure (1-17) respectively, these complexes have been diagnosed by many techniques as melting point, solubility, FTIR, CHN, UV-visible and atomic absorption, molar conductivity and magnetic measures. Data have suggested that the ligand was bi dentate and a four assortment tetrahedral geometry for Zn complexes and square geometry for Cu complexes.

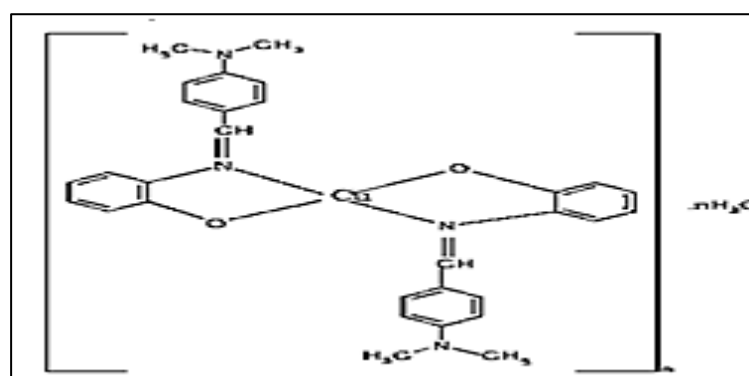


**Figure (1-16):** The structures of the Cu (II) complex



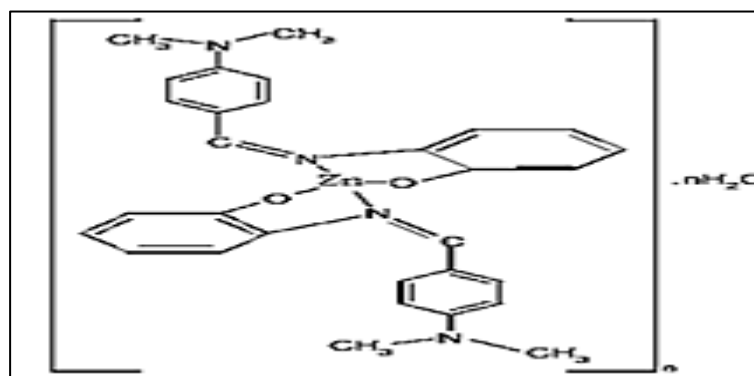
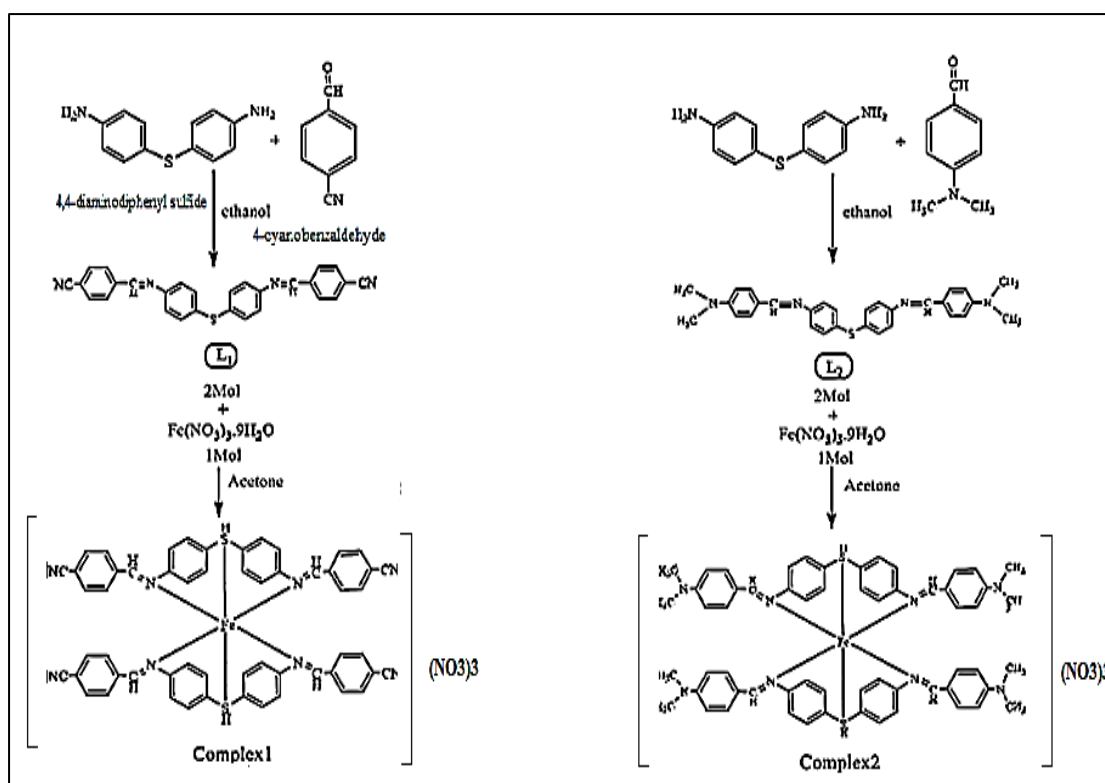


Figure (1-17): The structures of the Zn (II) complex

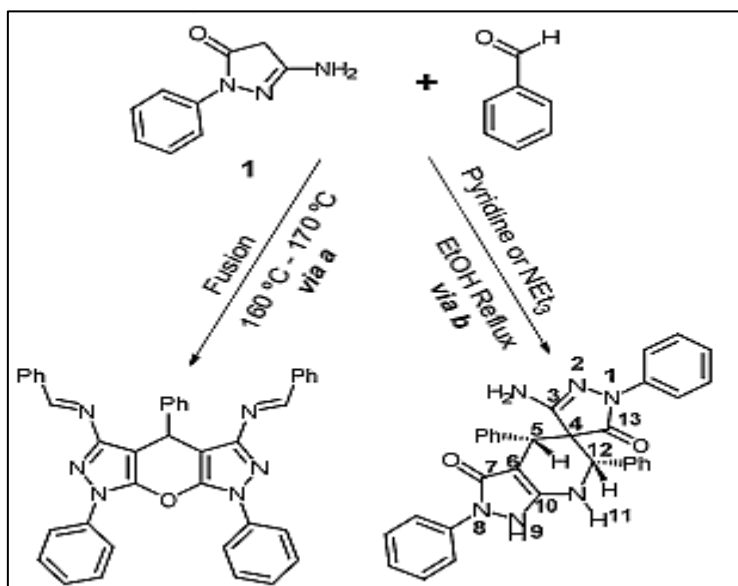
Noor *et al.*, in (2018)<sup>[64]</sup> prepared Schiff base with  $\text{Fe}^{+3}$  derived from 4,4-diaminodiphenyl sulfide with two kind of aromatic aldehyde to form L1 and L2. FTIR, job's method and electronic spectroscopy were used to characterize there complexes structure.



Scheme (1-4): The synthesis route of  $\text{Fe}^{+3}$ -complexes

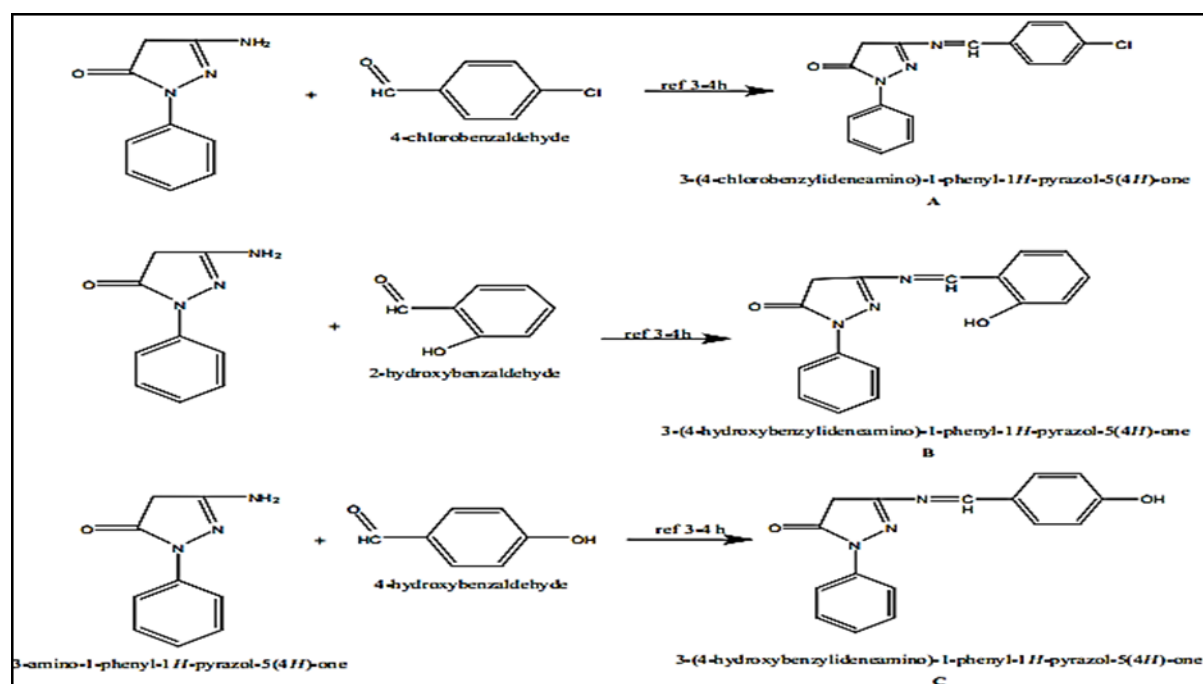
### 1.5.3 Complexes related to the Schiff base from 3-amino-1-phenyl-2-pyrazolin-5-one

Jamila Z. *et al.*, in (2015)<sup>[65]</sup> have synthesis of new derivatives ligands L1-5 see in Scheme (1-5) have attracted interest from the scientific community. Herein we report the formation of two unexpected spiro compounds containing pyrazole moieties using a tandem process involving the initial condensation of (3-amino-1-phenyl-2-pyrazolin-5-one) with benzaldehyde followed by dimerization.



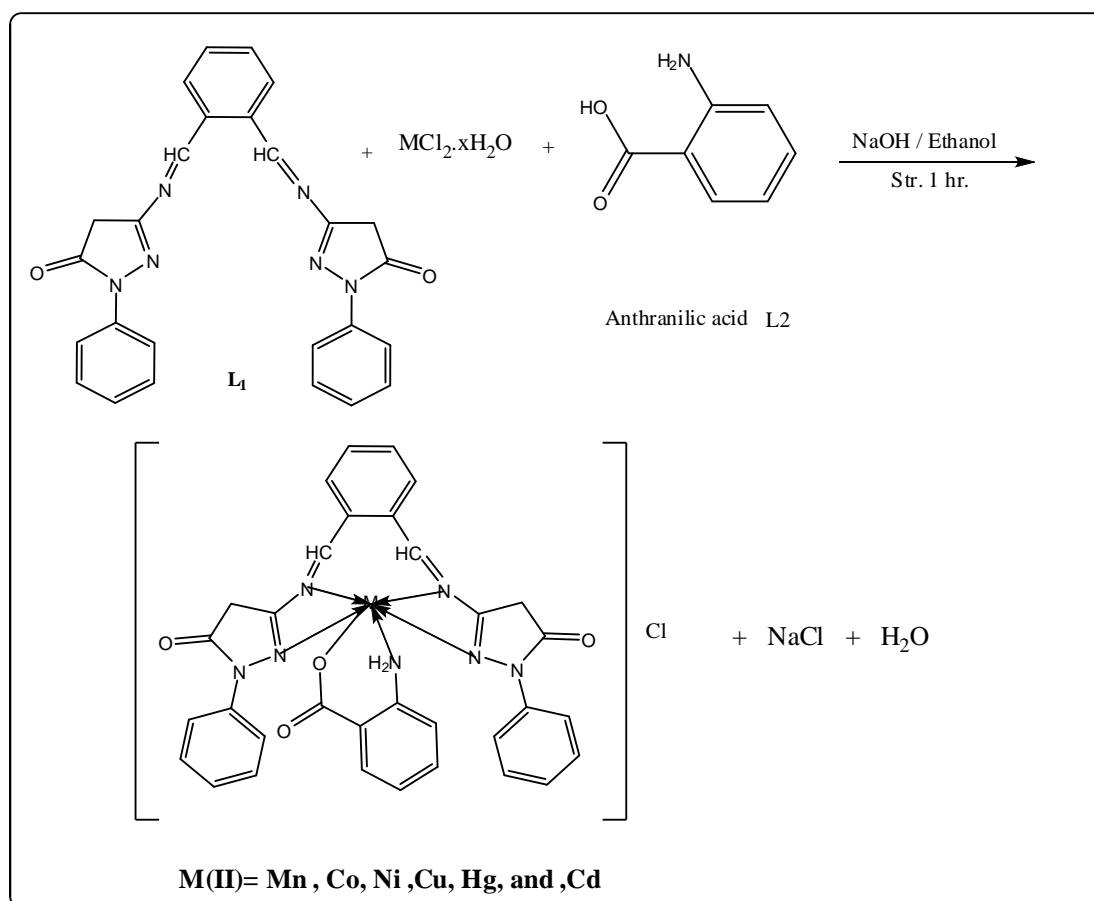
**Scheme (1-5): Synthesis route of L1-5 ligands**

Lekaa *et al.*, in (2018)<sup>[66]</sup>, prepared compounds of Cd(II) and Ni(II) which are related to the Schiff bases that are derived from 3-APO with three type of aromatic aldehyde. They were characterized by FT-IR, <sup>1</sup>HNMR, CHNO, mass spectrometer, molar conductivity measurements and magnetic susceptibility. Analytical information detected that these complexes were tetrahedral shape Scheme (1-6). The biological activity for the compounds was tested.



**Scheme (1-6): The prepared of the three ligands**

Lekaa *et al.*, (2019)<sup>[67]</sup> have prepared complexes of mixed ligands see in Scheme (1-7), that consist of Schiff bases derivative ligand (L1) that was formed through condensed 3-APO with anthranillic acid (L2) and o-phthalaldehyde as well as certain transition metal ions. Diagnosing the formed ligand (L1) was through UV-Visible, mass spectroscopy, <sup>1</sup>HNMR, and (CHN) elemental analysis. Complexes have been typified through elemental analysis, FTIR, atomic absorption, UV-visible, molar conductance, and magnetic susceptibility. The octahedral geometry was suggested for metal compounds according to analytical studies. The compounds have been determined against two bacteria types; Gram negative and Gram positive.



**Scheme (1-7): Synthesis of new mixed ligand complexes**

## 1.6 Mixed Ligands Complexes of Anthranilic Acid (A)

The complexes of mixed ligands are different from conventional complexes as they have more than two different types of ligands related to same metal ion in the complex. The existence of over one ligand type in the complex will increase the possibility of variations in the characteristics of the complex. Thus, the researchers will be more focused on the synthesis related to complexes of mixed ligands with changing features. Characterization and synthesis regarding the complexes of mixed ligands are of high importance now and more researchers are focusing on this field. Recently, a lot of papers were concerned about the characterization and the synthesis of mixed ligand complexes<sup>[68]</sup>.

Gehad *et al.*, in (2005)<sup>[69]</sup> prepared metal complexes which are related to the Schiff bases that is derived from 2-thiophene carboxaldehyde and 2-aminobenzoic acid (HL). They defined according to the elemental analyses, thermal analysis TGA, solid reflectance, molar conductance, IR, magnetic moment, and <sup>1</sup>HNMR Figure (1-18).

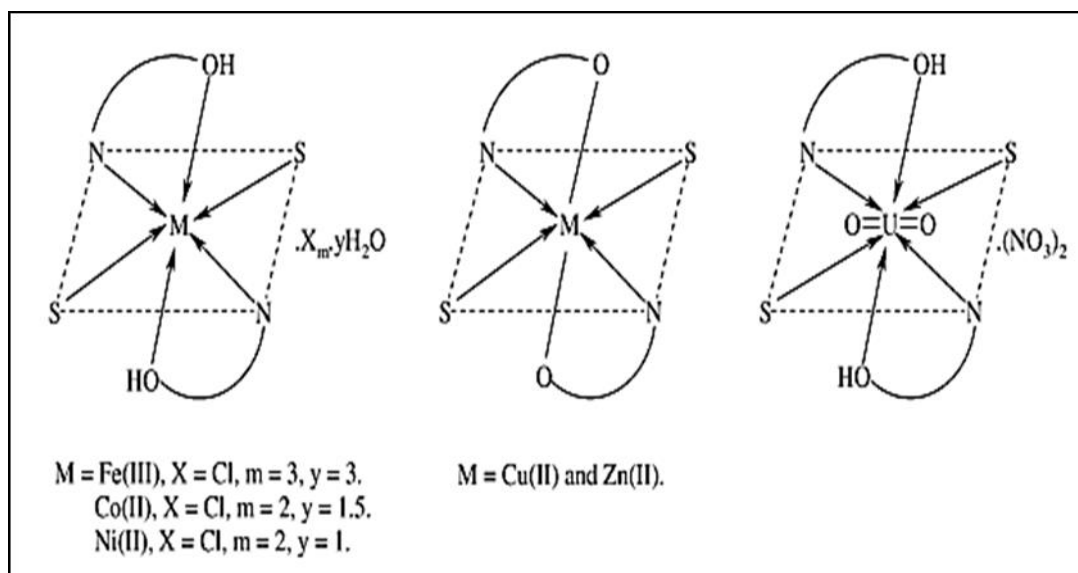
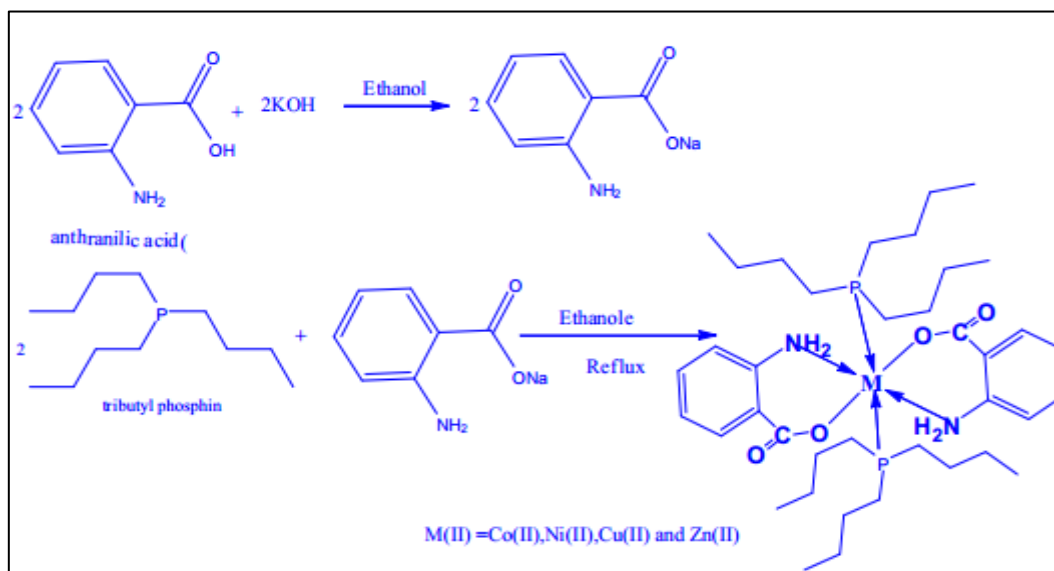


**Figure (1-18): The structural formulas related to mixed HL metal complexes**

Taghreed *et al.*, in (2013)<sup>[70]</sup> prepared a mixed ligand complexes from the reaction of tri butyl phosphine, anthranilate and metal ion such as Zn(II), Ni(II), Co(II), and Cu(II) see in Scheme (1-8). The prepared compounds were characterized using A.A., FT-IR, UV visible spectra methods, conductivity measurements and magnetic susceptibility. Metal compounds were tested in vitro against different types of pathogenic bacteria for the purpose of assessing their anti-microbial characteristics results. The research indicates that there is octahedral geometry in all the complexes.



**Scheme (1-8): Preparation route of the Complexes**

Taghreed *et al.*, in (2016) <sup>[71]</sup> prepared complexes of mixed ligands that are related to bivalent metal ions such as Hg(II), Zn(II), Ni(II), Co(II), Cu(II), and Cd (II) with Anthranilic acid and Trimethoprim (TMP) Figure (1-19), such complexes were characterized through electronic spectral data, molar conductivity, FT-IR, melting point, AAS, and a measurement of magnetic susceptibility. The two ligands in addition to their metal compounds have been screened for their bacterial activates against selected microbial strains Gram (+) and Gram (-).

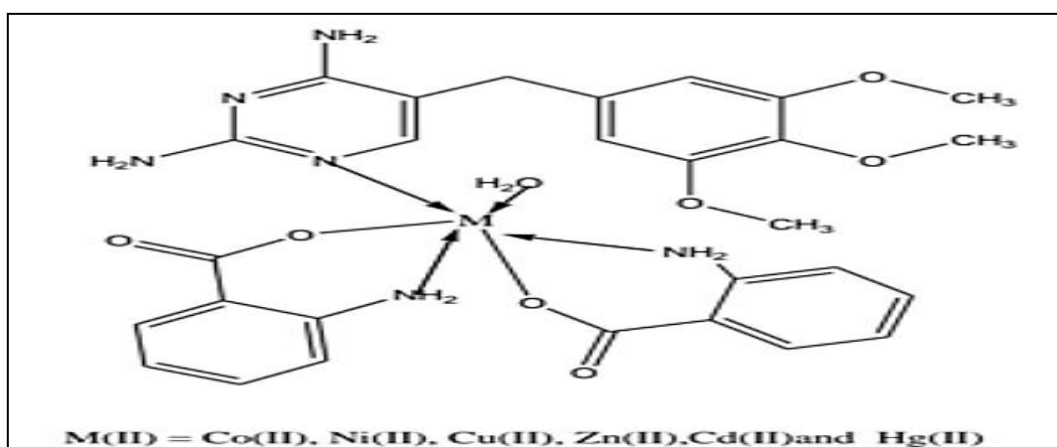


**Figure (1-19): The composition of mixed ligands complexes**

Oladipupo *et. al.*, in (2018) <sup>[72]</sup> reported synthesis of Mn(II), Ni(II), Co(II), Cu(II), Zn(II) and Cd(II) complexes of anthranilic acid (L1H) and pyridine-2-aldoxime (L2H) were synthesized in an alkaline medium see in Figure (1-20). The resulting complexes were characterized by CHN analysis, infrared and UV-Visible spectroscopies, molar conductance and magnetic susceptibility measurements. Cd(II) complex showed promising inhibitory activity against *Staphylococcus aureus*, *Bacillus subtilis*, *Escherichia coli*, *Pseudomonas aeruginosa* and *Candida albicans*.

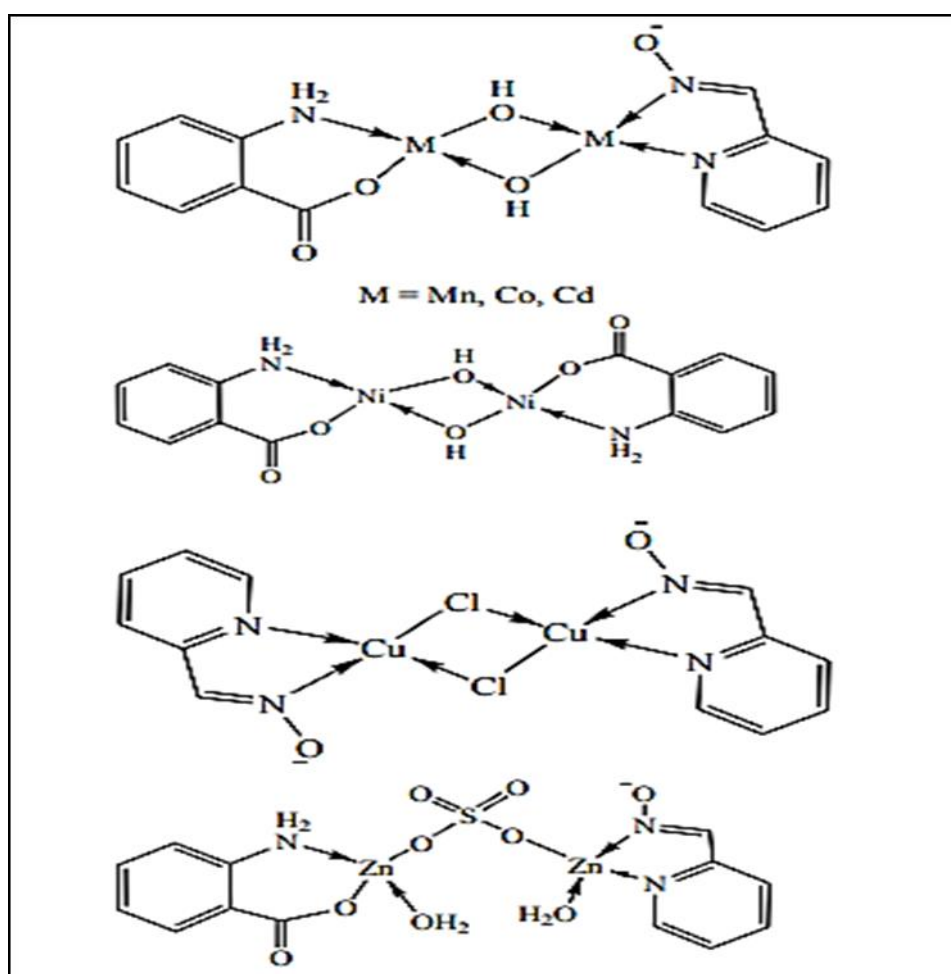


Figure (1-20): Structures of new complexes

## 1.7 Aim of the work

- Synthesize the Schiff base SB1 that is derived from vanillin with 3-Amino-1-phenyl-2-pyrazoline-5-one.
- Synthesize the Schiff base SB2 that is derived from 4-(dimethyl amino) benzaldehyde with 3-Amino-1-phenyl-2-pyrazoline-5-one.
- Characterize the synthesized ligands SB1 and SB2 by the use of elemental micro analysis (C.H.N.), FT-IR,  $^1\text{H-NMR}$ , UV-Vis, GC-MS and study they anti-bacterial activity that is tested against gram negative and gram-positive bacteria.
- Preparing mixed ligand compounds of Co(II), Ni(II), Cu(II), Cd(II) and Hg(II) ions with Schiff bases SB1 and SB2 considered as the primary ligand and (A) considered as the secondary ligand.
- Characterizing the prepared mixed ligands complexes by the use of elemental micro analysis (C.H.N.), UV-Vis, FT-IR, magnetic measurements as well as studying the anti-bacterial activity, that is tested against gram negative and gram positive bacteria.



## 2. Experimental section

### 2.1. Initial materials

The initial materials were of high purity (99%). Therefore, no further purification was needed. Table (2-1) lists the initial materials.

**Table (2-1): The initial materials**

Initial of materials	Company equipment
3-amino-1-pheneyl-2-pyrazoline-5-one	Merck
Acetone	Merck
Anthranillic Acid	Fluka
Cadmium chloride. Mono hydrate	Merck
Cobalt chloride. Hexa hydrate	Riedel-de Haën
Cupper chloride. Di hydrate	Merck
Dimethyl formamide (DMF)	Fluka
Dimethyl sulfoxide. (DMSO)	Fluka
4-dimethyl amino benzaldehyde	Fluka
Ethanol	Merck
Ethyl acetate	Merck
Glacial acetic acid	Bryce Dallas Howard
Mercury chloride	Merck
Methyl alcohol	Fluka
Nickel chloride. Hexa hydrate	Fluka
Vanillin(4-Hydroxy-3-methoxybenzaldehyde)	Fluka

## **2.2 Instrumental analysis**

The new compounds were characterized by using the following techniques:

### **2.2.1 Melting points measurement**

The melting points of the recorded vehicles were measured by using digital melting point apparatus, in Baghdad University Laboratories, Education for pure science Ibn Al Haitham.

### **2.2.2 Fourier Transform Infrared FT-IR**

The FT-IR of the new materials were on record as (KBr disc) pellets in range of (4000 to 400)  $\text{cm}^{-1}$  by using Shimadzu, 4800S spectrophotometer, in the laboratories of Ibn Sina in Baghdad.

### **2.2.3 Electronic spectra**

The electronic transfer's spectra of the new materials were using UV visible spectrophotometer type (double beam) in range (200 to 1100) nm, Shimadzu UV160A nm in the laboratories of Ibn Sina in Baghdad. The concentration of prepared solutions was  $0.001 \text{ mole.L}^{-1}$  in DMSO solvent and the cell is 1cm long, which is made of quartz.

### **2.2.4 Conductivity devices**

The conductivity devices of the new materials solution in DMSO were registered in 0.001M at room temperature, using the conductivity meter model (4070), Jew wary in the service laboratory at the University of Baghdad, Education for pure science Ibn Al Haitham.

### **2.2.5 Elementar micro analysis (CHNO)**

The CHNO was recorded in Euro vector model (EA3000) in the service laboratory at the University of Baghdad, Education for pure science Ibn Al Haitham.

### **2.2.6 Atomic Absorption Spectrometry A.A.S.**

The atomic absorption percentage of the metal in the complex was measured using Shimadzu AA(680) type Emission spectrophotometer in the laboratories of Ibn Sina in Baghdad.

### **2.2.7 Proton nuclear magnetic resonance (<sup>1</sup>HNMR)**

The <sup>1</sup>HNMR spectra of new ligands were recorded on Bruker DRX type system (500MHz) in TMS (Tetra methyl silane) as a standard in DMSO-d<sup>6</sup> solution in the laboratories of University of Tehran.

### **2.2.8 GC-mass Spectra**

The prepared SB1 and SB2 were measured the mass spectrometry in Shimadzu (E170ev) type GC-mass QP50A in the laboratories of University of Tehran.

### **2.2.9 Measurements of the Magnetic Susceptibility**

The magnetic sensitiveness for complexes SB1 and SB2 using in Balance Johnson Matthey. The  $\mu_{\text{eff}}$  was obtained in the solid state by Faraday's method in the laboratories of al Nahrain University.

### **2.2.10 Proposal of the molecular structure**

The proposals of the molecular structure for new compounds were done using Chem. Office program (2010).

### **2.2.11 Biological Activity**

The evaluation of starting materials, ligands and their metal complexes against two bacterial strains (Escherichia coli (G-) and Staphylococcus aureus (G+)) and one fungi species (Candida albicans) were performed using agar-well diffusion. In this method, the wells were dug in the media

with the help of a sterile metallic borer with centres at least 6 mm. Recommended concentration (100  $\mu$ L) of the test sample 1 mg/mL in DMSO was introduced in the respective wells. The plates were incubated immediately at 37 °C for 24h. Activity was evaluated by measuring the diameter of inhibition zones (mm). This test was done in the laboratories of the University of Baghdad, College of Science .

### **2.2.12 The materials and instrumental in Biological laboratory**

The materials and instrumental figure (2-1) used for testing the biological activity were:

Petri dish, nutrient agar medium, autoclave, spreader, McFarland tube, distilled water and control (DMSO).

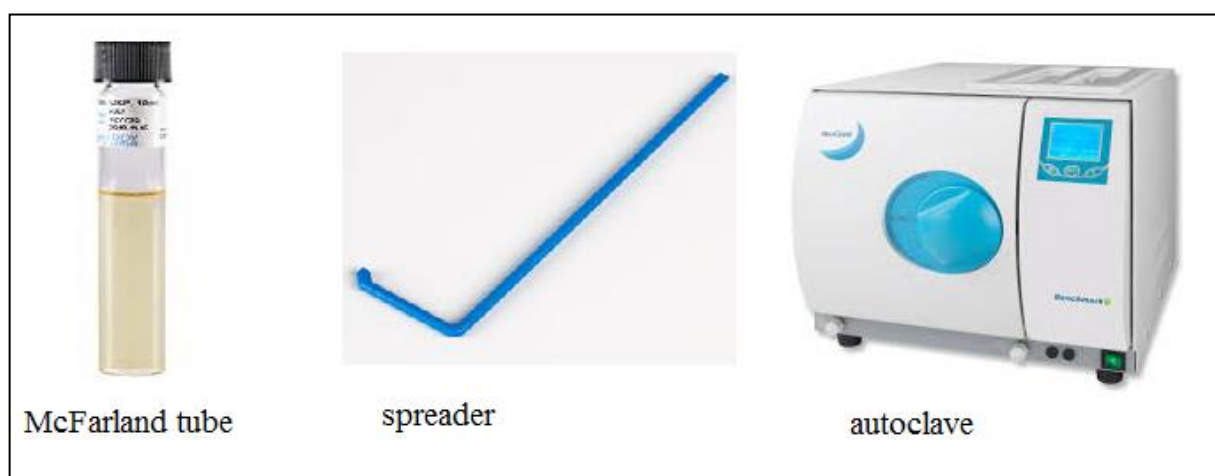
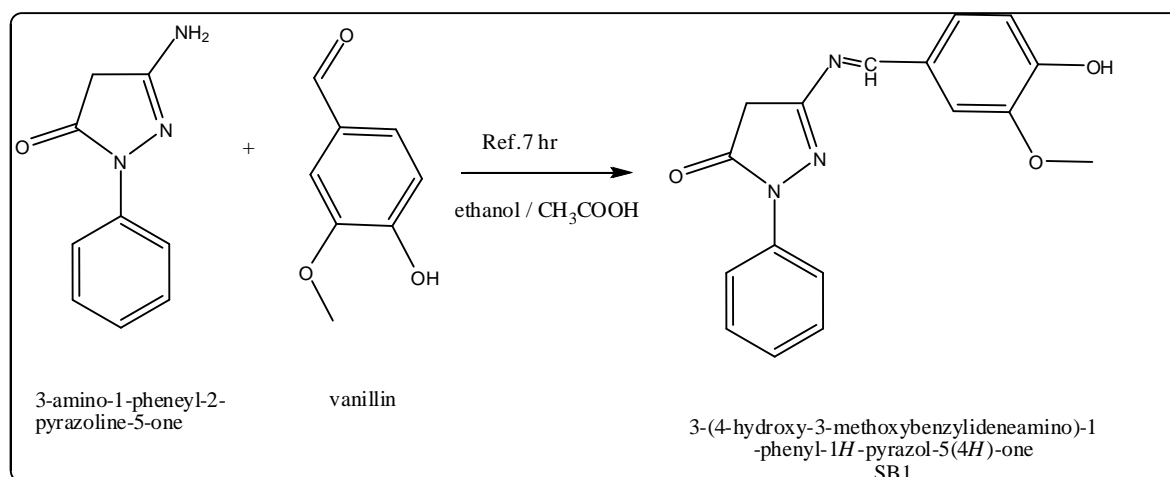


**Figure (2-1): Some of instruments in biological laboratory**

## 2.3 Preparation of the SB1 and SB2 ligands

### 2.3.1 3-(4-hydroxy-3-methoxybenzylideneamino)-1-phenyl-1H-pyrazol-5(4H)-one SB1

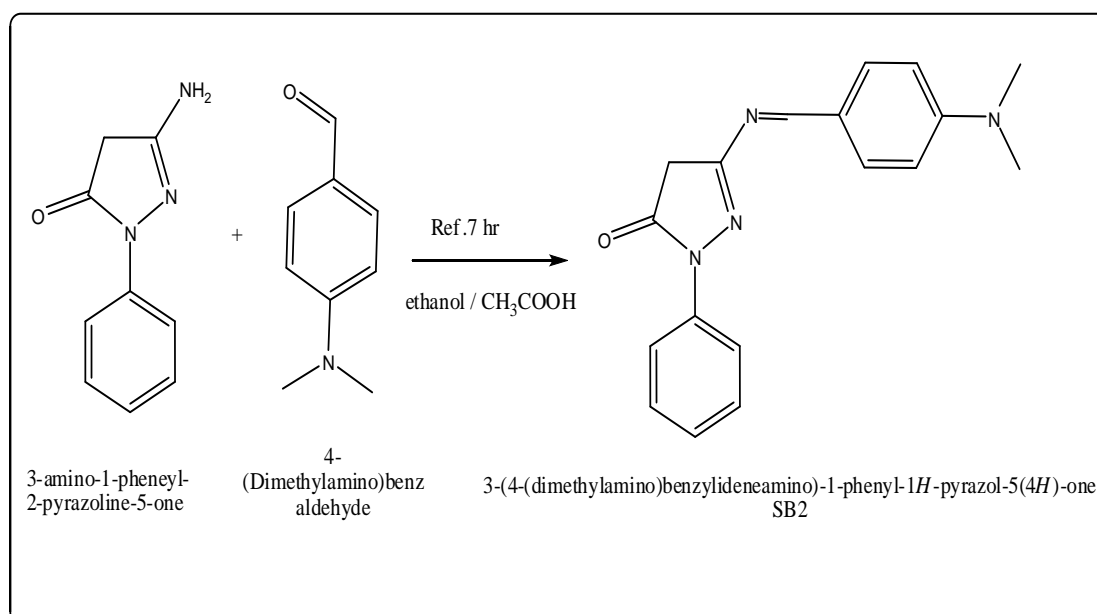
A mixture of 3-APO (1mmol, 0.175g) in 20mL of ethyl alcohol and solution of vanillin (1mmol, 0.152g) with 3-4 drops of (glacial acetic acid) were mixed in round bottomed flask. The mixture was then heated under reflux for 7h at 80°C with stirring. The product had been collected by filtration, washed with ethyl alcohol, dried and then recrystallization and dried at room temperature Scheme (2-1).



**Scheme (2-1): Synthesis of SB1 ligand**

### 2.3.2 3-(4-(dimethylamino)benzylideneamino)-1-phenyl-1H-pyrazol-5(4H)-one SB2

A mixture of 3-APO (1mmol, 0.175g) in 20mL of ethyl alcohol and solution of 4-DMAB (1mmol, 0.149g) with 3-4 drops of (glacial acetic acid) were mixed in round bottomed flask. The mixture was then heated under reflux for 7h at 80°C with stirring. The product had been collected by filtration, washed with ethyl alcohol, dried and then recrystallization dried at room temperature Scheme (2-2).



**Scheme (2-2): Synthesis of SB2 ligand**

## 2.4 Preparation of new complexes

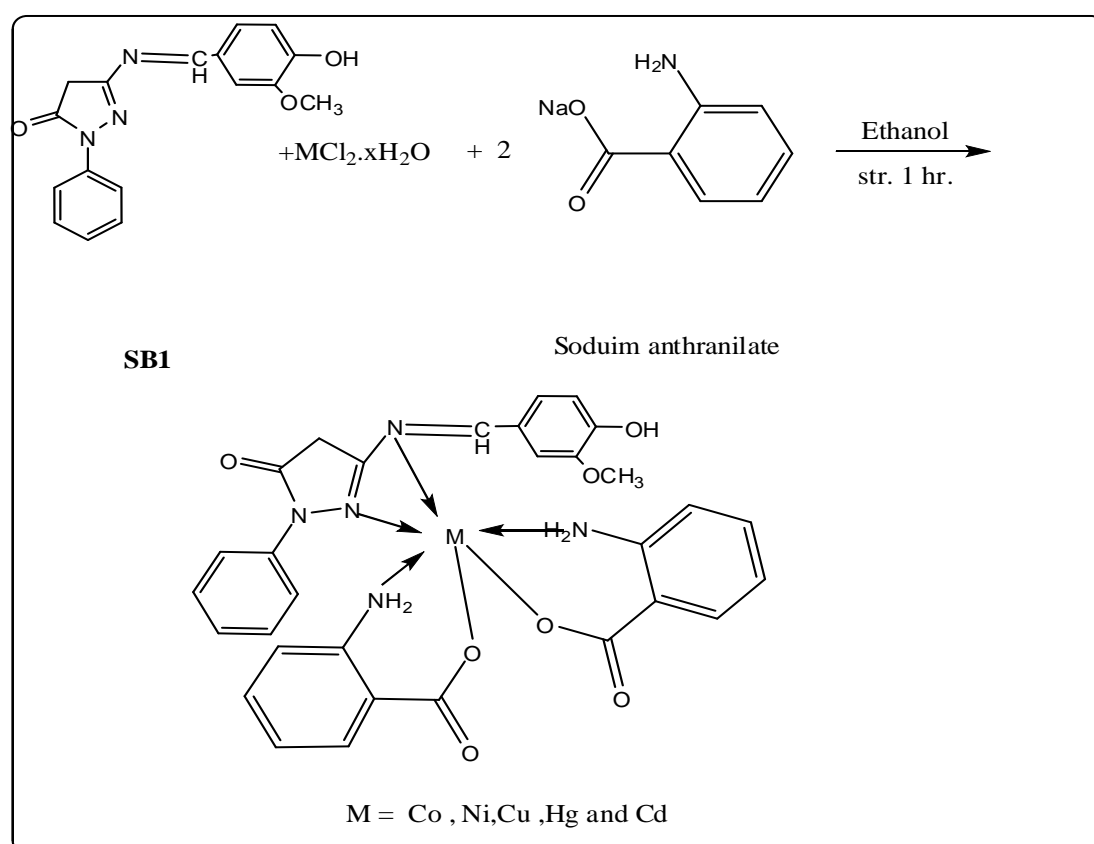
### 2.4.1 Preparation of SB1 complexes

#### 2.4.1.1 Preparation of [CoA<sub>2</sub>SB1] complex

[CoA<sub>2</sub>SB1] was prepared by mixing (A 0.274g, 2mmol & NaOH 0.08g, 2mmol) with (SB1 0.309g, 1mmol) and CoCl<sub>2</sub>.H<sub>2</sub>O (0.237g, 1mmol) in 15mL of ethyl alcohol. The mixture solution was mixed was whiskered for 1h to produce a green-bluish precipitation. The precipitate was filtered and dried at room temperature for one day<sup>[73]</sup>.

#### 2.4.1.2 Preparation of mixed complexes

Similar to the method for cobalt complex preparation (2.4.1.1) complexes such as [NiA<sub>2</sub>SB1], [CuA<sub>2</sub>SB1], [CdA<sub>2</sub>SB1] and [HgA<sub>2</sub>SB1] were prepared. The solid complexes with metal chloride listed in Table (2-2), see in Scheme (2-3).



**Scheme (2-3): Preparation of [MA<sub>2</sub>SB1] complexes**

**Table (2-2): Weights of materials involved in the preparation of complexes [MA<sub>2</sub>SB1]**

Complex	Wt. of Metal Chloride	Wt. of SB1	Wt. of A	wt. of complex	Yield %
[CoA <sub>2</sub> SB1]	CoCl <sub>2</sub> .6H <sub>2</sub> O 0.237g	0.309g	0.274g	0.640	78
[NiA <sub>2</sub> SB1]	NiCl <sub>2</sub> .6H <sub>2</sub> O 0.237g	0.309g	0.274g	0.639	81
[CuA <sub>2</sub> SB1]	CuCl <sub>2</sub> .2H <sub>2</sub> O 0.170g	0.309g	0.274g	0.645	85
[CdA <sub>2</sub> SB1]	CdCl <sub>2</sub> . H <sub>2</sub> O 0.201g	0.309g	0.274g	0.693	77
[HgA <sub>2</sub> SB1]	HgCl <sub>2</sub> 0.272g	0.309g	0.274g	0.783	87

## 2.4.2 Preparation of SB2 complexes

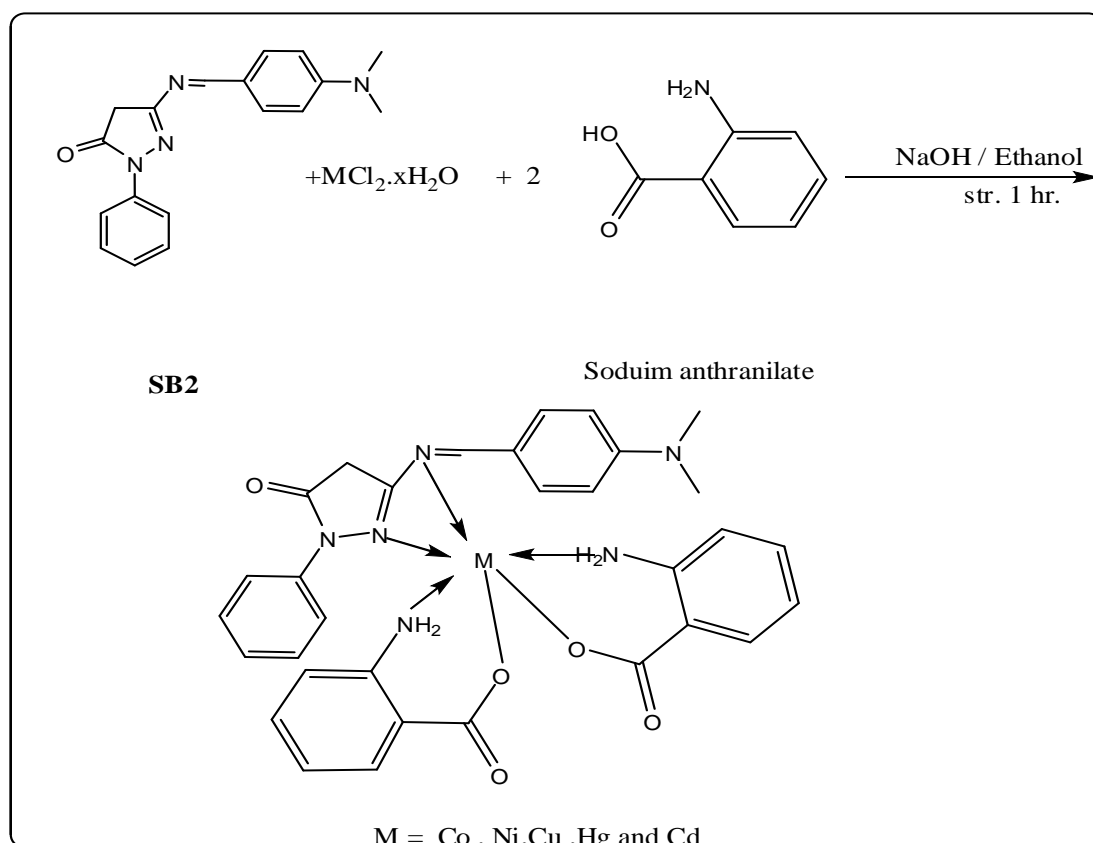
### 2.4.2.1 Preparation of [CoA<sub>2</sub>SB2] complex

[CoA<sub>2</sub>SB2] was prepared by mixing (A 0.274g, 2mmol and NaOH 0.08g, 2mmol) with (SB2 0.306g, 1mmol) and CoCl<sub>2</sub>.H<sub>2</sub>O (0.237g, 1mmol) in 15mL of ethyl alcohol. The mixture solution was mixed was whiskered for 1h to produce a green-bluish precipitation. The precipitate was filtered and dried at room temperature for one day.

### 2.4.2.2 Preparation of mixed complexes

Similar to the method for cobalt complex preparation (2.4.2.1) complexes such as [NiA<sub>2</sub>SB2], [CuA<sub>2</sub>SB2], [CdA<sub>2</sub>SB2] and [HgA<sub>2</sub>SB2] were prepared. The solid complexes with metal chloride listed in Table (2-3), Scheme (2-4).



Scheme (2-4): Preparation of  $[MA_2SB_2]$  complexesTable (2-3): Weights of materials involved in the preparation of complexes  $[MA_2SB_2]$ 

Complex	Wt.of Metal Chloride	Wt. of SB2	Wt.of A	wt. of complex	Yield %
$[CoA_2SB_2]$	CoCl <sub>2</sub> ·6H <sub>2</sub> O 0.237g	0.309g	0.274g	0.637	78
$[NiA_2SB_2]$	NiCl <sub>2</sub> ·6H <sub>2</sub> O 0.237g	0.309g	0.274g	0.637	81
$[CuA_2SB_2]$	CuCl <sub>2</sub> ·2H <sub>2</sub> O 0.17g	0.309g	0.274g	0.642	85
$[CdA_2SB_2]$	CdCl <sub>2</sub> 0.201g	0.309g	0.274g	0.691	77
$[HgA_2SB_2]$	HgCl <sub>2</sub> 0.272g	0.309g	0.274g	0.779	87

### 3. Result and Discussion

#### 3.1. Part one: Characterization of ligands SB1 and SB2

In this research, two Schiff base ligands were prepared and characterized by using spectroscopic techniques such as FT-IR, Uv-visble, <sup>1</sup>HNMR and mass spectrum in addition to detection of solubility, melting point and CHNO.

##### 3.1.1 Solubility

The solubility of prepared SB1 and SB2 in several solvents listed in Table (3-1)

**Table (3-1): Solubility of SB1 & SB2 in several solvents**

Ligands	Soluble (+),	insoluble (-)	Partially (÷)
SB1	DMSO , DMF	H <sub>2</sub> O, MeOH and Acetone	DME
SB2			

##### 3.1.2 Physical properties of new ligands

Some physical properties for SB1 and SB2 in addition to elemental microanalysis were listed in Table (3-2).

**Table(3-2): Some physical properties for SB1 and SB2**

Ligands formula	M.Wt (Color)	M.P	Practical (theoretical)			
			C	H	N	O
SB1 ( C <sub>17</sub> H <sub>15</sub> N <sub>3</sub> O <sub>3</sub> )	309.32 Deep Yellow	112-114	65.22 (66.01)	4.89 (4.78)	13.00 (13.58)	14.96 (15.52)
SB2 ( C <sub>18</sub> H <sub>18</sub> N <sub>4</sub> O )	306.36 Yellow	123-126	70.66 (70.57)	5.67 (5.92)	18.06 (18.29)	4.75 (5.22)

##### 3.1.3 FT-IR spectral data of starting material and new ligands

FTIR of the starting material (VA) Figure (3-1) showed the absorption bands at 3486 and 1730 cm<sup>-1</sup> due to the O-H and C=O stretching vibration respectively. The bands at (3021, 2975, 2738 and 1593) cm<sup>-1</sup>were due to (C-H

aromatic), (C-H aliphatic), (C-H aldehyde) and (C=C aromatic) stretching vibration respectively <sup>[74,75]</sup>. The FT-IR of the **4-DMAB** Figure (3-2) showed a weak absorption band at 3050, 2931, 2731, 1679 and 1584  $\text{cm}^{-1}$  which were assigned to the (C-H aromatic), (C-H aliphatic), (C-H aldehyde), (C=O aldehyde) and (C=C), stretching and vibration, respectively <sup>[74-77]</sup>. FTIR spectrum for **3-APO** Figure (3-3) showed bands at 3417, 3331, 3039 and 1681  $\text{cm}^{-1}$  due to  $\text{NH}_2$  asy. and sym., (CH aromatic) and (CO keto. ring), respectively <sup>[78,79]</sup>.

Spectrum of SB1 Figure (3-4) and Table (3-3) appeared bands at (3078, 1693 and 1566)  $\text{cm}^{-1}$  which were due to the (C-H aromatic), (C=O keton ring) (C=C) and new band at 1627 assigned to Schiff base stretching vibration <sup>[79]</sup>.

The infrared spectrum of SB2 Figure (3-5) and the same Table showed bands at 3062, 1701, 1643 and 1589  $\text{cm}^{-1}$  which were due to (C-H aromatic), (C=O ring pyrazole), (C=N new Schiff base group) and (C=C) stretching vibration <sup>[78]</sup>.

**Table (3-3): Distinguish between frequencies of the ligands and compare them with the initial materials**

Materials	OH	( $\text{NH}_2$ ) <sub>sym.&amp;asy.</sub>	C-H <sub>arom.</sub> C-H <sub>aliph</sub>	C-H aldehyde	C=O aldehyde	C=O Ketone	(C=N) <sub>SB</sub> (C=N)Pyr.	C=C
<b>VA</b>	3196	-----	3021 2975	2738	1666	----	-----	1593
<b>4-DMAB</b>	-----	-----	3050 2904	2731	1679	----	-----	1546
<b>3-APO</b>	-----	3425 3332	3221 2943	---	-----	1681	---- 1631	1597
<b>SB1</b>	3456	-----	3078 2997	----	-----	1693	1627 1597	1566
<b>SB2</b>	----	-----	3062 2974	----	-----	1701	1643 1627	1589

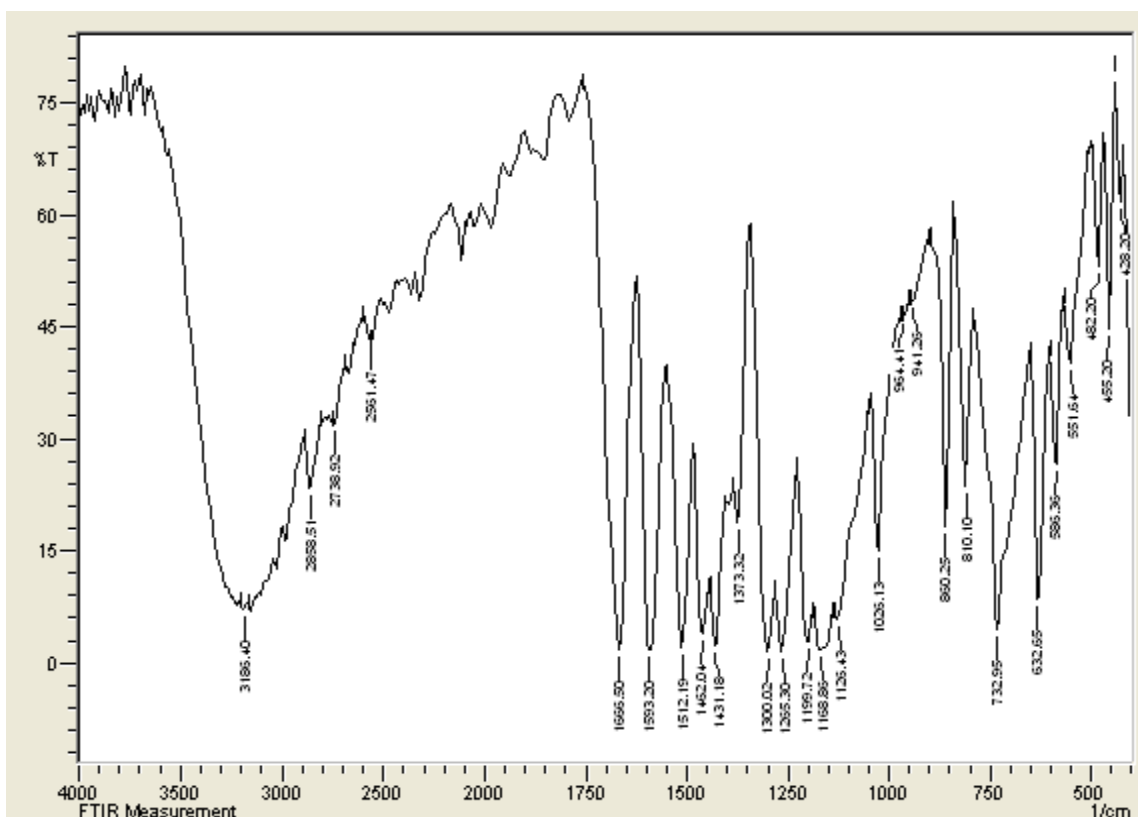


**Figure (3-1): The FTIR spectrum of vanillin**

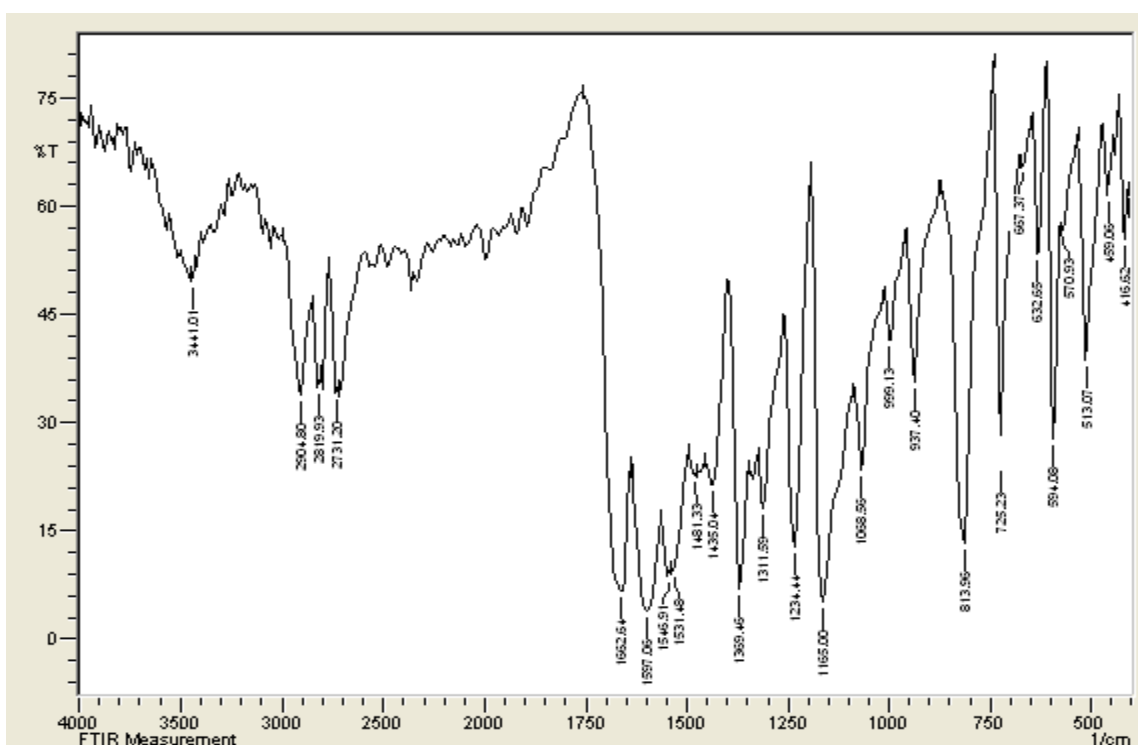


**Figure (3-2): The FTIR spectrum of [4-(Dimethylamino)benzaldehyde]**

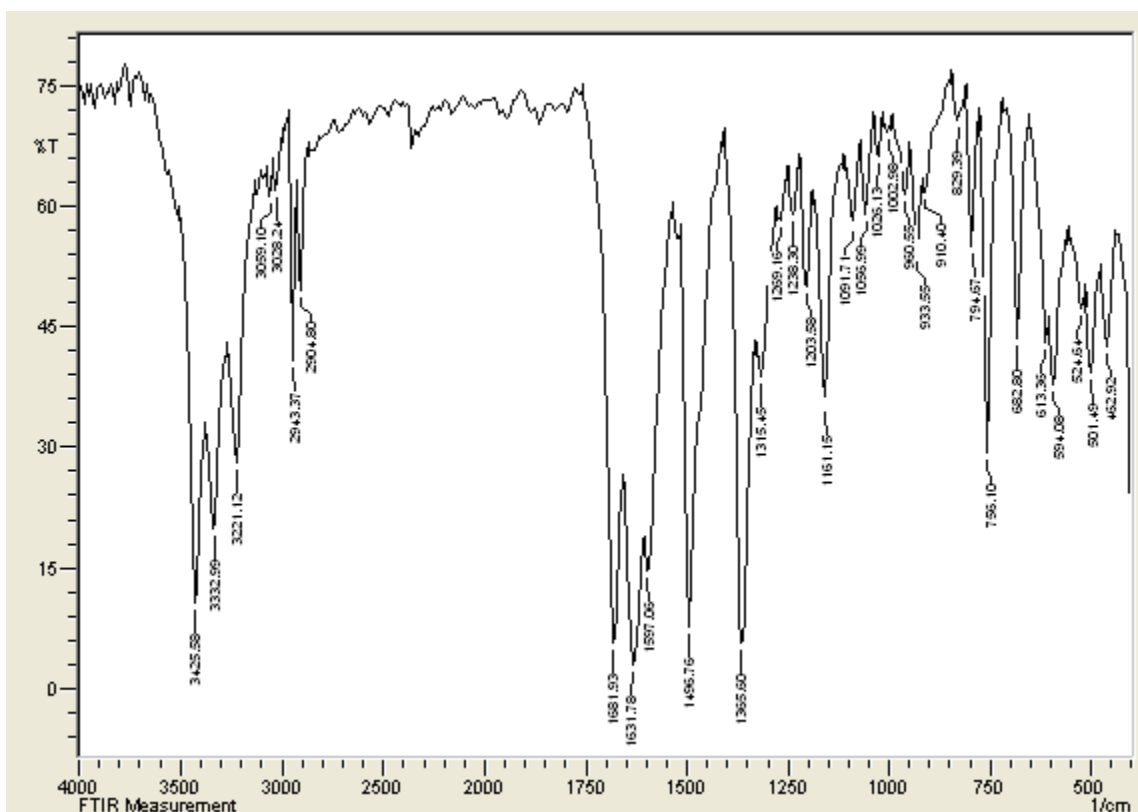


Figure (3-3): The FTIR spectrum of 3APO

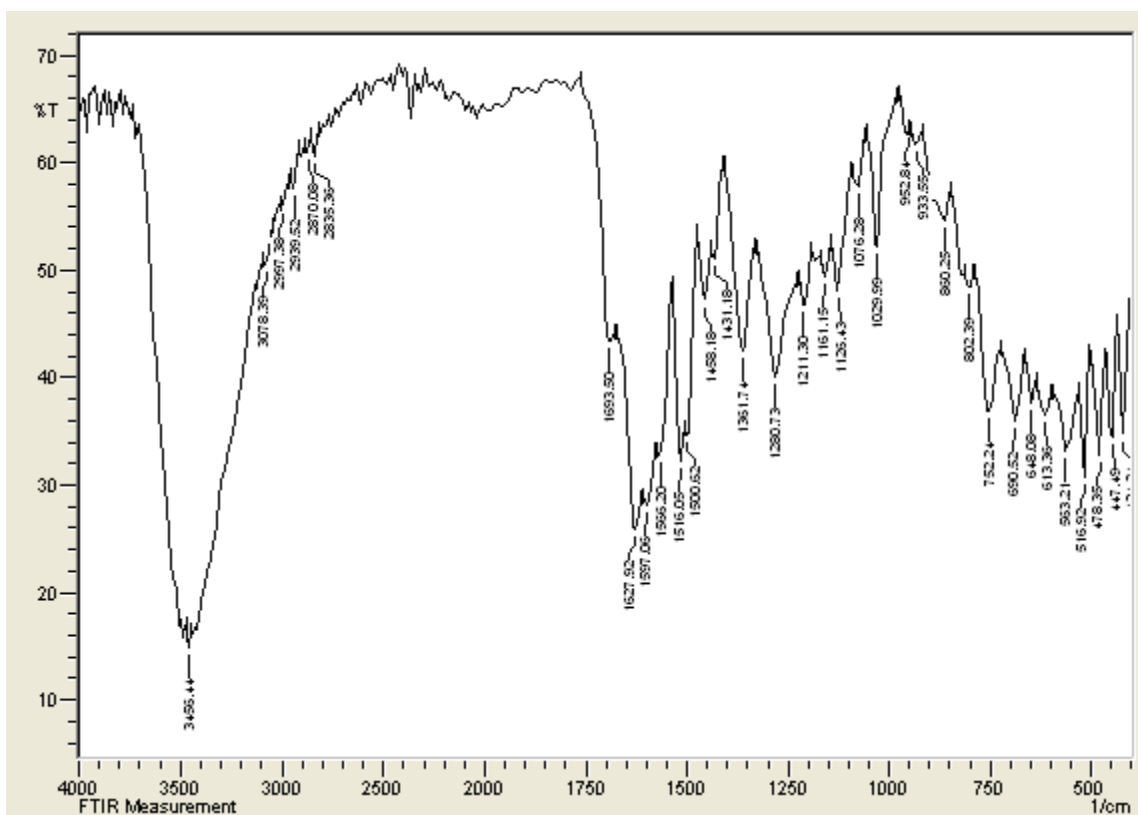


Figure (3-4): The FTIR spectrum of SB1 Ligand

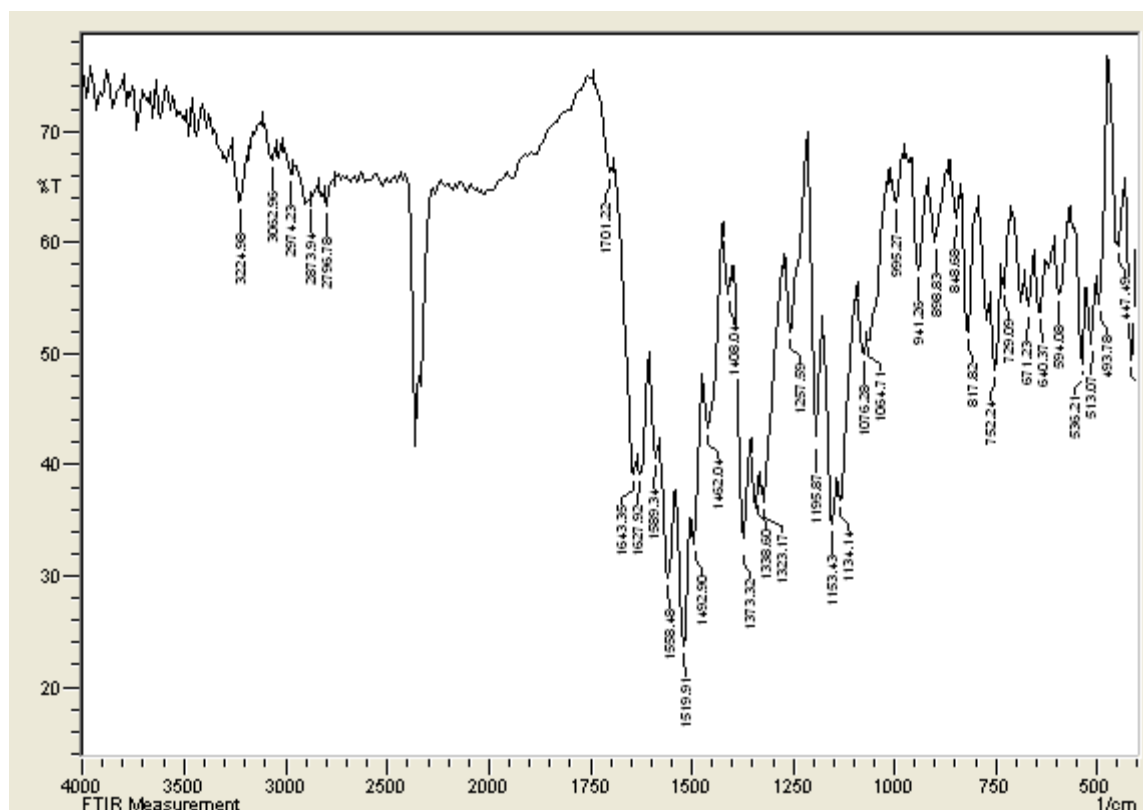


Figure (3-5) :The FTIR spectrum of SB2 Ligand

### 3.1.3 $^1\text{H-NMR}$ Spectral Data

#### 3.1.4.1 $^1\text{H-NMR}$ of ligand SB1

$^1\text{H-NMR}$  of SB1 is shown in Figure (3-6) and Table (3-4). The singlet signal in  $\delta$  (2.49, 2.53) ppm may be attributed to the  $\text{DMSO-d}^6$  solvent and (-CH<sub>2</sub>) of pyrazol ring respectively. The multiple signals ranged between  $\delta$  (6.25-7.75) ppm were assigned to the aromatic protons, and the singlet signal at  $\delta$  (8.94 and 9.76) ppm was due to the azomethine and OH protons [80,81].

Table (3-4):  $^1\text{H-NMR}$  Data for SB1

Efficacious group	The singlet in $\delta$ (ppm)
$\text{DMSO-d}^6$	2.49
(-CH <sub>2</sub> ) ring , Aromatic H	2.53 , (6.25-7.75)
HC=N, OH	8.94(1H, s), 9.76(1H,m)

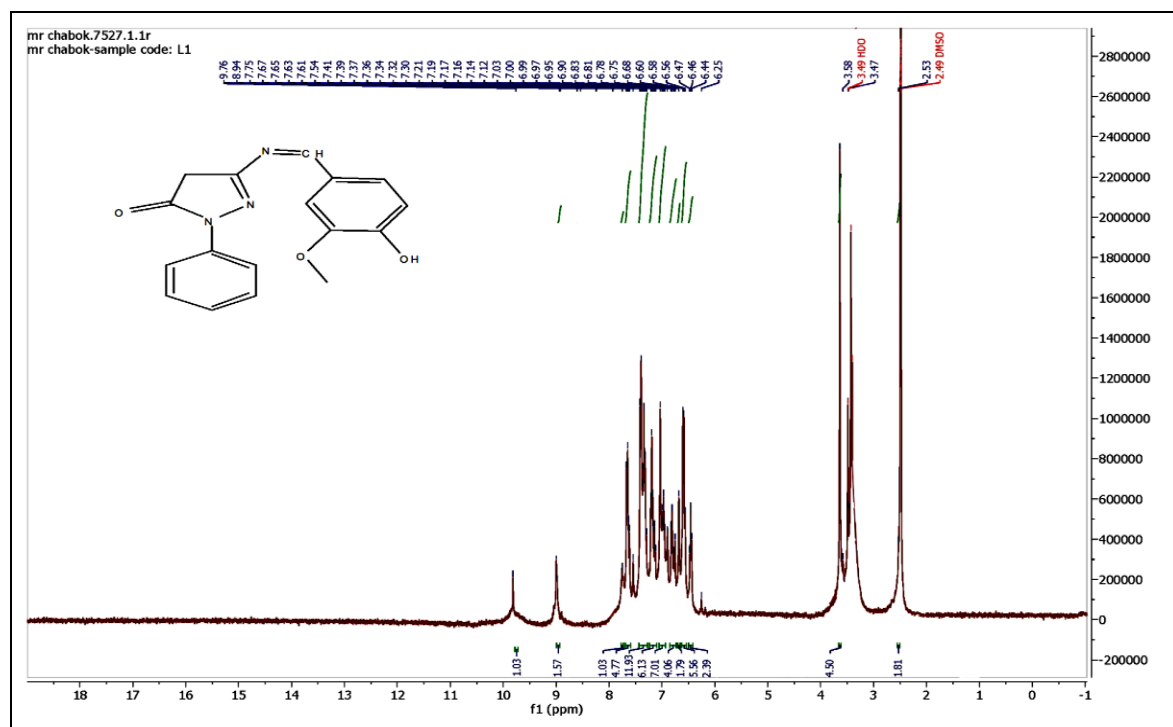


Figure (3-6): The  $^1\text{H}$ NMR spectrum of the Ligand SB1

### 3.1.4.2 $^1\text{H}$ -NMR spectrum of the ligand SB2

$^1\text{H}$ NMR of SB2 was shown in Figure (3-7) and Table (3-5). The singlet signal in  $\delta$  (2.53, 2.31 and 3.37) ppm may be attributed to the  $\text{DMSO-d}_6$  solvent,  $(\text{CH}_2)$  of pyrazol ring and methyl group respectively. The multiple signals ranged between  $\delta$  (6.45-7.83) ppm were assigned to the aromatic protons, and the singlet signal at  $\delta$  (8.80) ppm was due to the azomethine proton<sup>[80,81]</sup>.

Table (3-5): The  $^1\text{H}$ NMR for SB2

Efficacious group	The singlet in $\delta$ (ppm)
$\text{DMSO-d}_6$	2.49
Aromatic-H	6.45-7.83
$-\text{CH}_2\text{pyzol}$ , $-\text{CH}_3$	2.53, 2.31, 3.37
$\text{HC}=\text{N}$	8.51 (2H, s)

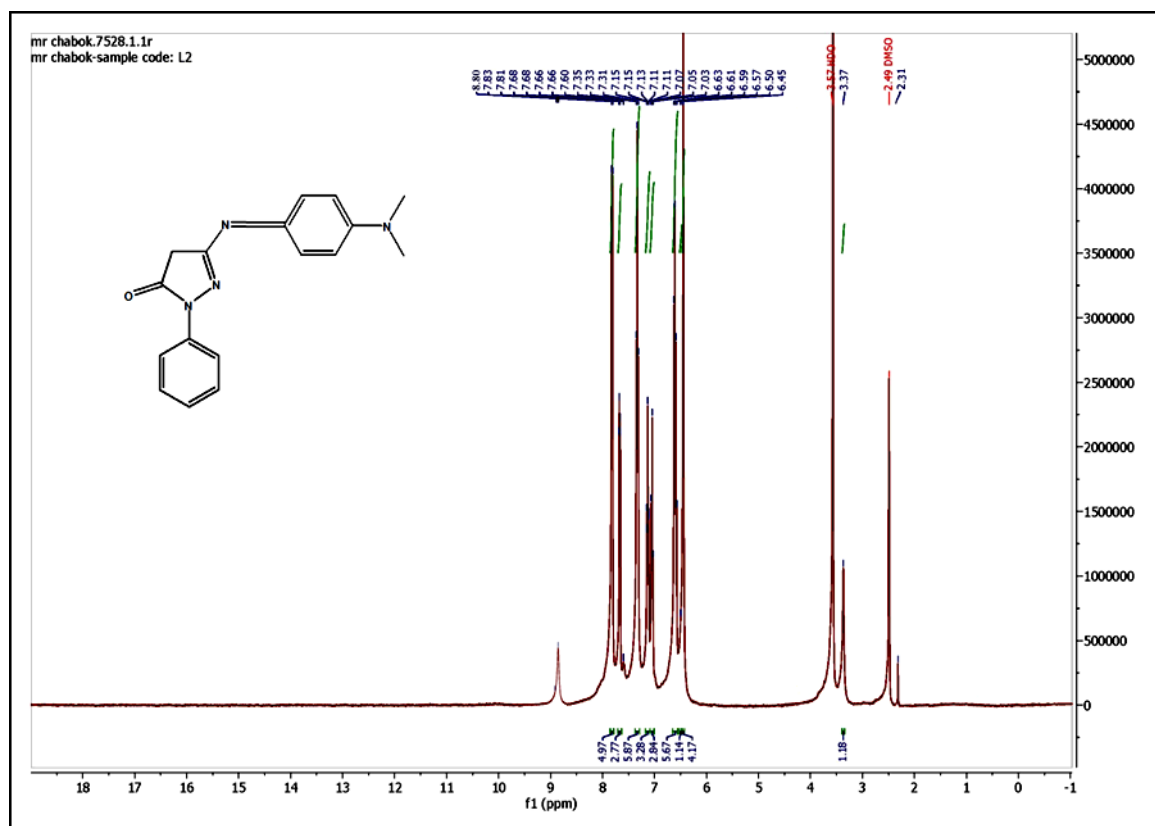


Figure (3-7): The  $^1\text{H}$ NMR spectrum of SB2

### 3.1.5 The Electronic Transfers for SB1 and SB2

#### 3.1.5.1 The spectrum of ligand SB1

The spectrum of SB1 in DMSO, (Table (3-6) and Figure (3-8)), show peaks at (289 and 390) nm which are due to  $\pi \rightarrow \pi^*$  and  $n \rightarrow \pi^*$  electronic transition [82, 83].

Table (3-6): Type of electronic transition of SB1

	$\lambda_{\text{max}}$ nm( $\text{cm}^{-1}$ )	$\epsilon_{\text{max}}$	Type of transition
SB1	289(34702)	92	$\pi \rightarrow \pi^*$
	390(25641)	222	$n \rightarrow \pi^*$



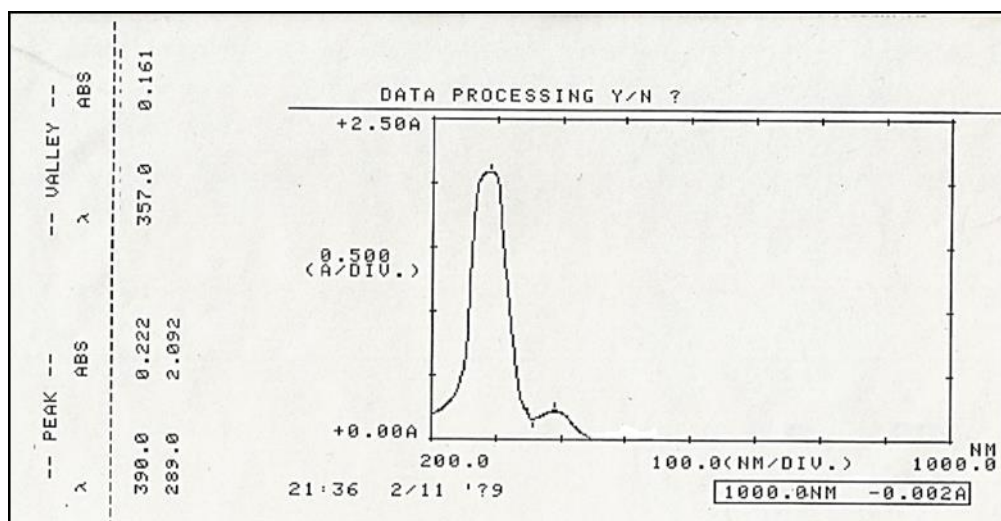


**Figure (3-8): Electronic spectrum of SB1 ligand**

### 3.1.5.2 The spectrum of ligand SB2

Spectrum of SB2 shows peaks in 271 and 399 nm which are assigned to  $\pi \rightarrow \pi^*$  and  $\pi \rightarrow \pi^*$  electronic transition, figure (3-9) and Table (3-7)<sup>[82, 83]</sup>.

**Table (3- 7): type of electronic transition of SB2**

	$\lambda$ nm( $\text{cm}^{-1}$ )	$\epsilon_{\text{max}}$	Type of transition
SB2	271(35211)	1334	$\pi \rightarrow \pi^*$
	399(25575)	247	$\pi \rightarrow \pi^*$

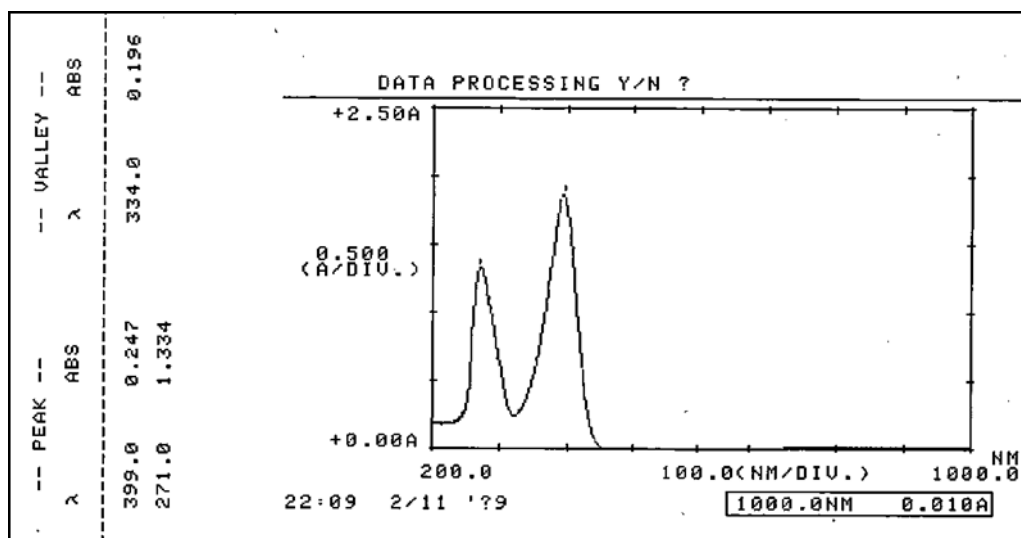


Figure (3-9): Electronic spectrum of SB2 ligand

### 3.1.6 The GC-mass spectral for ligands SB1 and SB2

#### 3.1.6.1 Mass spectrum of SB1

SB1 spectrum was shown in Figure (3-10) and scheme (3-1), the M.wt ion peak for  $C_{18}H_{18}N_4O$  equal 309m/z which was very much steady with the theoretical value<sup>[80, 84]</sup>.

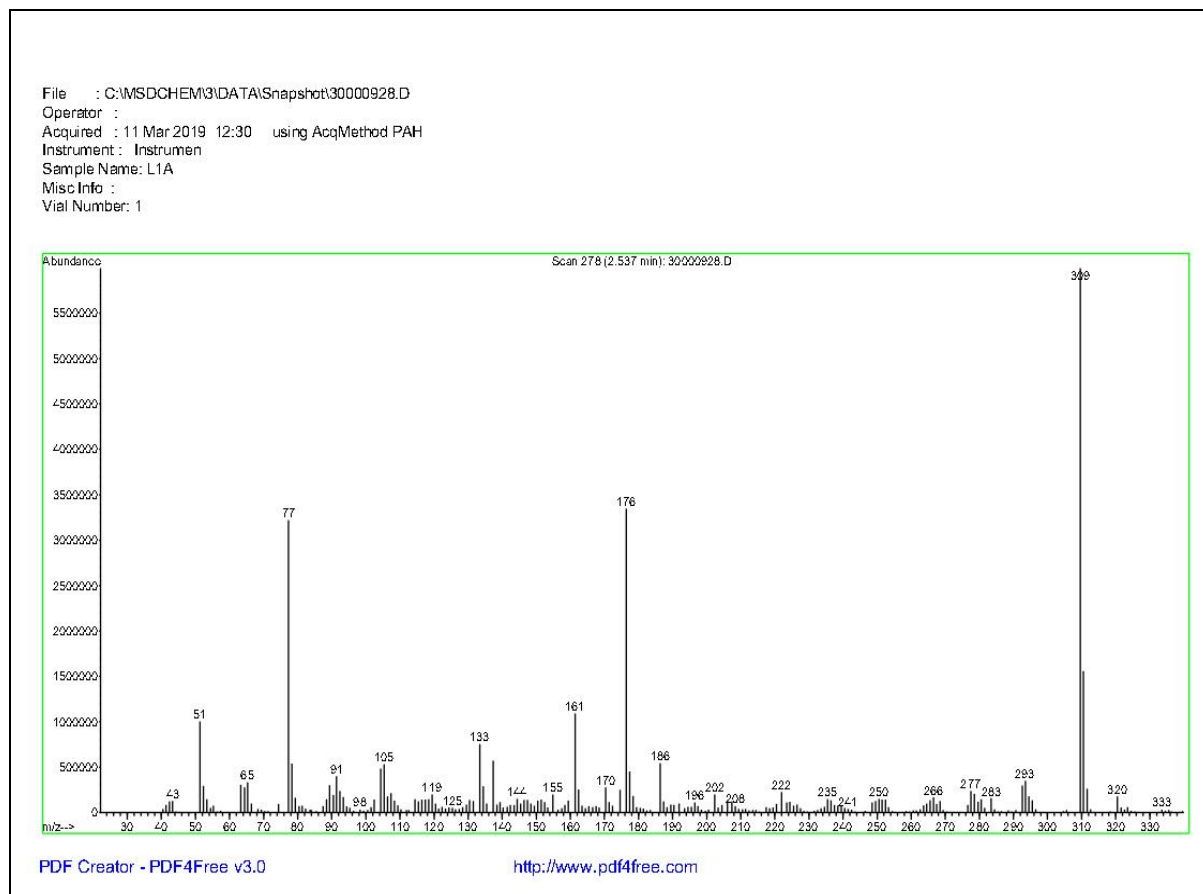
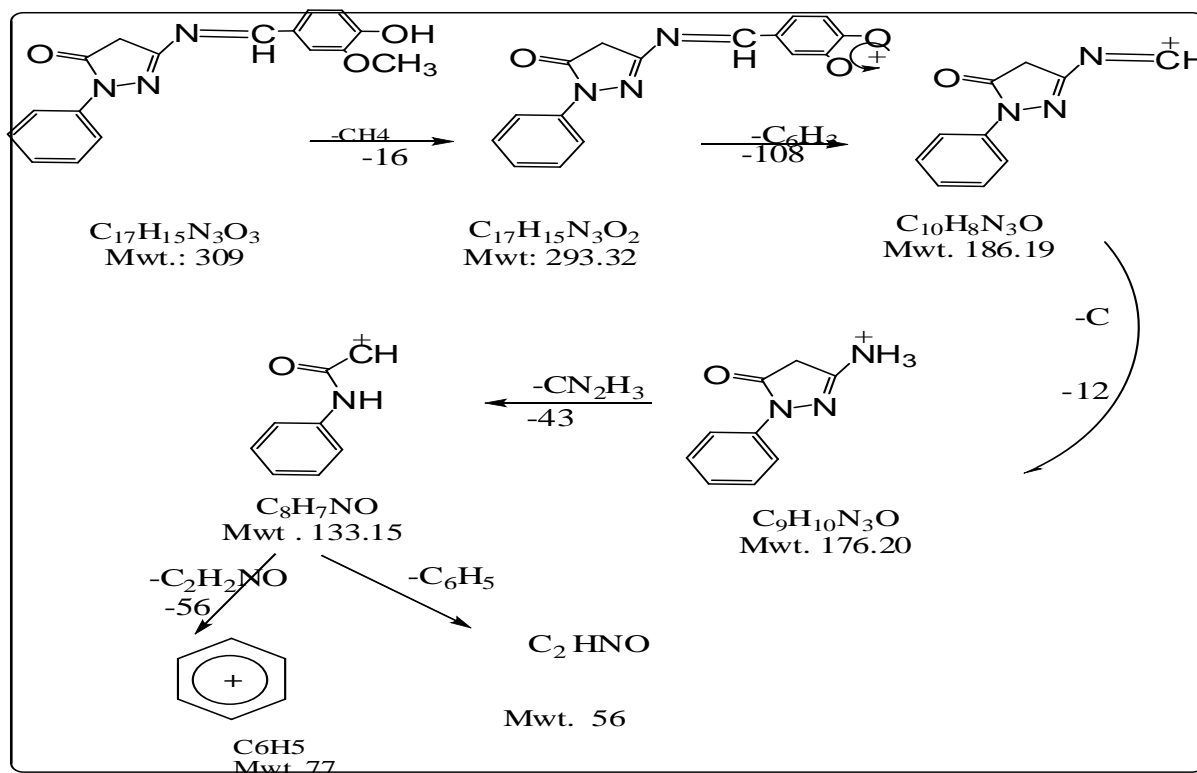


Figure (3-10):The mass spectrum of SB1



Scheme (3-1): The fragmentation pattern of the ligand SB1

### 3.1.6.2 Mass spectrum of SB2

Ligand SB2 spectrum was shown in Figure (3-11) and scheme (3-2), the M.wt ion peak for ( $C_{18}H_{18}N_4O$ ) equal 306 m/z which was very much steady with the theoretical value [79,85].

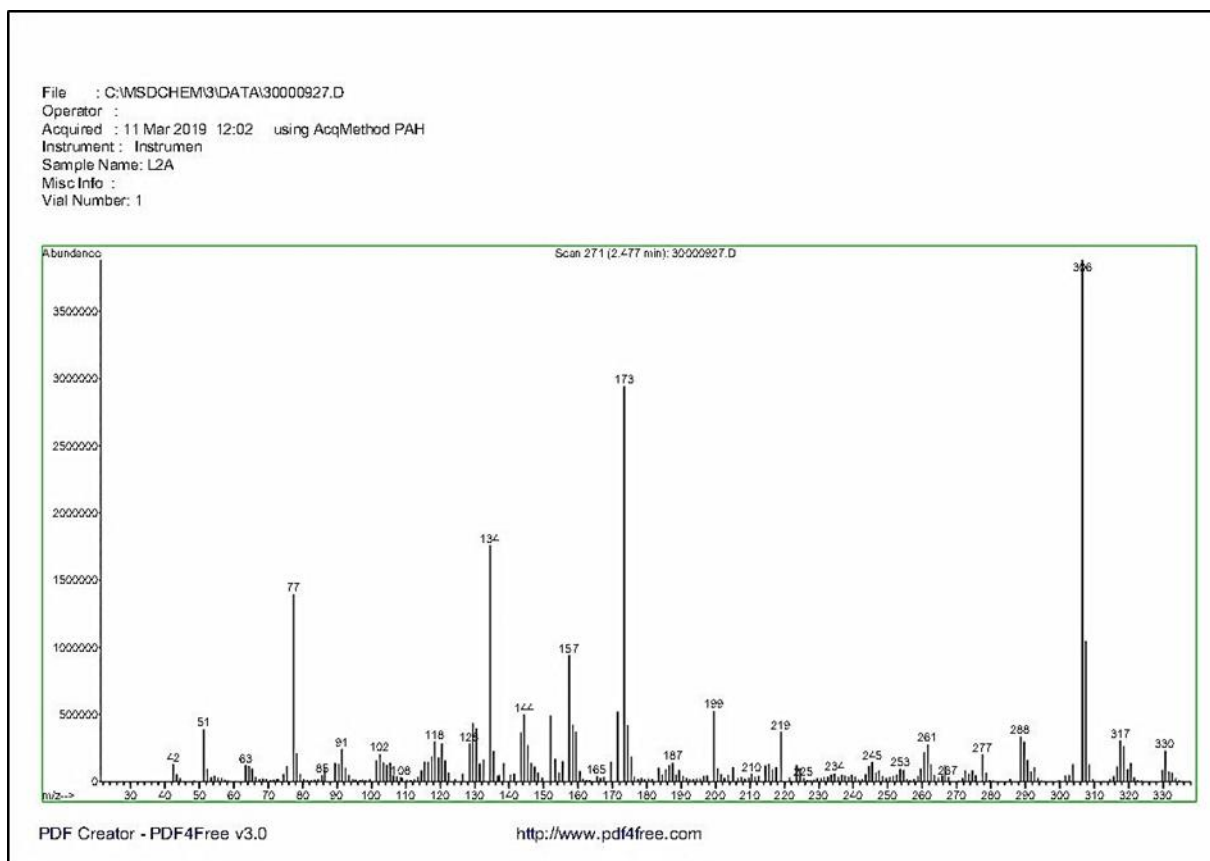
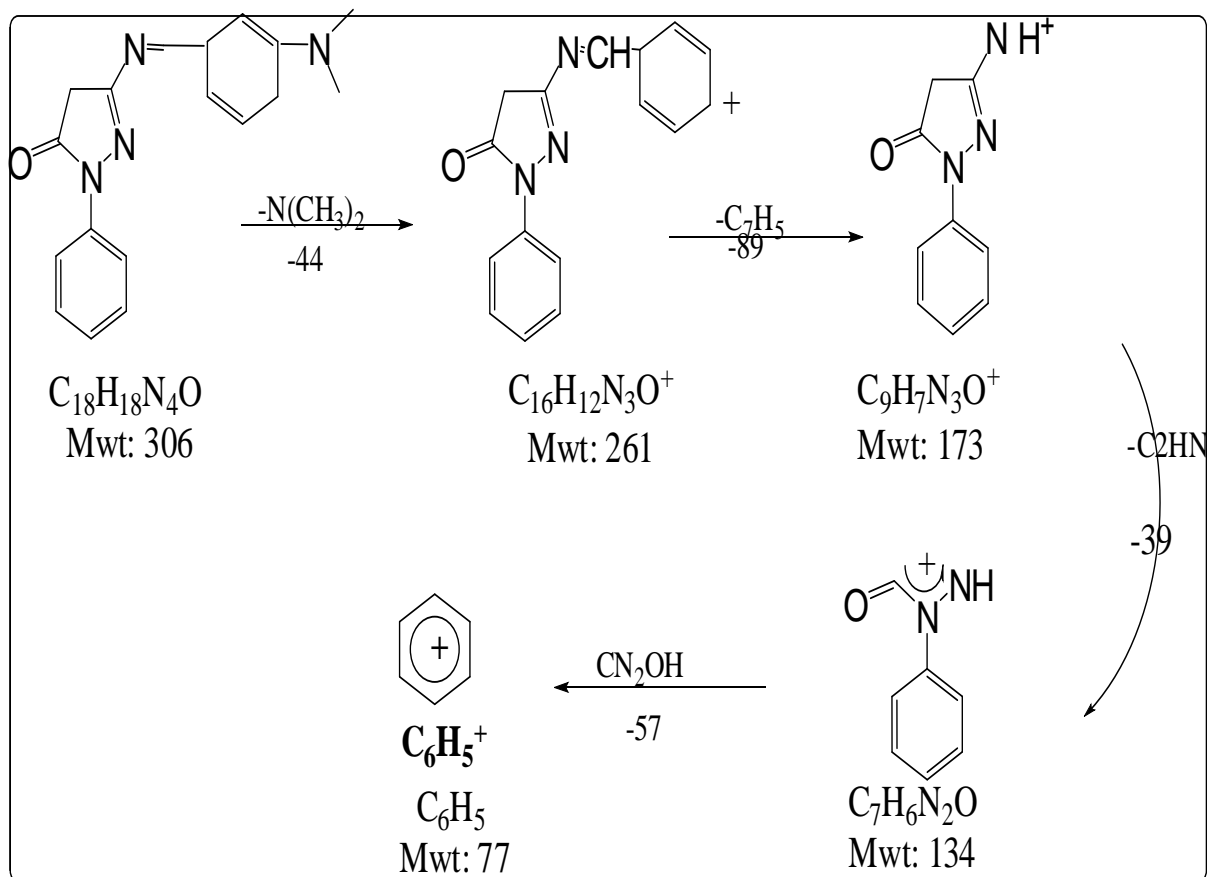


Figure (3-11): The mass spectrum of SB2



Scheme (3-2): Fragmentation pattern of the ligand SB2

### 3.2 Part two: Characterization of complexes with SB1 and SB2

The compounds were displayed in different colors and solubility was obtained in different solvents. The new prepared complexes were characterized by melting point, analysis of the elements CHNO, atomic absorption A.A, FT-IR, UV-Vis spectra, molar conductivity.

#### 3.2.1 Solubility

The solubility of prepared complexes was tested using several solvents as shown in the Table (3-8).

Table (3-8): Solubility of SB1 and SB2 Complexes

Complexes	Soluble (+)	insoluble (-)	Partially (÷)
[CoA <sub>2</sub> SB1]	DMSO, DMF	H <sub>2</sub> O, MeOH and EtOH	Acetone
[NiA <sub>2</sub> SB1]			
[CuA <sub>2</sub> SB1]			
[CdA <sub>2</sub> SB1]			
[HgA <sub>2</sub> SB1]			
[CoA <sub>2</sub> SB2]			
[NiA <sub>2</sub> SB2]			
[CuA <sub>2</sub> SB2]			
[CdA <sub>2</sub> SB2]			
[HgA <sub>2</sub> SB2]			

### 3.2.2 The Physical properties and CHNO and M for SB1 and SB2 complexes

Table (3-9) shows the physical properties and elemental microanalysis CHNO and M for the complexes SB1 and SB2.

**Table (3-9): The Physical Properties and Elemental Microanalysis for SB1 and SB2 Complexes**

The Chem. formula of complexes	m.p	Color	Theoretic ( calculated )				
			C	H	N	O	M
[CoA <sub>2</sub> SB1] C <sub>31</sub> H <sub>27</sub> CoN <sub>5</sub> O <sub>7</sub>	185- 187	Green- Bluish	58.13 (57.88)	4.25 (4.05)	10.93 (10.67)	17.49 (16.90)	9.20 (9.11)
[NiA <sub>2</sub> SB1] C <sub>31</sub> H <sub>27</sub> N <sub>5</sub> NiO <sub>7</sub>	210- 212	Dark orange	58.15 (57.78)	4.25 (4.10)	10.94 (10.91)	17.90 (16.87)	9.17 (9.11)
[CuA <sub>2</sub> SB1] C <sub>31</sub> H <sub>27</sub> CuN <sub>5</sub> O <sub>7</sub>	180- 182	Greenish yellow	57.71 (56.99)	4.22 (4.18)	10.86 (10.55)	17.36 (17.20)	9.85 (9.77)
[CdA <sub>2</sub> SB1] C <sub>31</sub> H <sub>27</sub> CdN <sub>5</sub> O <sub>7</sub>	218- 220	Light- yellow	53.65 (52.53)	3.65 (3.34)	10.09 (9.56)	16.14 (15.78)	16.20 15.83)
[HgA <sub>2</sub> SB1] C <sub>31</sub> H <sub>27</sub> HgN <sub>5</sub> O <sub>7</sub>	197- 199	dark yellow	47.60 (46.66)	3.48 (3.33)	8.95 (7.96)	14.32 13.76)	25.65 (24.23)
[CoA <sub>2</sub> SB2] C <sub>32</sub> H <sub>30</sub> CoN <sub>6</sub> O <sub>5</sub>	-185 183	Orange	60.28 (59.18)	4.74 (4.63)	13.18 (12.90)	12.55 (12.21)	9.24 (8.65)
[NiA <sub>2</sub> SB2] C <sub>32</sub> H <sub>30</sub> N <sub>6</sub> NiO <sub>5</sub>	202- 204	Dark orange	60.31 (59.87)	4.74 (4.56)	13.19 (12.95)	12.55 (12.35)	9.21 (8.89)
[CuA <sub>2</sub> SB2] C <sub>32</sub> H <sub>30</sub> CuN <sub>6</sub> O <sub>5</sub>	-244 242	Dark brown	59.85 (58.88)	44.71 (44.14)	13.09 (12.79)	12.46 (12.12)	9.90 (9.54)
[CdA <sub>2</sub> SB2] C <sub>32</sub> H <sub>30</sub> CdN <sub>6</sub> O <sub>5</sub>	-228 226	Yellow	55.62 (54.93)	4.38 (4.12)	12.16 (11.76)	11.58 (11.23)	16.27 (15.97)
[HgA <sub>2</sub> SB2] C <sub>32</sub> H <sub>30</sub> HgN <sub>6</sub> O <sub>5</sub>	-240 238	Yellow	49.32 (48.67)	3.88 (3.65)	10.79 (9.97)	10.27 (10.05)	25.74 (24.87)

### 3.2.3 Molar conductivity

The molar conductivity values of SB1 and SB2 complexes in DMSO ( $10^{-3}$ M solution) were found (19.4-12.8) and (16.6-12.9) respectively, these indicate that all complexes are non-electrolytic <sup>[86]</sup>, Table (3-10) shows molar conductivity in some general solvents and Table (3-11) shows the molar conductivity for SB1 and SB2 Complexes.

**Table (3-10): Molar Conductivity in some solvents**

	solvent	Non Electrolyte	Electrolyte Type			
			1:1	1:2	1:3	1:4
1	Water	0	120	240	360	480
2	Ethanol	0-20	35-45	70-90	≈120	≈ 160
3	Nitromethane	0-20	75-95	150-180	220-260	290-330
4	Methyl cyanide	0-30	120-160	220-300	340-420	≈ 500
5	Dimethyl formamide	0-35	65-90	130-170	200-240	≈ 300
6	Dimethyl sulfoxide	0-20	30-40	70-80	-	-



**Table (3-11): Molar conductivity for SB1 and SB2 Complexes**

Complexes	Molar Conductivity in ( $\text{Ohm}^{-1} \cdot \text{Cm}^2 \cdot \text{mol}^{-1}$ )
[CoA <sub>2</sub> SB1]	13.4
[NiA <sub>2</sub> SB1]	14.6
[CuA <sub>2</sub> SB1]	19.4
[CdA <sub>2</sub> SB1]	12.8
[HgA <sub>2</sub> SB1]	15.6
[CoA <sub>2</sub> SB2]	11.4
[NiA <sub>2</sub> SB2]	12.6
[CuA <sub>2</sub> SB2]	10.3
[CdA <sub>2</sub> SB2]	12.9
[HgA <sub>2</sub> SB2]	16.6

### 3.2.4 FT-IR spectral data for complexes

#### 3.2.4.1 FT-IR spectral for SB1 complexes

The infrared spectra of the prepared complex appeared the basic absorbance bands as compared to the (SB1) and anthranilate spectra. Table (3-11) and Figure (3-12) - (3-17) show that:

FTIR spectrum of Anthranilic acid show band of  $\nu(\text{OH})$  at  $3390 \text{ cm}^{-1}$  which was disappearance in all complexes. The band  $\nu(\text{NH}_2)$  at ( $3344$  and  $3244$ )  $\text{cm}^{-1}$  were shifted from its position compared to the spectrum of the base material. This indicates that complexes are coordinated with this group. The group of  $\nu(\text{COO})_{\text{asy}}$  and  $\nu(\text{COO})_{\text{sym}}$  appeared at ( $1679$  and  $1486$ )  $\text{cm}^{-1}$ , respectively in complexes. These band were shifted to lower frequency at rang ( $1581$ - $1523$ ) and ( $1377$ - $1315$ )  $\text{cm}^{-1}$  respectively. Therefore, the difference between  $\Delta_{(\text{ays-sym})}$  is equal to ( $216$ - $204$ )  $\text{cm}^{-1}$  which indicate that the carboxylate ion coordination with the metal ions is as mono dentate donor<sup>[78,87, 90]</sup>.

The absorption bands of the stretching vibration for imine group (C=N) of pyrazole ring and (HC=N) group have appeared in the spectrum of complexes at a lower frequency 1589-1581  $\text{cm}^{-1}$  and 1616-1612  $\text{cm}^{-1}$  compared to the free ligand spectrum at (1597 and 1627)  $\text{cm}^{-1}$  respectively. This change in the form and location of the band is an evidence of the coordination between the nitrogen atom in this groups and the metal ion <sup>[75, 88]</sup>.

The IR spectra for complexes showed the new absorption bands that proved the coordination of the ligand with the central metal ion through nitrogen atoms of azomethine and imine groups at (505-520)  $\text{cm}^{-1}$  and (516-582)  $\text{cm}^{-1}$  could be referred to  $(\text{M-N})_{\text{sch., pyr.}}$  and  $(\text{M-N})_{\text{A}}$  respectively. The spectra appeared absorption band within the range (408-439)  $\text{cm}^{-1}$  were due to correlation the metal ion with oxygen atom in anthranilate  $(\text{M-O})_{\text{A}}$  <sup>[76,78,91]</sup>.

Table (3-12): The FTIR Spectra for the SB1 Complexes

Compound	$\nu(\text{OH})_{\text{SB}}$ $\nu(\text{NH}_2_{\text{asy\&sym}}) \text{ A}$	$\nu(\text{CHarom.})$	CO ring	$\nu(\text{COO})_{\text{asy\&sym}}$	$\Delta_{\text{asy-sym}}$	$\nu(\text{HCN})_{\text{SB}}$	$\nu(\text{CN})_{\text{py}}$	$\nu(\text{MN})_{\text{SB.}}$ $\nu(\text{MN}) \text{ A.}$	$\nu(\text{MO})$
SB1	3456 ----	3078	1693	----	----	1627	1597	----	----
Anth	3390 3344- 3244	2586	----	1679 1486	193	-----	-----	----	----
[CoA <sub>2</sub> SB1]	3305 3244	3140	1695	1543 1327	216	1612	1585	505 559	439
[NiA <sub>2</sub> SB1]	3437 3305	3124	1692	1543 1327	216	1612	1581	520 532	420
[CuA <sub>2</sub> SB1]	3444 3275	3124	1696	1581 1377	204	1612	1581	505 516	428
[CdA <sub>2</sub> SB1]	3417 3294	3035	1695	1539 1337	212	1616	1589	516 582	408
[HgA <sub>2</sub> SB1]	3336 3325	3182	1694	1523 1315	208	1612	1581	509 520	432

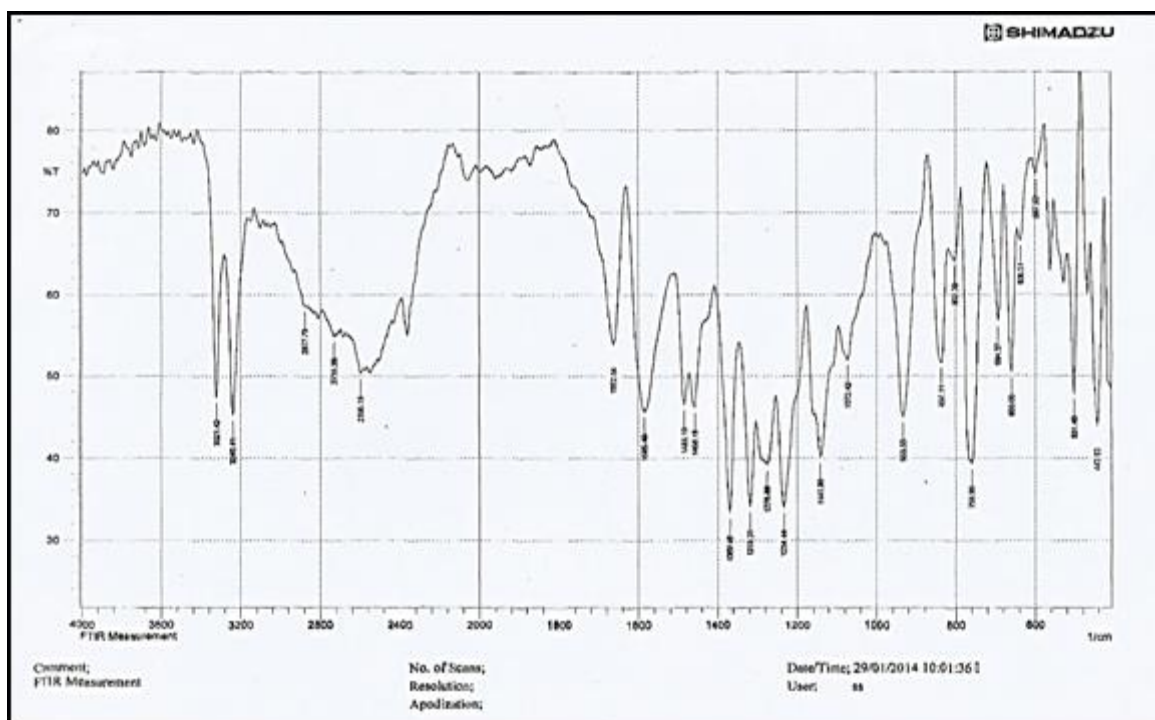


Figure (3-12): FTIR spectrum of (Anthranilic acid)

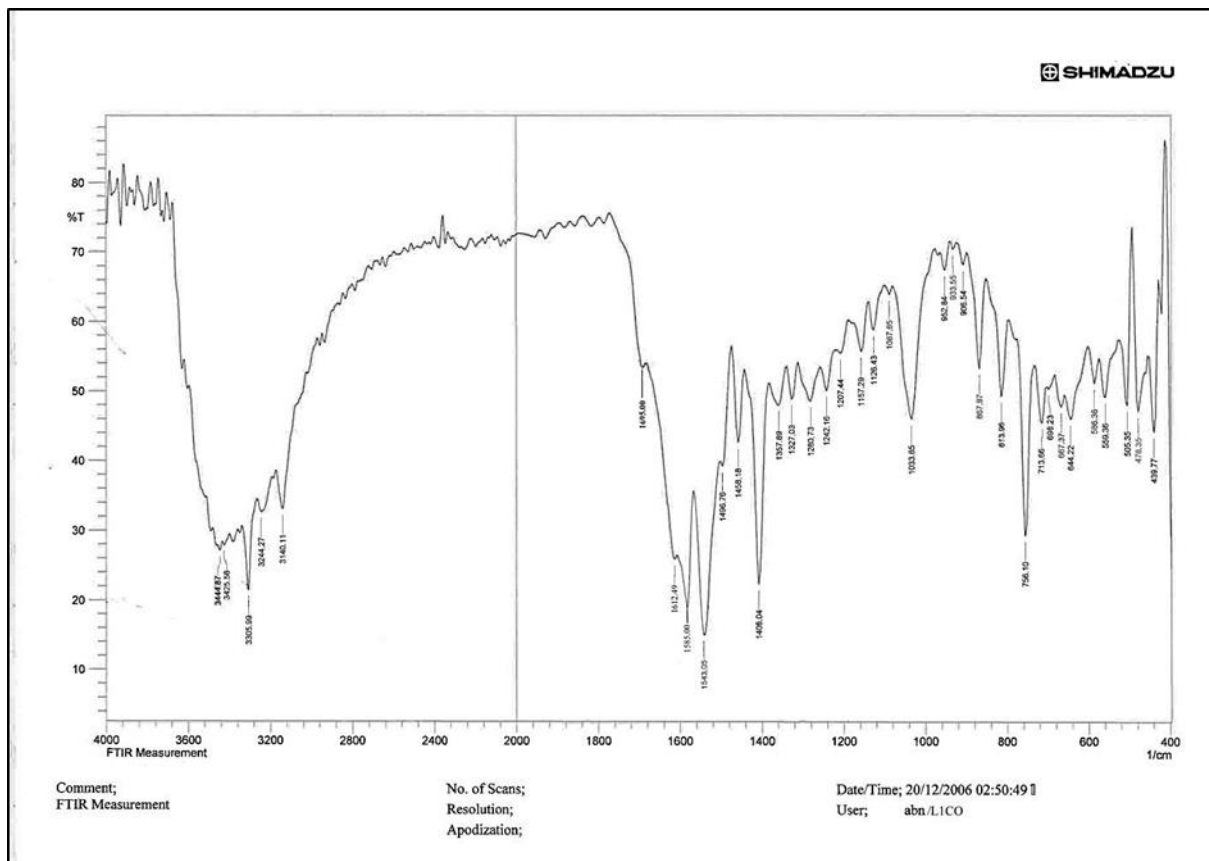


Figure (3-13): FTIR spectrum of [CoA2SB1]

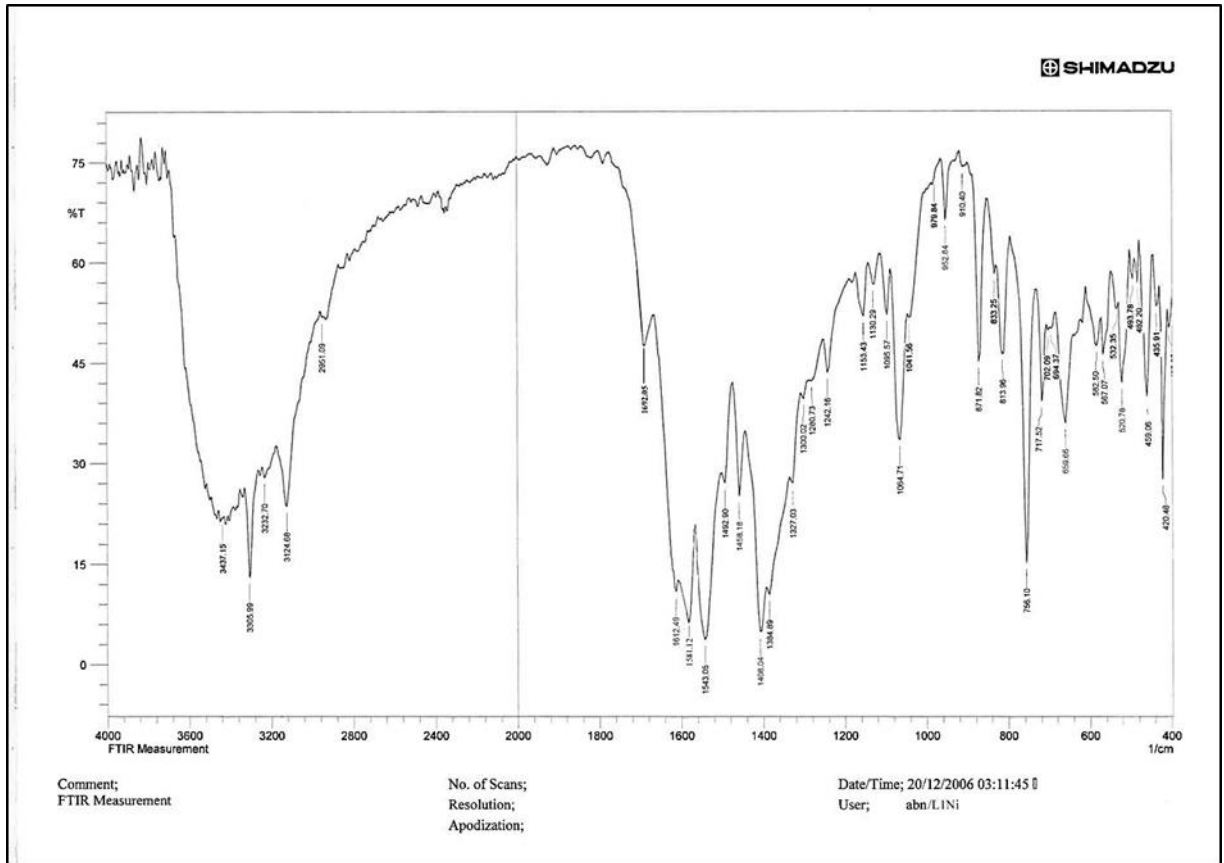


Figure (3-14): FTIR spectrum of [NiA2SB1]

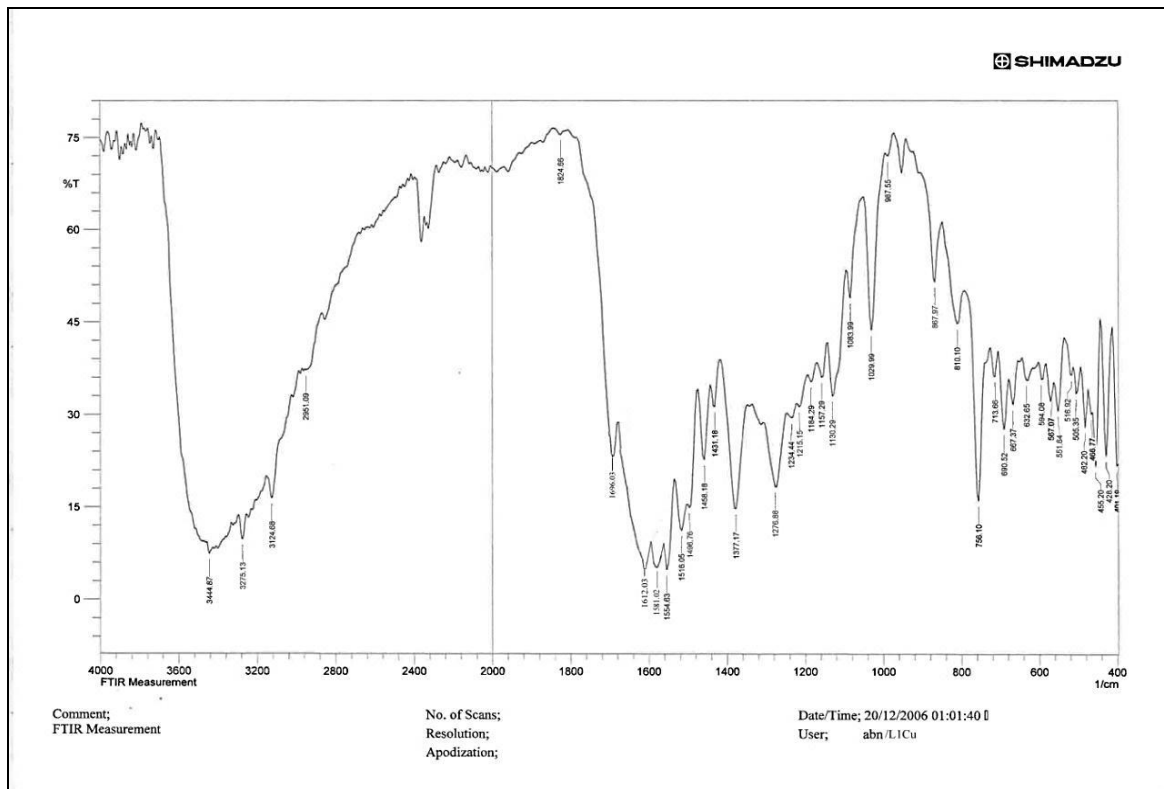


Figure (3-15): FTIR spectrum of [CuA2SB1]

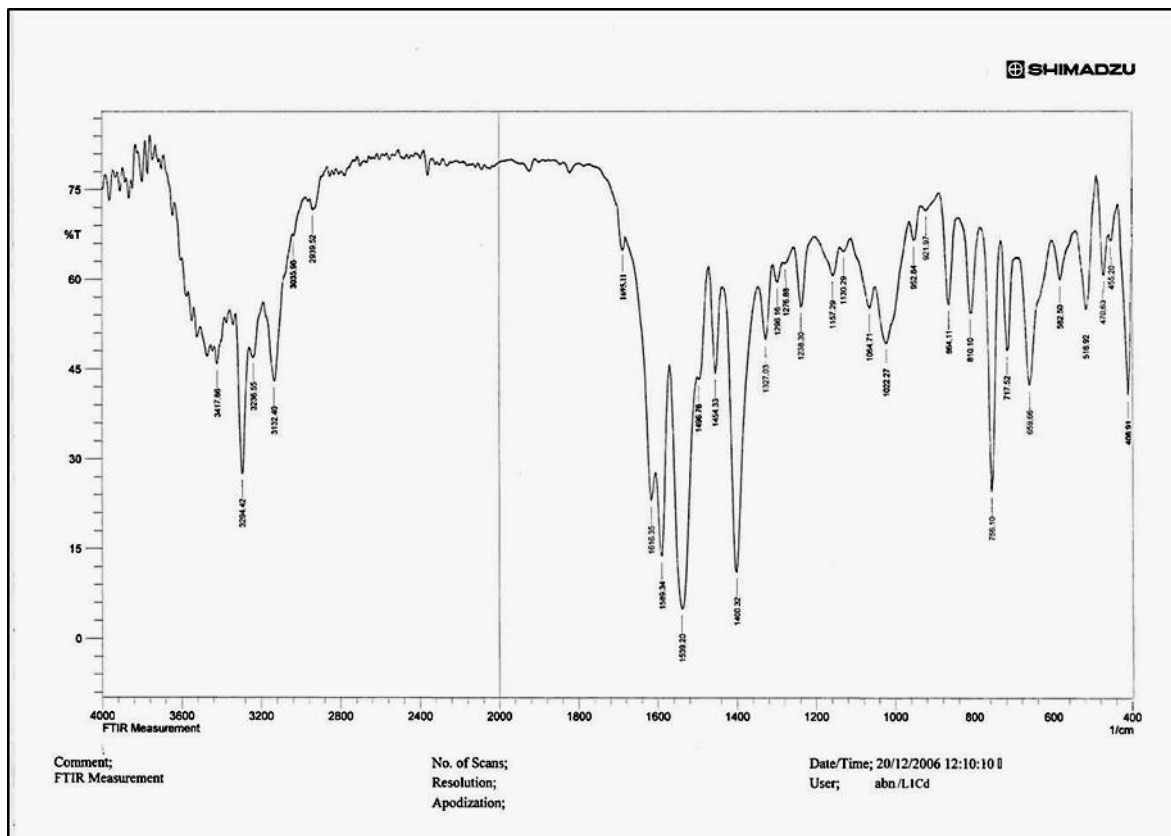


Figure (3-16): FTIR spectrum of [CdA2SB1]

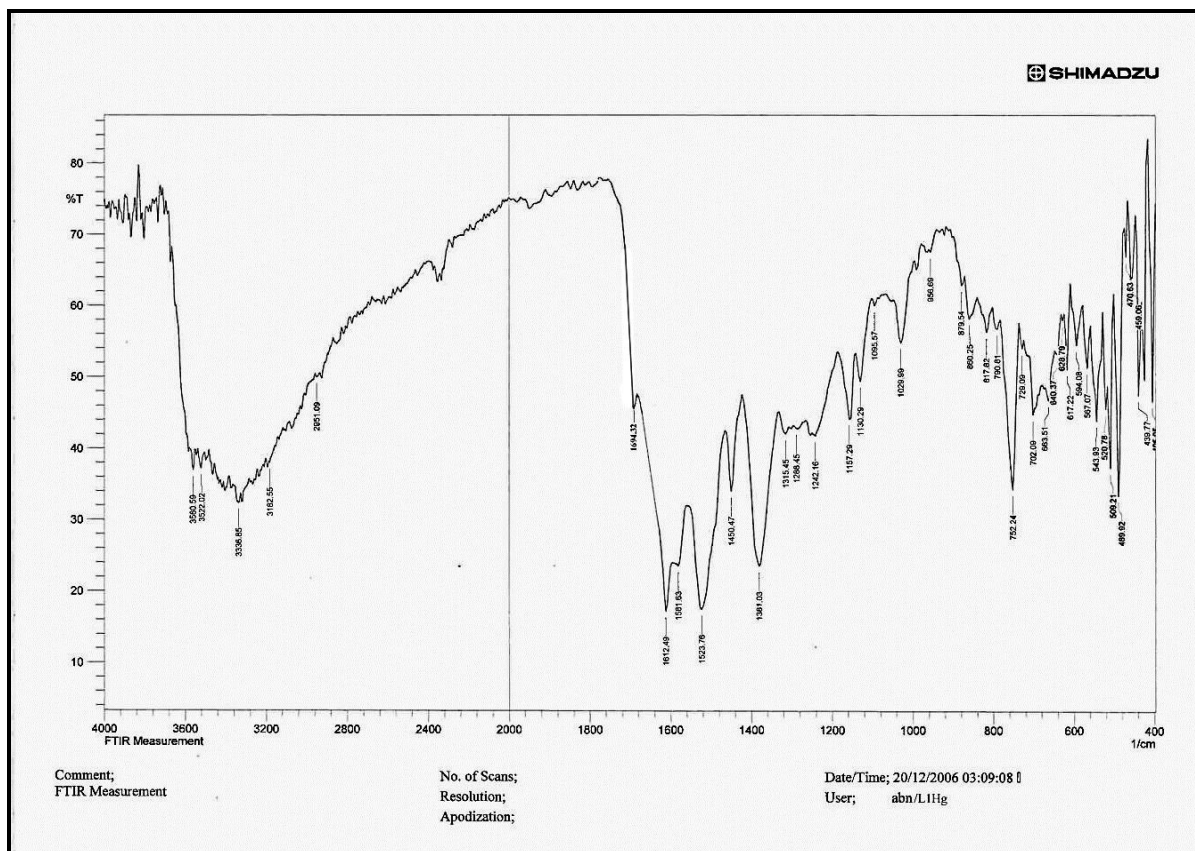


Figure (3-17): FTIR spectrum of [HgA2SB1]

### 3.2.4.2 FT-IR Spectral Data for SB2 Complexes

The spectrum FTIR for all complexes tested in Table (3-12) and Figure (3-18) to (3-22), the broad band of hydroxyl group for (A) was disappeared in complexes, bands at range  $(3410-3448)\text{cm}^{-1}$  and  $(3275-3321)\text{cm}^{-1}$  which due to  $\nu(\text{NH}_2_{\text{asy. \& sym}})$  stretching vibration for (A) respectively. This indicates that the metal ions are connected with N atom of this group<sup>[78,89]</sup>.

Bands of the stretching vibration for imine (Schiff base and pyrazole ring), have become clear in the complexes at a lower frequency at  $(1612-1620)\text{cm}^{-1}$  and higher frequency at  $(1581-1604)\text{cm}^{-1}$  comparing with the free ligand spectrum at  $1643$  and  $1627\text{cm}^{-1}$  respectively, these shifting indicates the correlation between the metal ions from these groups, the bands at  $(3032-3140)\text{cm}^{-1}$  in complexes referred to  $\nu(\text{C-H})$  aromatic<sup>[77,90]</sup>.

The carboxylic group for (A) asymmetric and symmetric in complexes shifted to lower frequencies at  $(1527-1554)\text{cm}^{-1}$   $(1310-1327)\text{cm}^{-1}$ . Therefore, the  $\Delta$  between them in  $\text{Co}^{+2}$ ,  $\text{Ni}^{+2}$ ,  $\text{Cu}^{+2}$ ,  $\text{Cd}^{+2}$  and  $\text{Hg}^{+2}$  complexes are  $(212, 223, 227, 208, 217)\text{cm}^{-1}$  respectively, which reference that the carboxylate ion coordinate with the  $(\text{M}^{+2})$  from one-sided<sup>[78]</sup>.

In the complexes appeared a new absorption band at  $(551-578)\text{cm}^{-1}$  and  $(509-536)\text{cm}^{-1}$  due to nitrogen atom for Schiff and pyrazole ring coordinated with metal ions, and appeared band  $(\text{M-O})$  at range  $(447-478)\text{cm}^{-1}$  were due to linked metal ions with oxygen from carboxylic group<sup>[91]</sup>.

The absorption bands of the prepared complexes which are ranged between  $(1697-1696)\text{cm}^{-1}$  were referred to CO pyrazole ring.

Table (3-13): The FTIR Spectra for the SB2 Complexes

Compound	(OH) <sub>A</sub>	(NH <sub>2</sub> <sub>asy&amp;sym</sub> ) <sub>A</sub>	(C-H <sub>arom.</sub> )	CO( ketone ring)	(COO) <sub>asy&amp;sym</sub>	Δ <sub>asy-sym</sub>	(HCN) <sub>schif</sub>	(CN) <sub>py</sub>	(MN) Sch. ν(MN) <sub>A</sub>	(MO)
SB2	----	----	3062	1701	---	----	1643	1527	----	----
Anth	3390	3321 3210	2586	---	1679 1486	193	-----	-----	----	----
[CoA <sub>2</sub> SB2]	---	3429 3305	3140	1695	1539 1327	212	1616	1593	551 513	455
[NiA <sub>2</sub> SB2]	----	3410 3305	3124	1695	1543 1320	223	1612	1593	574 536	478
[CuA <sub>2</sub> SB2]	----	3448 3275	3124	1697	1554 1327	227	1620	1604	578 516	447
[CdA <sub>2</sub> SB2]	-----	3421 3290	3032	1696	1535 1327	208	1616	1589	559 509	474
[HgA <sub>2</sub> SB2]	-----	3421 3321	3062	1697	1527 1310	217	1612	1581	563 532	459



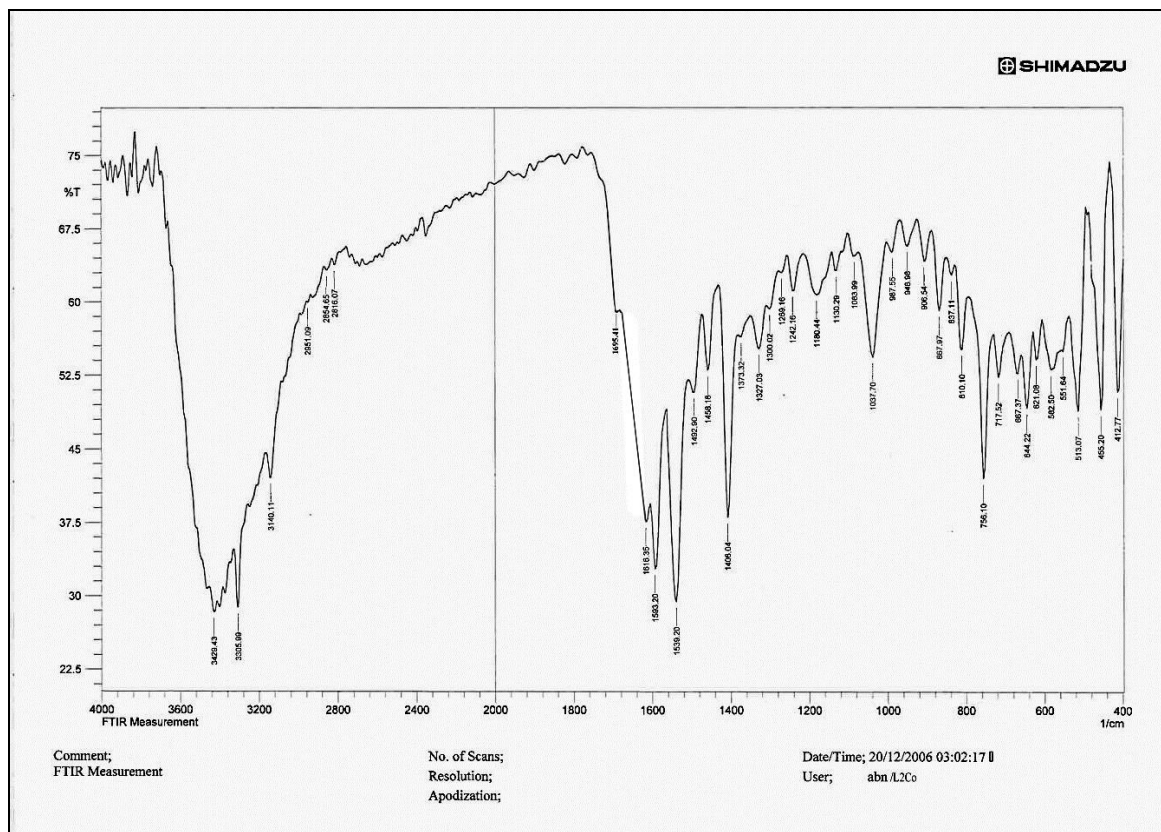


Figure (3-18): FTIR spectrum of [CoA2SB2]

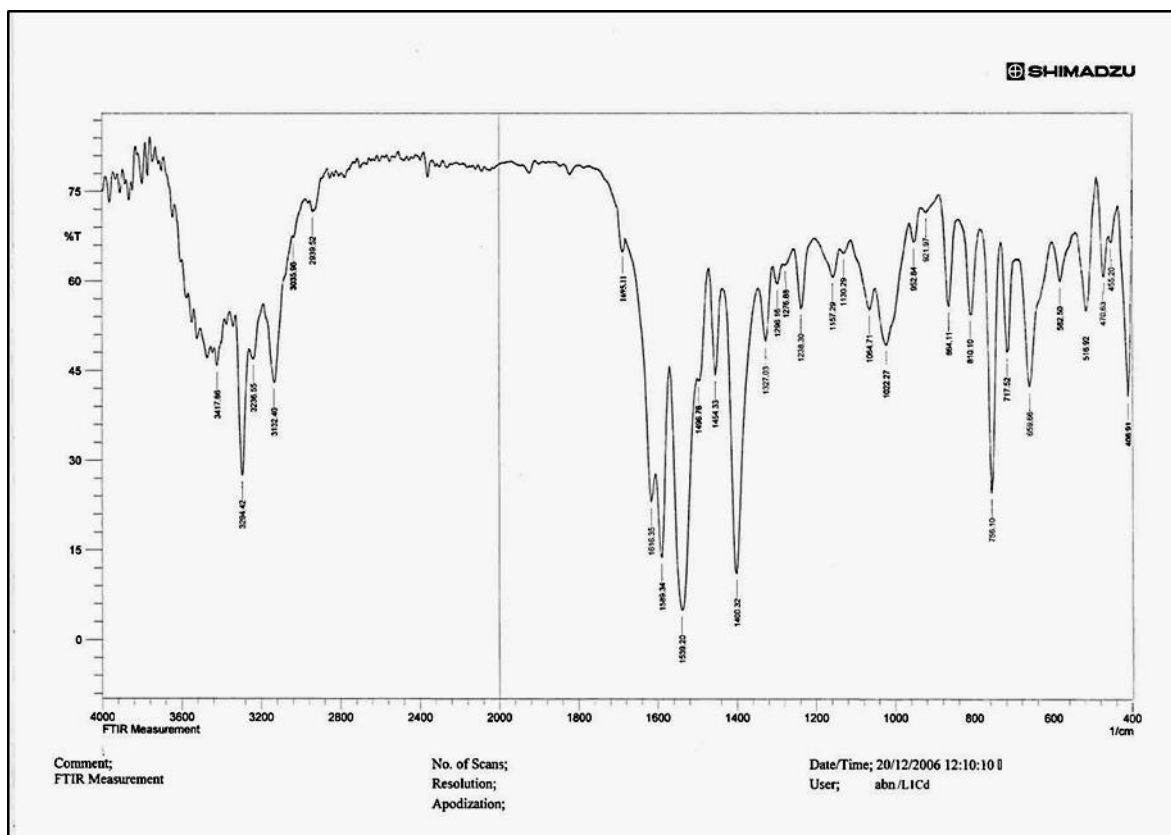


Figure (3-19): FTIR spectrum of [NiA2SB2]

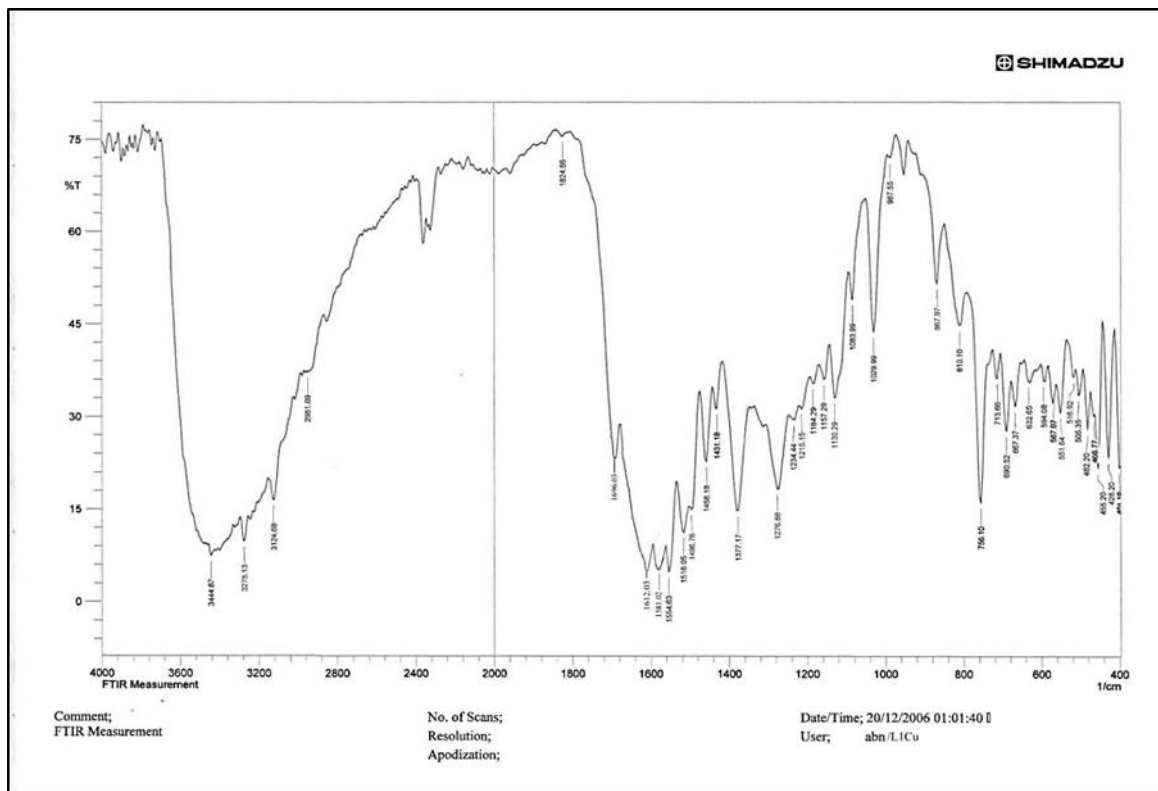


Figure (3-20): FT-IR Spectrum of [CuA2SB2]

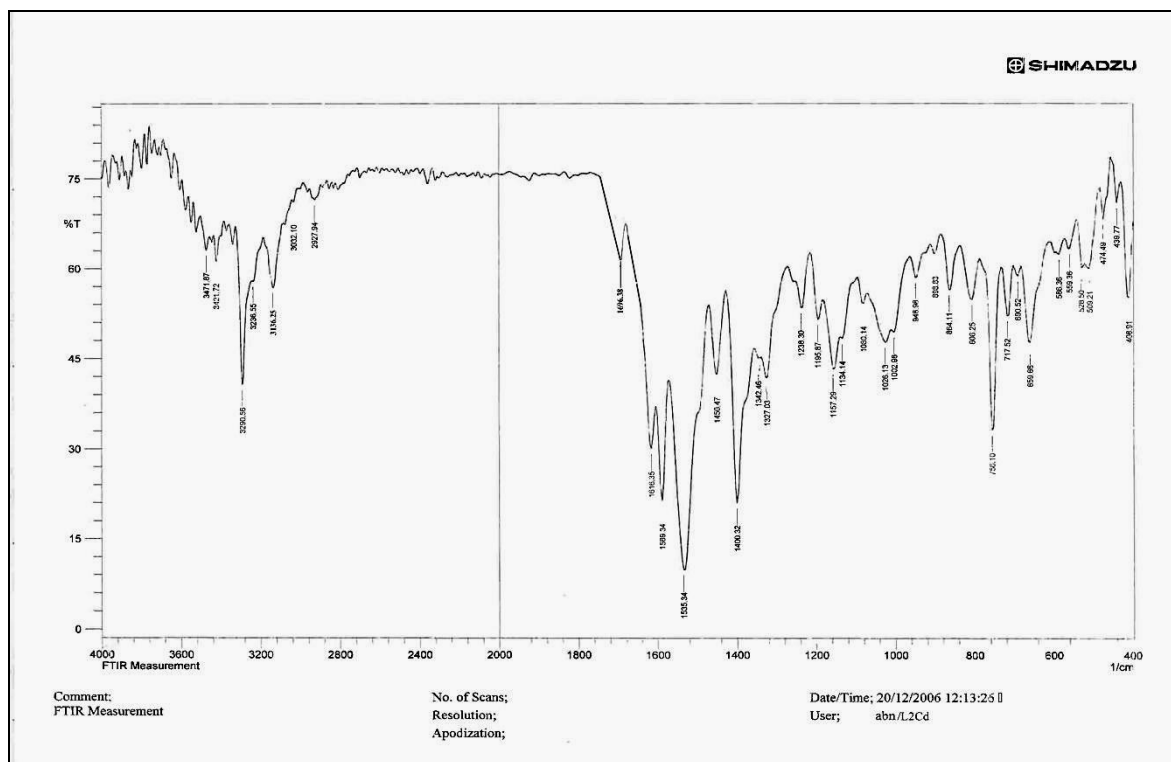


Figure (3-21): FTIR spectrum of [CdA2SB2]

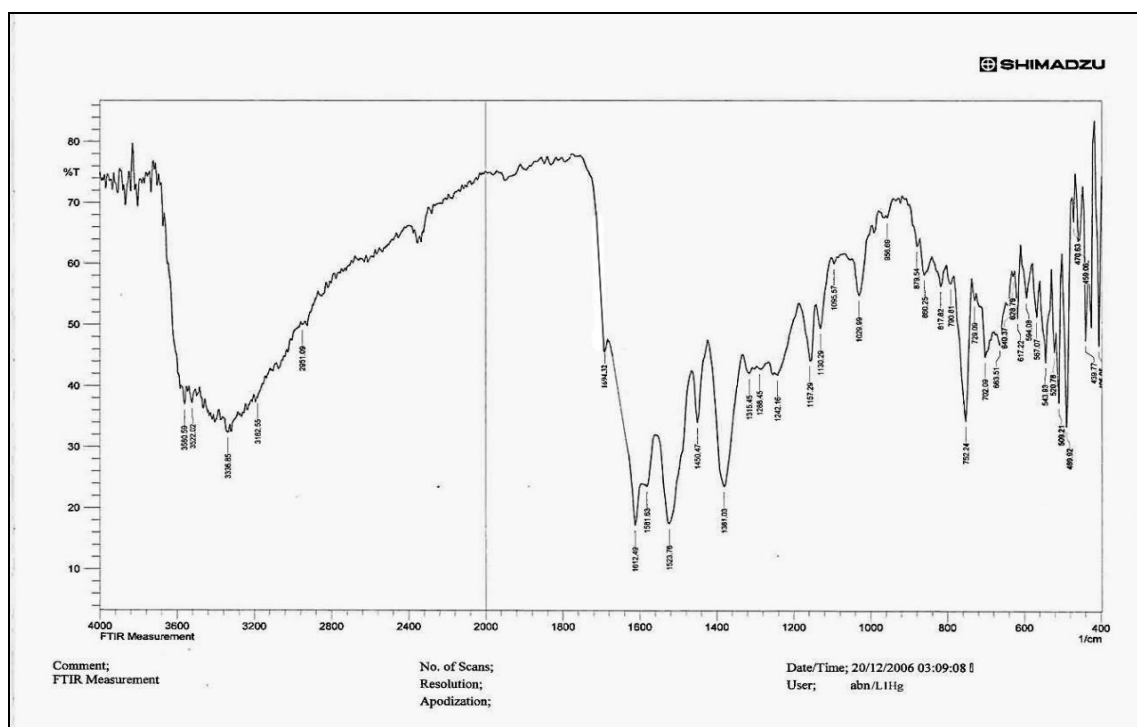


Figure (3-22): FTIR spectrum of [HgA<sub>2</sub>SB<sub>2</sub>]

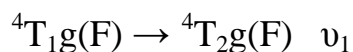
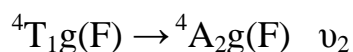
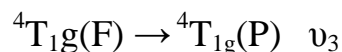
### 3.2.5 Electronic spectra

#### 3.2.5.1 Electronic spectra of SB1 complexes

All electronic transitions of the five complexes are listed in the Table (3-13)

#### 3.2.5.2 CoA<sub>2</sub>SB1 Complex

[CoA<sub>2</sub>SB1] complex displayed six absorption peaks. The two absorption peaks at 277 and 397 nm are assigned to intra ligand and charge transfer. The new absorption peaks at 500, (652,709) and 813nm were due to:



These peaks are characteristic in location with that mention for octahedral Co<sup>+2</sup> complexes, Fig. (3-23)<sup>[92-93]</sup>.

### 3.2.5.3 NiA<sub>2</sub>SB1 Complex

[NiA<sub>2</sub>SB1] complex showed six absorption peaks, the three absorption peaks at 275, 350 and 394 nm are due to intra ligand and C.T when compare with the SB1. The peaks with weak intensity 489 nm, (777, 826) nm and 958nm are due to (d-d) electronic transition type  $^3A_{2g}(F) \rightarrow ^3T_{1g}(p)$ ,  $^3T_{1g}(F)$  and  $^3T_{2g}(F)$  respectively. These peaks environment were quite close to an octahedral one Figure (3-24) <sup>[94,95]</sup>.

### 3.2.5.4 CuA<sub>2</sub>SB1 Complex

[CuA<sub>2</sub>SB1] complex showed absorption peaks, the high peaks at (275, 314 and 345) nm are due to intra (SB1) ligand. The peak at (423 nm) is assigned to charge transfer. Weak intensity at 693 nm is due to (d-d) electronic transition type  $^2E_g$  to  $^2T_{2g}$ . These values environment were quite close to a distorted octahedral Figure (3-25) <sup>[96,97]</sup>.

### 3.2.5.5 CdA<sub>2</sub>SB1 Complex

[CdA<sub>2</sub>SB1] complex showed four absorption peaks, the two absorption peak at (264 and 342 nm) are assigned to intra ligand comparably with the spectrum of SB1 and the peak at (450 nm) is due to charge transfer (C.T). These peaks environment were very close to a distorted octahedral Figure (3-26) <sup>[98]</sup>.

### 3.2.5.6 HgA<sub>2</sub>SB1 complex

[HgA<sub>2</sub>SB1] complex appeared four absorption peaks, the two peaks at (272,332,346 and 395 nm) are assigned to intra ligand in comparison with the spectrum of (SB1) and the absorption peak at 463 nm is attributed to charge transfer (C.T) Figure (3-27). The bands are congruence in the location with the researches for octahedral Hg (II) <sup>[99]</sup>.

Table (3-14): Electronic spectral data of SB1 complexes

Compound	$\lambda$ nm ( $\text{cm}^{-1}$ )	Type of transitions
SB1	289(34602) 390(25641)	$\pi \rightarrow \pi^*$ $n \rightarrow \pi^*$
[Co A2SB1]	277(36101) 397(25188) 500(20000) 652,709(15337,14104) 813(12300)	Intra ligand C.T. ${}^4T_{1g}(F) \rightarrow {}^4T_{1g}(P)$ ( $\nu_3$ ) ${}^4T_{1g}(F) \rightarrow {}^4A_{2g}(F)$ ( $\nu_2$ ) ${}^4T_{1g}(F) \rightarrow {}^4T_{2g}(F)$ ( $\nu_1$ )
[Ni A2SB1]	275(36363) 350(28571) 394(25380) 489(20449) 777,826(12870,12106) 958(10438)	Intra ligand Intra ligand C.T. ${}^3A_{2g}(F) \rightarrow {}^3T_{1g}(P)$ ( $\nu_3$ ) ${}^3A_{2g}(F) \rightarrow {}^3T_{1g}(F)$ ( $\nu_2$ ) ${}^3A_{2g}(F) \rightarrow {}^3T_{2g}(F)$ ( $\nu_1$ )
[Cu A2SB1]	275,314(36363,31847) 345(28985) 423(23640) 693(14430)	Intra ligand Intra ligand C.T. ${}^2E_g \rightarrow {}^2T_{2g}$
[Cd A2SB1]	264(37735) 342 (30769) 450(22222)	Intra ligand Intra ligand C.T.
[Hg A2SB1]	272,332(36764,30120) 346,395(28901,25316) 463(21598)	Intra ligand Intra ligand C.T.

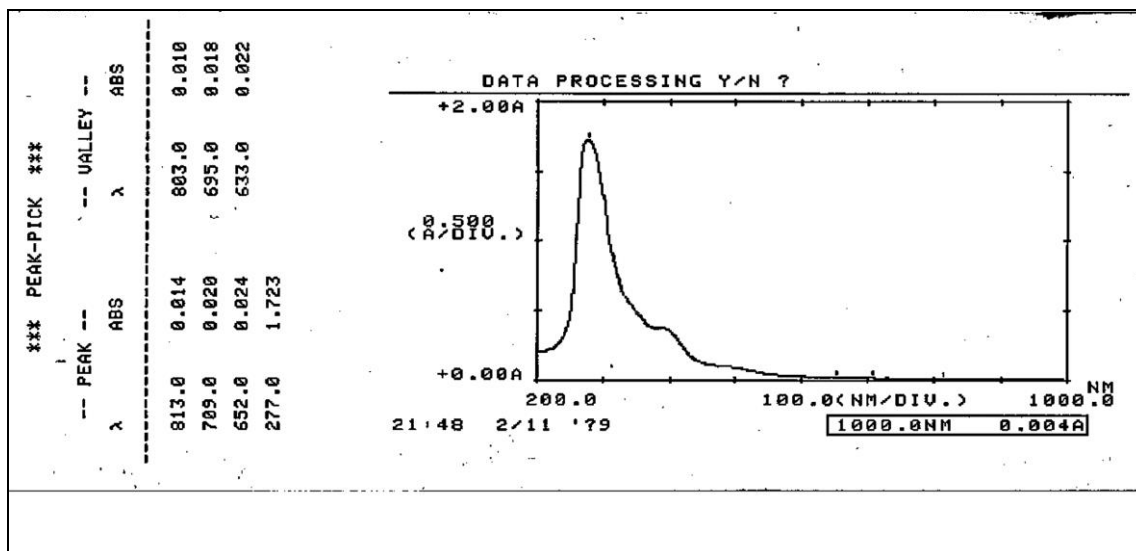


Figure (3-23): Electronic spectrum of [CoA<sub>2</sub>SB1] complex

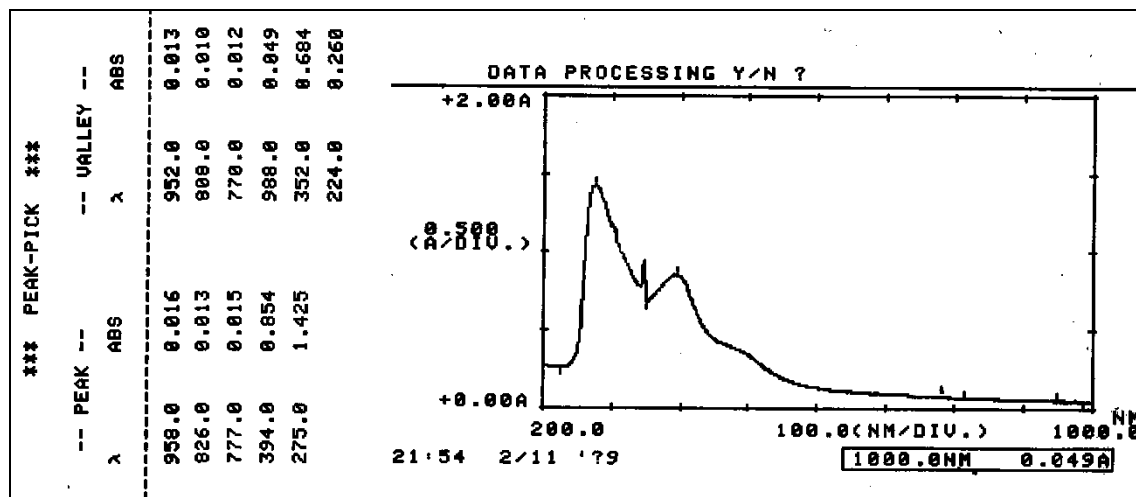


Figure (3-24): Electronic spectrum of [NiA<sub>2</sub>SB1] complex

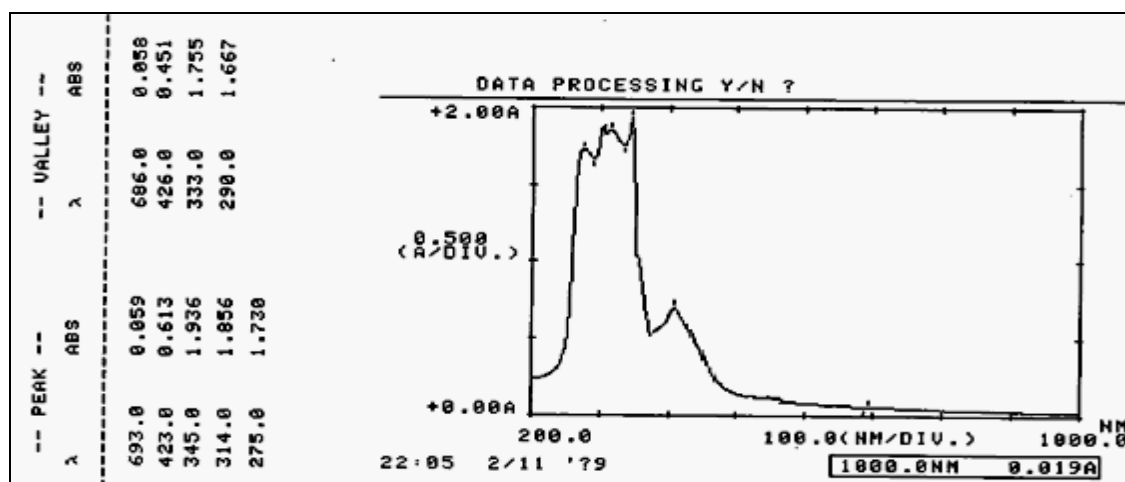
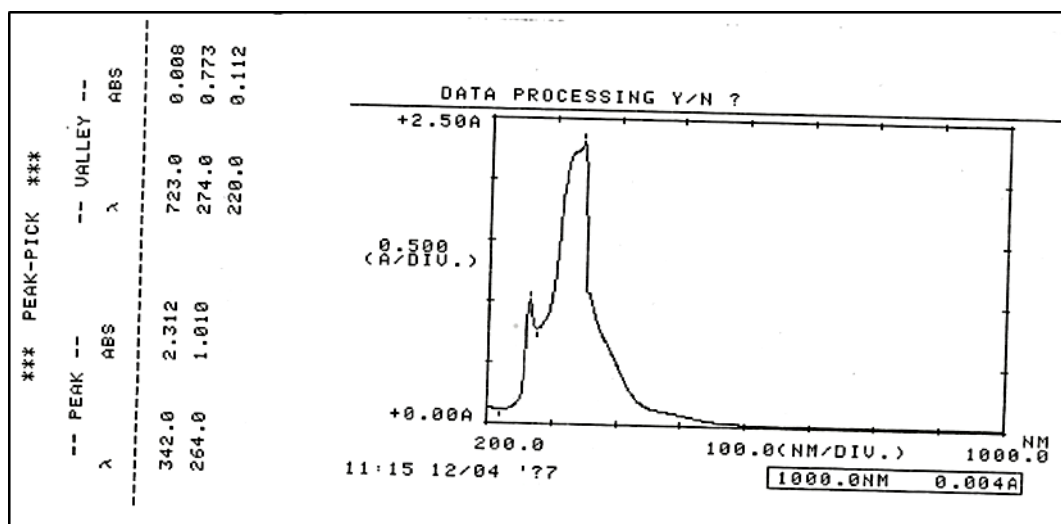
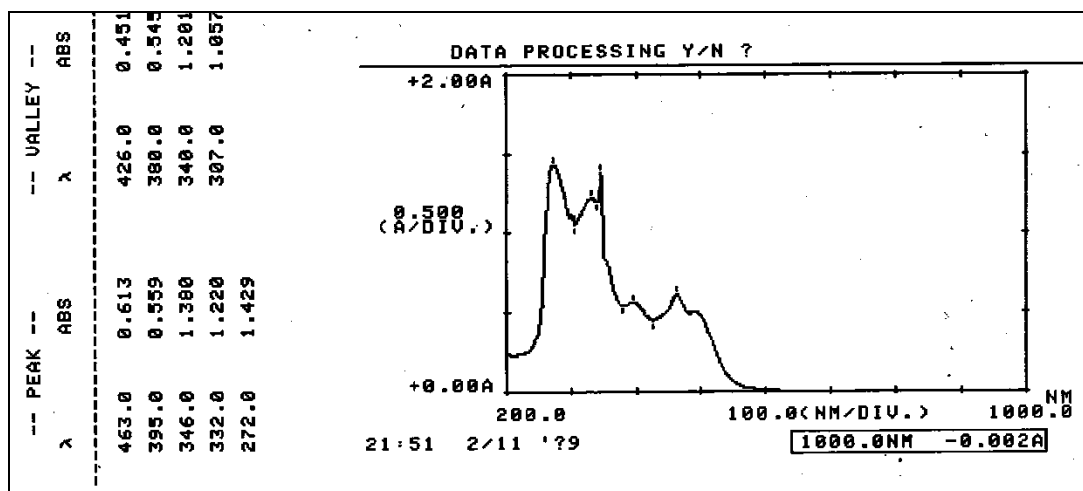


Figure (3-25): Electronic spectrum of [CuA<sub>2</sub>SB1] complex

Figure (3-26): Electronic spectrum of [CdA<sub>2</sub>SB1] complexFigure (3-27): Electronic spectrum of [HgA<sub>2</sub>SB1] complex

### 3.2.6 Electronic spectra for SB2 Complexes

All electronic transitions of the five complexes are listed in the Table (3-14)

#### 3.2.6.1 CoA<sub>2</sub>SB2 Complex

CoA<sub>2</sub>SB2 complex displayed five absorption peaks, the absorption peaks at (271 and 348) nm is due to intra ligand comparably with the spectrum of SB2. The peak at 448nm is due to charge transfer. Two absorption peaks at 695 nm and 823nm are due to d-d transition type as  ${}^4T_{1g}(F)$  into  ${}^4A_{2g}(F)$  and  ${}^4T_{2g}(F)$

respectively Fig. (3-28). These peaks are characteristic in the location with the reported for octahedral cobalt complexes [92-93].

### 3.2.6.2 NiA<sub>2</sub>SB2 Complex

NiA<sub>2</sub>SB2 complex shown six absorption peaks, the two absorption peaks at (272,346 and 448) nm are assigned to intra ligand and charge transfer and <sup>3</sup>A<sub>2g</sub>(F) to <sup>3</sup>T<sub>1g</sub>(P) third transition. New three absorption peaks with weak intensity at (778 and 950 nm) are due to <sup>3</sup>A<sub>2g</sub>(F) to <sup>3</sup>T<sub>1g</sub>(F) second transition and <sup>3</sup>A<sub>2g</sub>(F) into <sup>3</sup>T<sub>2g</sub>(F) transition, Fig. (3-29) these peaks are characteristic in the location with the reported for octahedral Ni complexes [94].

### 3.2.6.3 CuA<sub>2</sub>SB2 Complex

CuA<sub>2</sub>SB2 complex displayed four absorption peaks Fig. (3-30), the two absorption peaks at (269 and 346 nm) are assigned to intra ligand comparably with the spectrum of SB2, and the peak at (449 nm) is due to charge transfer. The new peak at 658 nm is due to d-d electronic transition type <sup>2</sup>E<sub>g</sub> to <sup>2</sup>T<sub>2g</sub>. These peaks are harmony in the location with the researches of octahedral Cu (II) [95-98].

### 3.2.6.4 CdA<sub>2</sub>SB2 Complex

CdA<sub>2</sub>SB2 complex shown three absorption peaks, the two absorption peak at 262 and 342 nm is assigned to intra ligand comparably with the spectrum of SB2 and the peak at 400nm is due to (charge transfer) Fig.(3-31). These peaks are compatibility in the position with the researches for octahedral Cd (II) [98].

### 3.2.6.5 HgA<sub>2</sub>SB2 Complex

HgA<sub>2</sub>SB2 complex appeared three absorption peaks, the peaks at (282 and 344) nm are assigned to intra ligand in comparison with the spectrum of SB2 and the absorption peak at 420 nm is attributed to (charge transfer C-T)



Fig. (3-32), these bands are congruence in the location with the researches for octahedral Hg (II) [99].

**Table (3-15): Electronic spectral data of SB2 complexes**

Compound	$\lambda$ nm ( $\text{cm}^{-1}$ )	Type of transitions
SB2	271(35211) 399(25575)	$\pi \rightarrow \pi^*$ $n \rightarrow \pi^*$
[Co A2SB2]	271(36900) 348(28735) 448(22321) 695(14388) 823(12150)	Intra ligand Intra ligand C.T. ${}^4T_{1g}(F) \rightarrow {}^4A_{2g}(F) \nu_2$ ${}^4T_{1g}(F) \rightarrow {}^4T_{2g}(F) \nu_1$
[Ni A2SB2]	272 (36764) 346 (28571) 448 (22321) 778 (12853) 950 (10526)	Intra ligand Intra ligand C.T + ${}^3A_{2g} \rightarrow {}^3T_{1g}(P) (\nu_3)$ ${}^3A_{2g}(F) \rightarrow {}^3T_{1g}(F) \nu_2$ ${}^3A_{2g}(F) \rightarrow {}^3T_{2g}(F) \nu_1$
[Cu A2SB2]	269(37174) 346(28901) 449(22271) 658(15197)	Intra ligand Intra ligand C-T ${}^2E_g \rightarrow {}^2T_{2g}$
[Cd A2SB2]	262(38167) 342 (23809) 400(25000)	Intra ligand Intra ligand C-T
[Hg A2SB2]	282,344(35461,34722) 420(23809)	Intra ligand CT

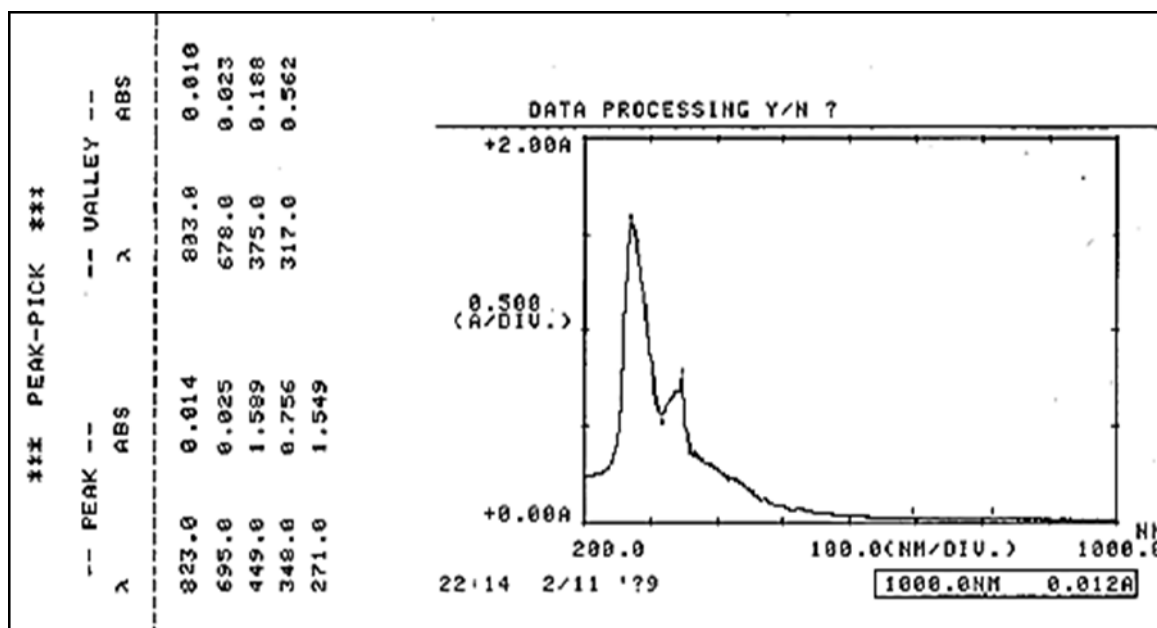


Figure (3-28): Electronic spectrum of [CoA<sub>2</sub>SB<sub>2</sub>] complex

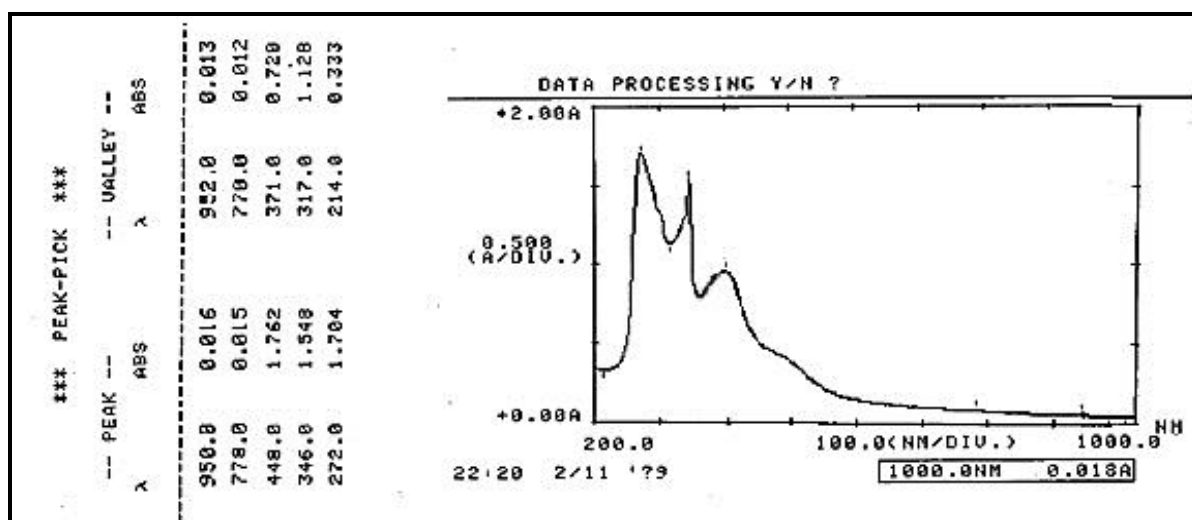


Figure (3-29): Electronic spectrum of [NiA<sub>2</sub>SB<sub>2</sub>] complex

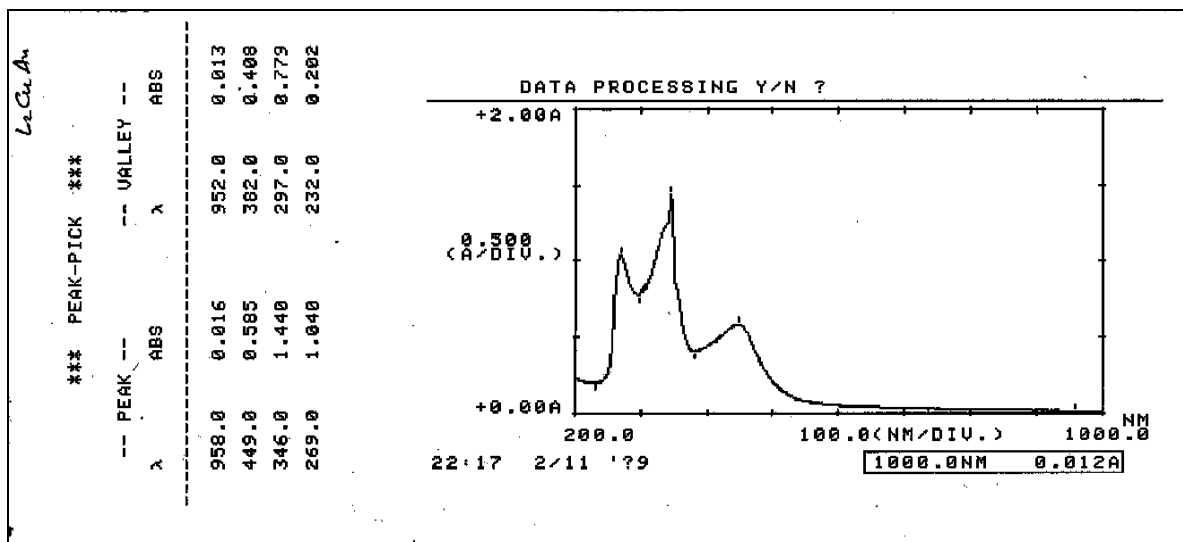


Figure (3-30): Electronic spectrum of [Cu<sub>2</sub>SB<sub>2</sub>] complex

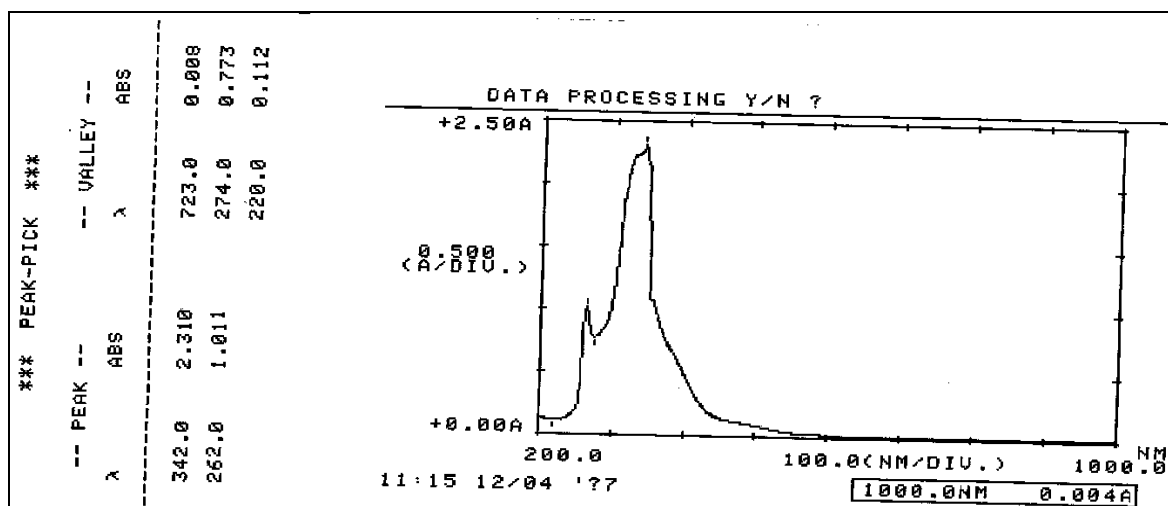


Figure (3-31): Electronic spectrum of [CdA<sub>2</sub>SB<sub>2</sub>] complex

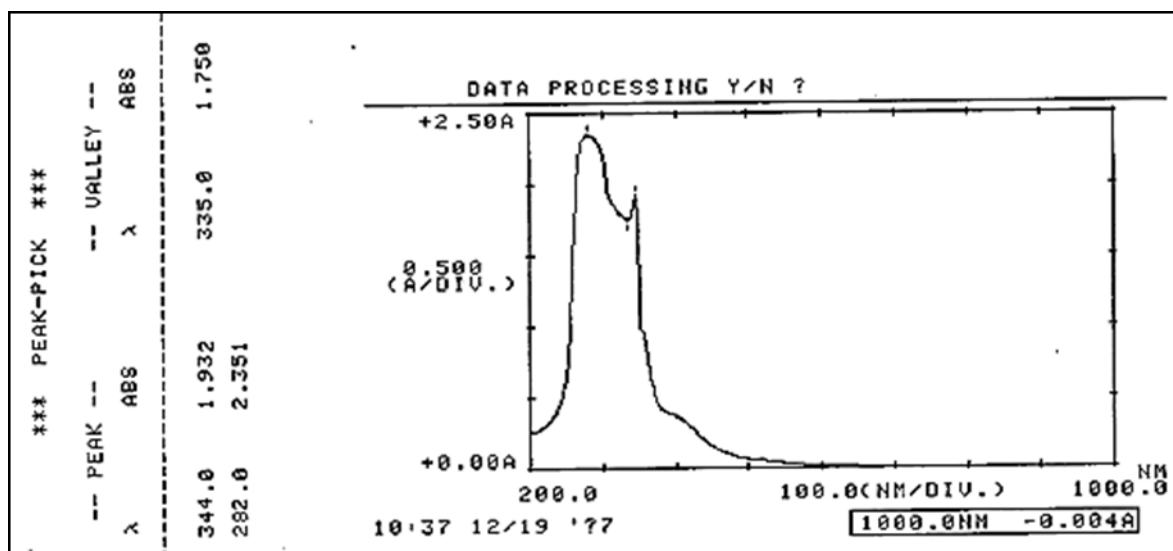


Figure (3-32): Electronic spectrum of [HgA<sub>2</sub>SB<sub>2</sub>] complex

### 3.3 Magnetic susceptibility of SB1 and SB2 complexes

Magnetic measurements were used to diagnose and study the complexes of transitional elements in 298 °C after the correction of the presence of diamagnetism has been used. Tables for the values of magnetic sensitivity of atoms in organic molecules (Pascal constants) and metal ions <sup>[100,101]</sup>. The magnetic momentum is calculated according to the following equations were used in Table (3-15).

$$X_M = X_g \cdot M \text{ wt.}$$

$$X_A = X_M - (-D)$$

$$\mu_{\text{eff.}} = 2.828 \sqrt{X_A} \cdot T$$

Where:  $\mu_{\text{eff.}}$  = effective magnetic moment  $X_M$  = molar magnetic susceptibility

$X_A$  = atomic susceptibility  $X_g$  = gram magnetic susceptibility

D = diamagnetic function T = absolute temperature

For exp: [NiA<sub>2</sub>SB<sub>1</sub>] complex

$$X_g = 4.6 \cdot 10^{-6}$$

$$X_M = 4.6 \cdot 10^{-6} \cdot 639.13 = 2939.99 \cdot 10^{-6} \text{Z}$$

$$X_A = 2939.99 \cdot 10^{-6} + 319.56 \cdot 10^{-6} = 3259.55 \cdot 10^{-6}$$

$$\mu_{\text{eff.}} = 2.828 \sqrt{3259.55 \cdot 10^{-6} \cdot 298} = 2.78$$

**Table (3-16): Measurements of the magnetic of prepared complexes**

Compound	Weight Sensitivity $X_g \cdot 10^{-6}$	Molar Sensitivity $X_m \cdot 10^{-6}$	Atomic Sensitivity $X_A \cdot 10^{-6}$	- D. $10^{-6}$	$\mu_{\text{eff}}$ B.M
[CoA <sub>2</sub> SB1]	8.5	5508.38	5828.63	320.25	3.72
[NiA <sub>2</sub> SB1]	4.6	2939.99	3259.55	319.56	2.78
[CuA <sub>2</sub> SB1]	1.5	967.68	1294.74	327.06	1.75
[Co A2SB2]	9.4	5992.97	6311.74	318.77	3.87
[Ni A2SB2]	4.8	3059.08	3377.73	318.65	2.83
[Cu A2SB2]	1.45	931.13	1252.21	321.08	1.72

### 3.4 Conclusions and the proposed molecular structure for all prepared complexes

According to the characterization data for new Schiff base (SB1) derived from 3-amino-1-phenyl-2-pyrazoline-5-one with vanillin and (SB2) derived from 3-amino-1-phenyl-2-pyrazoline-5-one with 4-dimethylaminobenzaldehyde by FT-IR, U.V-Vis, atomic absorption, <sup>1</sup>H-NMR, Mass, elemental microanalysis addition with melting point, we found that:

- 1- Schiff base as a primary ligand SB1 and SB2 behavior as bidentate chelating through N atom of imine group and nitrogen atoms from pyrazole ring and anthranilic acid as secondary ligand behavior as bidentate chelating through N atom for amine group (-NH<sub>2</sub>) and oxygen from carboxylic group.
- 2- Schiff bases and anthranilic acid reacts with Co(II), Ni(II), Cu(II), Cd(II) and Hg(II) metal ions forming complexes with general molecular formula: [MA<sub>2</sub>SB1], Figure (3-37) and [MA<sub>2</sub>SB2] Figure(3-38).

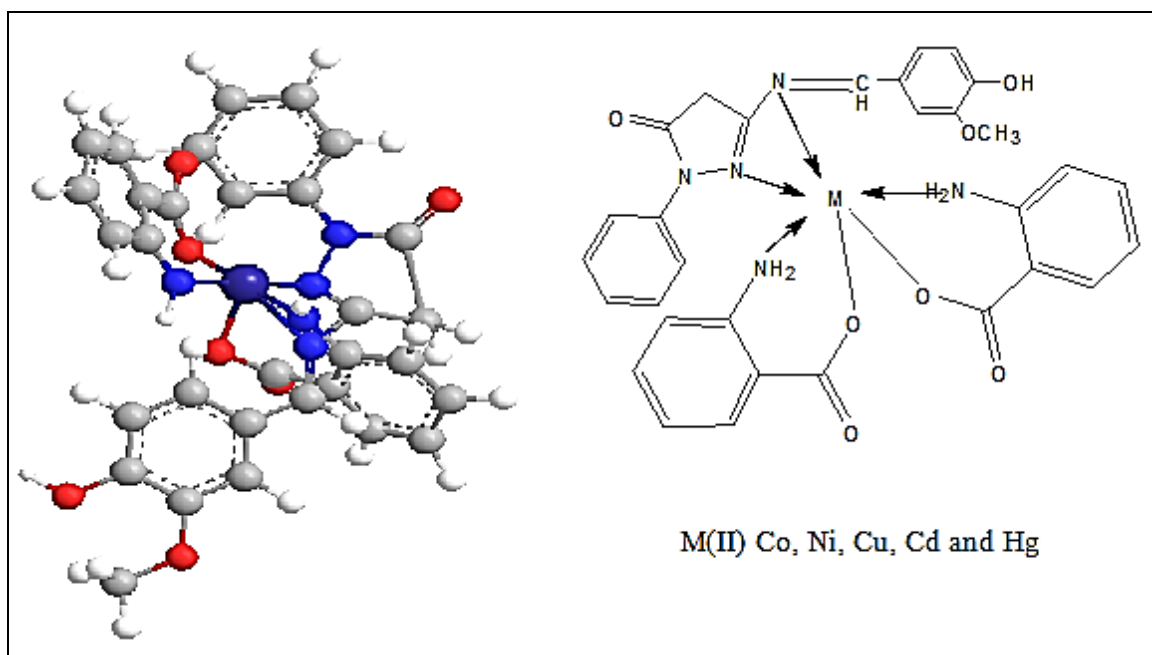


Figure (3-33): The suggested geometry for metal complexes of SB1

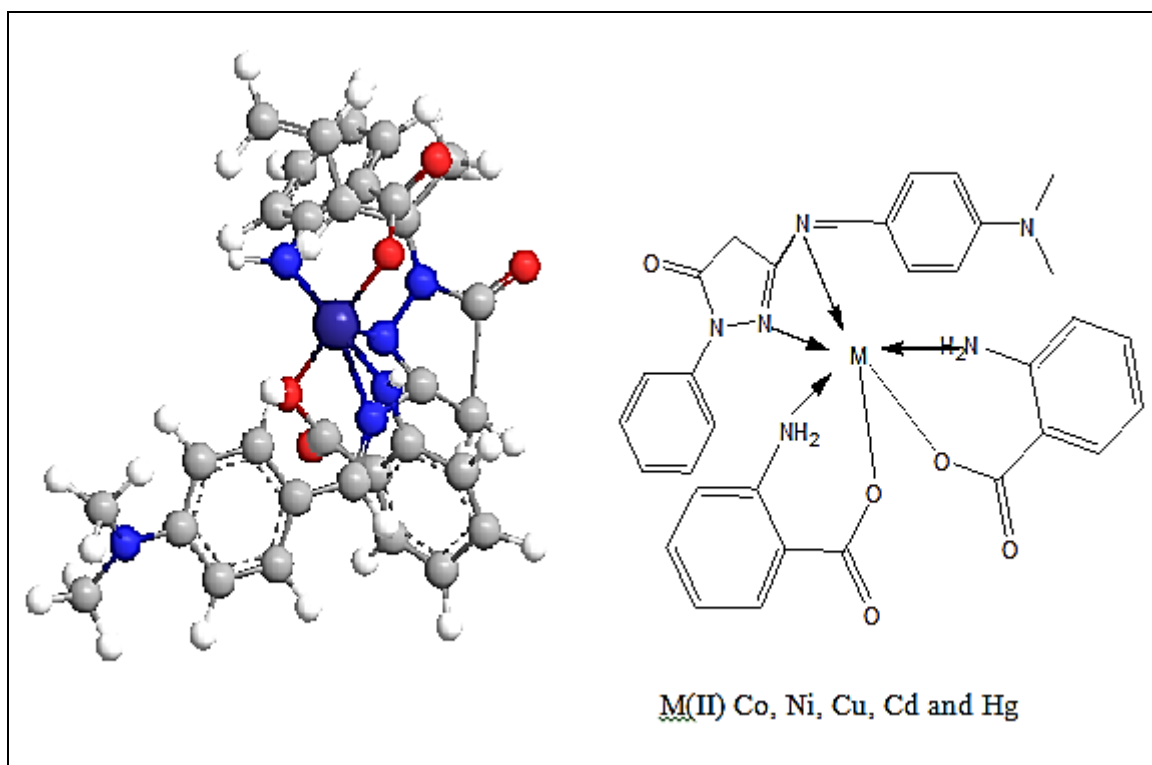


Figure (3-34): The suggested geometry for metal complexes of SB2

#### 4. Biological activity

The complexes of ligands SB1 and SB2 were tested for two types of bacteria, G+ (*Staphylococcus aureus*) and G- (*Escheria coli*) in nutrient agar <sup>[102,103]</sup>. Biological activity of all compounds was set by measuring the inhibition diameter of the millimeter unit.

#### 4.1 Biological activity of Ligands Complexes

##### 4.1.1 SB1 Complexes

The prepared ligand SB1 and their metal complexes of this study were tested against types of bacteria gram positive and gram negative using well plate method in nutrient agar <sup>[104]</sup>. The diameter of the inhibition for the bacterial medium growth of the complexes was listed in the Table (4-1). The study showed the prepared compounds of ligand SB1, Anthranillic acid<sup>[105]</sup>, [CoA<sub>2</sub>SB1], [CuA<sub>2</sub>SB1], [HgA<sub>2</sub>SB1] and [CdA<sub>2</sub>SB1] were having different efficacy against *E.coli* except. The complex NiA<sub>2</sub>SB1 did not show any effectiveness towards the same type of bacteria and all complexes showed efficacy against *Staphylococcus aureus* except ligand SB1 which showed no efficacy against the same type of bacteria. Figure (4-1), (4-2), (4-3) and Chat(1) show the variation in ligands and their complexes effectiveness towards of bacteria used. <sup>[106]</sup>.

**Table (4-1): Biological activity of SB1 complexes**

Compound	<i>Escheria coli</i>	<i>Staphylococcus</i>
DMSO	-	-
SB1	11	-
A	18	21
[CoA <sub>2</sub> SB1]	14	24
[NiA <sub>2</sub> SB1]	-	10
[CuA <sub>2</sub> SB1]	28	19
[CdA <sub>2</sub> SB1]	18	32
[HgA <sub>2</sub> SB1]	32	29

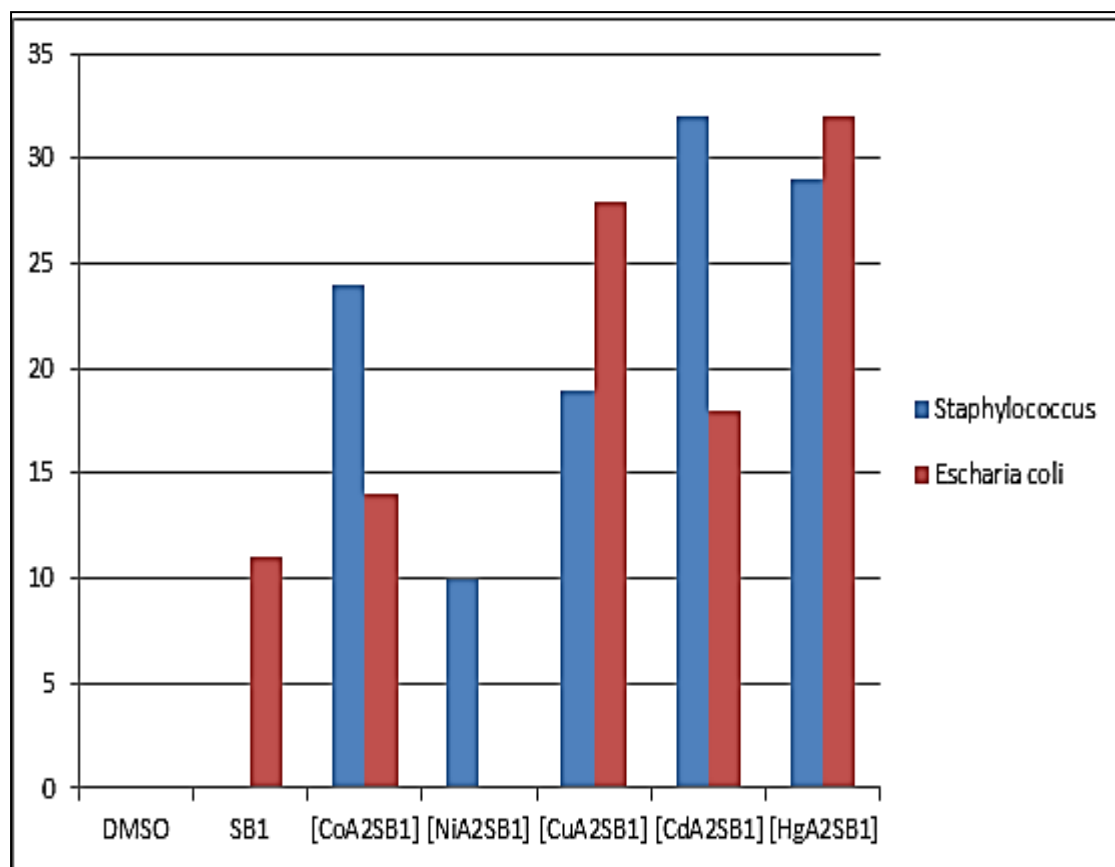


**Chart1: biological activity for prepared compounds [MA<sub>2</sub>SB1]**

#### 4.1.2 SB2 Complexes

The prepared ligand SB2 and their metal complexes of this study were checked against two types of bacteria (G+ and G-) by using well plate method in nutrient agar. The diameter of inhibition for the bacterial medium growth of the complexes was listed in the Table (4-2), Figure (4-4), (4-5), (4-6) and Chart (2). The study showed they prepared compounds of ligand SB2, Anthranillic acid, [CoA<sub>2</sub>SB2], [CuA<sub>2</sub>SB2], [HgA<sub>2</sub>SB2] and [CdA<sub>2</sub>SB2] were different efficacy against *E.coli* except the complex NiA<sub>2</sub>SB2 did not show any effectiveness towards the same type of bacteria while all complexes a showed good effectiveness towards *Staphylococcus aureus* except for ligand SB2, there was no effect on the same type of bacteria <sup>[106,107]</sup>.



The various inhibition activities of metal complexes can be explained by:

- According to "Tweedy's" chelation theory <sup>[105]</sup>.
- In the complexes, the polarity of the metal ion will be reduced to a greater extent leads to the overlap of the ligand orbital and partial sharing of the  $M^{+n}$  where n; (1,2 or 3) with donor groups.
- The delocalization of ( $\pi$  electrons) over the whole chelate ring.
- The large ring size of ligands moiety makes the complexes more lipophilic <sup>[107]</sup>.

**Table (4-2): The Biological Activity of SB2 Complexes**

Compound	<i>Escharia coli</i>	<i>Staphylococcus aureus</i>
<b>DMSO</b>	-	-
<b>SB2</b>	10	-
<b>A</b>	18	21
<b>[CoA<sub>2</sub>SB2]</b>	15	18
<b>[NiA<sub>2</sub>SB2]</b>	-	15
<b>[CuA<sub>2</sub>SB2]</b>	33	27
<b>[CdA<sub>2</sub>SB2]</b>	16	28
<b>[HgA<sub>2</sub>SB2]</b>	35	31

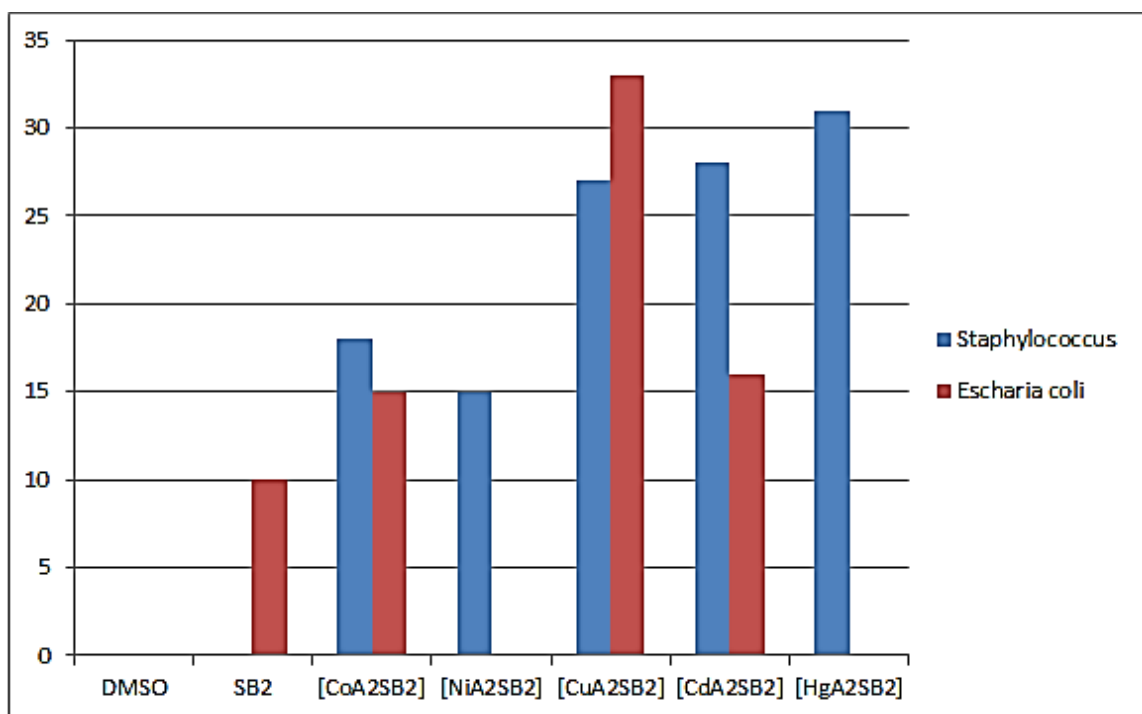


Chart 2: Biological activity for prepared compounds [MA<sub>2</sub>SB<sub>2</sub>]

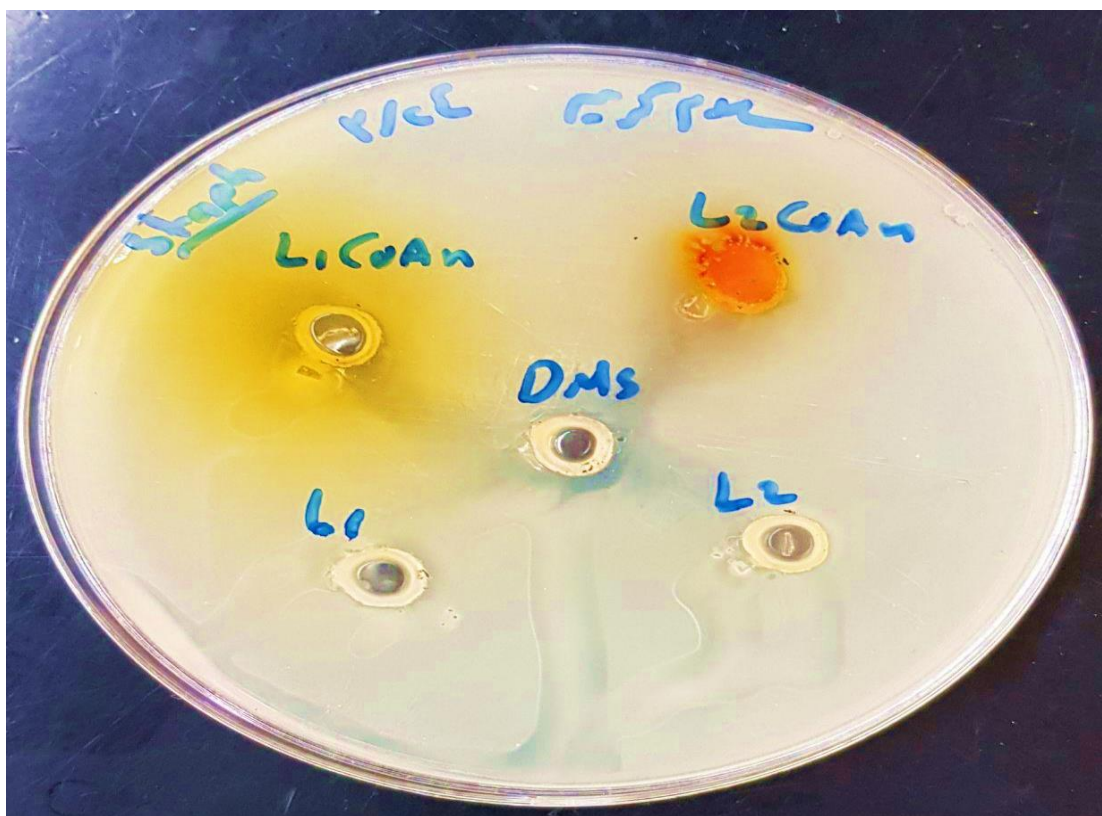
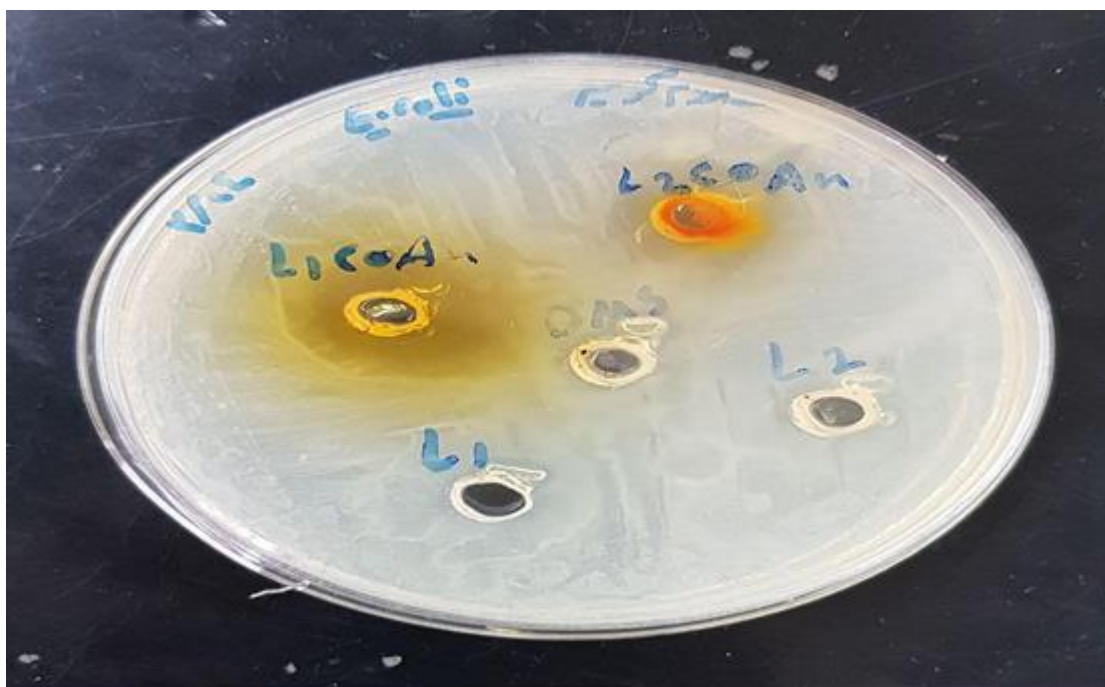




Figure (4-1): Inhibition zone of ligands and their complexes towards *Staphylococcus aureus* bacteria



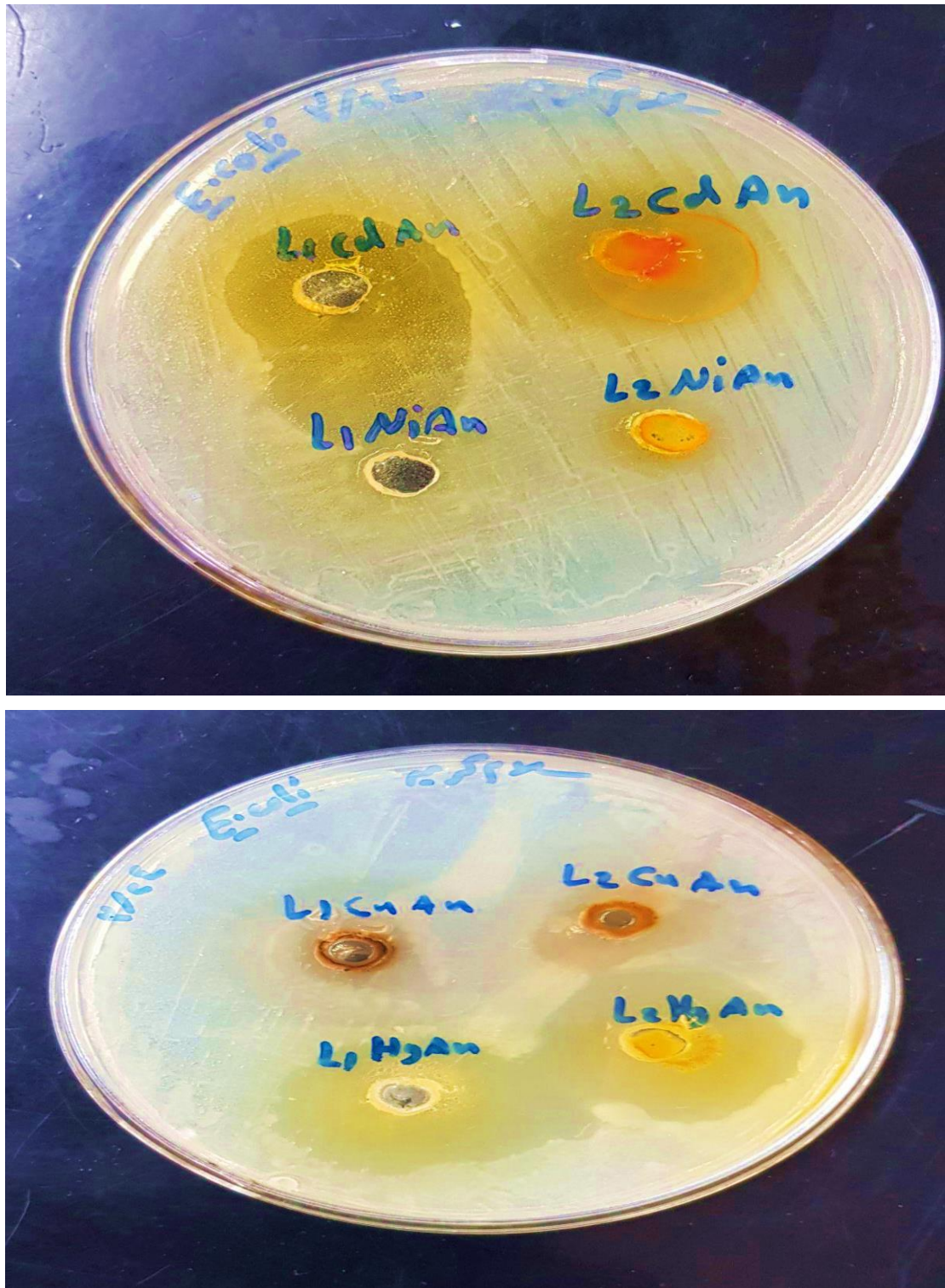


Figure (4-2): Inhibition zone of complexes towards *E.coli* bacteria

**4.2 Prospective studies**

1. Preparation of new metal chelate using other metal ions.
2. Schiff Bases are used in analytical chemistry for determination of metal ions.
3. Study TG and DTG of the Schiff base ligands and their metal complexes.
4. Study enzymes activity for the produced Schiff base ligands and their metal chelates.

## References

- 1- Wasi N.; *Inorganica Chimica Acta*, 135(1987):133-137.
- 2- Johan T.H. Roos and David R. Williams; *Journal of Inorganic and Nuclear Chemistry*, 39(1977): 367-369.
- 3- Samina K. Tadavia, Abhijit A. Yadavb and Ratnamala S. Bendrea; *Journal of Molecular Structure*, 1152(15) 2018: 223- 231.
- 4- Cozzi P. G.; *Chemical Society Reviews*, 33(2004) 410-421.
- 5- Ali H.Kianfar and Roghayeh H. Fath; *Egyptian Journal of Petroleum*, 26(4)2017: 865- 874.
- 6- Keerthi K. Ct., Keshavayya J., Rajesh T.,Peethambar Sk.; *International Journal of Pharmacy and Pharmaceutical Sciences*, 5(2)2013: 639-647.
- 7-Wail Al Zoubi; *International Journal Of Organic Chemistry*, 3 (2013) : 37-95.
- 8- Tanaka K., Shimora R. and Caira; *Tetrahedron Letters*, 51(2)2010: 449- 452.
- 9-Basil M. Ahmed, Nicholas A. Rudell, Ixtlazihuatl Soto, and GellertMezei; *Journal of Organic Chemistry*, 82(19)2017:10549–10562.
- 10- Rajkumar G. Momle, Suresh G. Vedpathak and Gopal K. Kakade; *European Journal of Pharmaceutical and Medical Research*,5(03)2018, 225-235.
- 11- Lekaa K.AbdulKarem, FawziY.Waddai and Nisreen H. Karam; *Journal of Pharmaceutical Sciences and Research*,10(8)2018: 1912-1917.
- 12- Saurabh N. Devi, Choudhary D. and Khokra S. L.; *European Journal of Pharmaceutical and Medical Research*, 3(11)2016:598-609.

- 13- Wail Al Zoubi, Abbas Ali Salih Al-Hamdani & Young Gun Ko; *Separation Science and Technology*, 52(6)2017:1052-1069.
- 14- Clodoaldo V., Italo N.Ribeiro, João Victor B. Soares, Basílio Baseia and Francisco A. P. Osório; *Advances in Condensed Matter Physics*, 139(31)2019:1-12.
- 15- Ali M. Yimer; *Review of Catalysts*, 2(1)2015:14- 25.
- 16- Schiff H.; Justus Liebigs Annalen der Chemie., 131(1864): 118-119.
- 17- Kalaivani S., Padma P.N., and Arunachalam S.; **International Journal of Applied Biology and Pharmaceutical Technology**, 3(1)2012:219-223.
- 18- Skyes P.; Longmans London, (1974).
- 19- Paryzek W. R., Patroniak V. and Lisowski J.; *Coordination Chemistry Reviews*, 249(2005): 2156-2175.
- 20- Hassan I.A.; **Research Journal of Chemical Sciences**, 3(12)2013:50-53.
- 21- Nabeel B. H., and Farah S.T.; *Research Journal of Chemical Sciences*, 2(6) 2012:43-49.
- 22- Kabeer A. S., Baseer M. A. and Mote N.A.; **Asian Journal of Chemistry**, 13(2) 2001:496–500.
- 23- Rajasekar K., Ramach and ramoorthy T. and Balasu bramaniyan S.; **Research Journal of Chemical Sciences**, 3(3)2013: 48-51.
- 24- Jyothi S., Sreedhar K., Nagaraju D. and Swamy S. J.; *Canadian Chem. Trans.*, 3 (4)2015: 368- 380.
- 25- Abu-Dief A.M. and Mohamed I. M. A.; *Journal of Basic and Applied Sciences*, 4, (2015):119- 133.
- 26- Rajasekar K., Ramachandramoorthy T., and S. Balasubramaniyan; *Chemical Science Transactions*, 2(3)2013:877-882.
- 27- TharmarajP., KodimunthiriD., Sheela C. D. and C.S. Shanmugapriya ; *Journal of the Serbian Chemical Society*, 74 (8- 9)2009: 927- 938.

- 28- Dongmei Xu, Mi Zhang, Jun Gao, Lianzheng Zhang and Shixue Zhou; *Chemical Engineering Communications*, 206(9) 2019 : 1199-1217.
- 29- Mossaraf H. and Ashis K. N.; *Science Journal of Chemistry*, 6(5)2018: 83-94.
- 30- Theophil E., Siegfried H., and Andreas S.; *The Chemistry of Heterocycles*, 3(2013): 646.
- 31- Neha M., Nisha J. and Sharma A.K.; *Open Chemistry Journal*, 5(2018):182-195.
- 32- Clementina M. M. Santos, Vera L. M. Silva, and Artur M. S. Silva; *Molecules*, 22(10)2017:1- 47.
- 33- Magda A. Abdallah, Sobhi M. Gomha, Ikhlass M. Abbas, Mariam S. H. Kazem, Seham S. Alterary, and Yahia N. Mabkhot; *Applied Sciences*, 7(8)2017:1-13.
- 34- Alexandria P. Taylor, Ralph P. Robinson, Yvette M. Fobian, David C. Blakemore, Lyn H. Jones and Olugbeminiyi Fadey; *Organic and Biomolecular Chemistry*, 14(28)2016: 6611-6637.
- 35- Mehta B.H., and Chavan V. L.; *Research Journal of Chemistry and Environment*, 2(2011):57-61.
- 36- Wu Q., Chen W. L., Liu D., Liang C., Li Y. G., Lin S. W., and Wang E. ; *Dalton Transactions*, 40(1)2011:56-61.
- 37- Kerler J., and Verpoorte R., *Technological Chemical, and Biosynthetic Aspects Food Reviews International*, 17(2)2001: 119–120.
- 38- Mohamed A., Rene J., Heijden A., and Udo A.; *Environmental science and technology* 1(1998):295–305.
- 39- Sen A., and Grosch W.; *Journal De Pharmacie Et De Chimie*, 3(1992): 239–245.



- 40- Maxence F., Bernard B., and Sylvain C.; *ACS Sustainable Chemistry & Engineering*, December 14(2015):1-23.
- 41- Ravendra K., Sharma P. K., and Prem S. M.; *International Journal of Pharmtech*, 4(1) 2012: 266-279.
- 42- Ehmann, A.; *Journal of Chromatography A.*, 132(2)1977: 267–276.
- 43- Watt G. W., and Chrisp J. D.; *Analytical Chemistry*, 24 (12)1952: 2006–2008.
- 44- Kawski A., Kuklinski B., and Bojarski P.; *Chemical Physics Letters*, 448(4-6)2007:208–212.
- 45- Rehman W., Haq S., Rahim F., Khan S., Waseem M., Nawaz M., and Guo; *Pharmaceutical Chemistry Journal*, 51(2)2017:115-118.
- 46- Laila A. B., Haque M.M., Islam M.S., Saddam H. Md. Matin M.A., and Kudrat E. Md.; *Russian Journal of General Chemistry*, 89(6)2019: 1197–1201.
- 47- Ibragimov A. B., Ashurov J. M., and Zakirov B. S.; *Journal of Chemical Crystallography*, 46(8-9)2016: 352-363.
- 48- Mark R Hardy ; *Techniques in Glycobiology*, 78 (2)1997:359-366.
- 49- Ana B. Miltojević and Niko S. Radulović; *Physics Chemistry and Technology*, 13(2)2015:121- 132.
- 50- Logullo F. M., Seitz A. H., and Friedman L.; *Organic Syntheses*, 5(1973): 54.
- 51- Wagner E. C., and Fegley M. F.; *Organic Syntheses*; 27(1947): 45.
- 52- Rakitskaya, T. L., Bandurko, A. Y., Truba, A. S., Raskola, L. A., and Golub, A. A; *Russian journal of general chemistry*, 67(8) 2006: 1266-1271.
- 53- Sivasankaran N. M., Selwin J.R.; *Spectro chimica Acta Part A*, 70(2008):749–753.
- 54- Suresh M. S. and Prakash V.; *International Journal of The Physical Sciences*, 5(14)2010: 2203-2211.

- 55- Fugu M. B., Ndahi N. P., Paul B. B. and Mustapha A. N.; *Journal of Chemical and Pharmaceutical Research*, 5(4) 2013:22-28.
- 56- Roji J.; *International Journal of Multidisciplinary Research and Development*, 2(7)2015: 472-473.
- 57- Dostani M., Kianfar A. H., and Momeni M. M.; *Journal of Materials Science Materials in Electronics*, 28(1)2017: 633-640.
- 58- Abduljleel M. A., Jasim A., Maitham N. A.; *Journal of Chemical, Biological and Physical Sciences*, 8(2)2018:135-153.
- 59- El-Ajaily M.M., Malhub A.A., Hudere S.S., and Ben-Saber S.M.; *Asian Journal of Chemistry*, 18(4)2006:2427-2430.
- 60- Devendra K. S., Raman K. and Mithlesh K. S.; *International Journal Chemistry Science*, 9(3) 2011:1140-1146.
- 61- Anu M., Lakshmi P.P., Banukarthy G., Raxy K., Rajeshwari K.; *International Journal of Institutional Pharmacy and Life Sciences*,3(6)2013: 23-32.
- 62- Alassbaly F.S., Maihub A. A., Ben-Gweirif S. F., El-Ajaily M. M., and Al-Noor T. H.; *Saudi Journal of Pathology and Microbiology*, 1(2) 2016:29-35.
- 63- Abubakar A.A., Yusuf Y. and Hussaini A. U.; *International Journal of Science and Applied Research*,2(3)2017:8-16.
- 64- Noor S. N., Tahseen A. Z. and Mohammad F. M.; *International Research Journal of Pharmacy*, 9(12)2018:57-63.
- 65- Jamila Z., Hanane A., Ouafa A., Abderrafia H. and Mostsfs K.; *New Journal of Chemistry*, 39,2015:6738-6741.
- 66- Lekaa K. A. K. and, Fawzi Y. W.; *Journal of Global Pharma Technology*,10(08)2018:201-208.
- 67- Lekaa K. A. K. and Saba H. M.; *The 1st International Scientific Conference On Pure Science*, 1234(2019): 1-13.

- 68- Dnyaneshwar S. Wankhede, Nileshkumar D. Mandawat and Atit H. Qureshi; *Journal of Current Chemical Pharmaceutical Science*, 4(3)2014, 135-141.
- 69- Gehad G. M., Omar M.M. and Ahmed M.M. Hindy; *SpectrochimActa A*, 62(2005): 1140–1150.
- 70- Taghreed, H. Al-Noor, Khalid, F. A., Amer J. J ., and Aliea, S. K.; *Chemistry of Materials*, 3 (3) 2013:126-133.
- 71- Taghreed, H. Al-Noor, Lekaa, K. A. K.; *TOFIQ Journal of Medical Sciences*, 3(2), 2016: 64-75.
- 72- Oladipupo, O. E., Ibukun, D. T. and Olalekan, T. E; *Nigerian Journal of Chemical Research*, 23(2) 2018:39-50.
- 73- Khudheyer J. Kadhimand Murad G. Munahi; *Journal of Global Pharma Technology*, 10(6) 2018: 1613-1614.
- 74- Nakamoto, K.; 1997,"*Infrared and Raman Spectra of Inorganic and Coordination Compounds*", 5th Edit., Part B; Wiley; New York.
- 75- Rashd M. El-Ferjani, Musa Ahmad and Farah Wahida Harun ; *Journal of Applied Chemistry*, 10( 6) 2017: 6-13.
- 76- Almarhoon Z. M., Al-Onazi W. A., Alothman A. A., Al-Mohaimeed A. M., and Al-Farraaj E. S. ; *Journal of Chemistry*, 8152721(2019) : 1- 14.
- 77- Saba H. M. and Lekaa K. A.K., *Oriental Journal of Chemistry*; 34(3)2018: 1565-1572.
- 78- Saba H.M. Al-Azzawi; A *Thesis, University of Baghdad Department of Collage of Education Ibn Al-Haitham*,2018
- 79- Smith J. G. ; *McGraw-Hill, New York*, 1(2006):522.
- 80- Robert M. S., Francis X. W., and David J. K.; *John wiley and Sons Inc., Hoboken*, 7(2005):106.

- 81-El-Sonbati A.Z., Mahmoud W.H., Gehad G. M., Diab M. A., Morgan S.M. and Abbas S.Y.; *Applied Organometallic Chemistry*, 33(7)2019:4945.
- 82- Lever, A.B.P.; 1984 "*Inorganic spectroscopy*" Elsevier publishing company, 3th Edit; Wiley; New York.
- 83- Světlík J., Pronayov N. , Frečer V. and Ciez D. ; *Tetrahedron*, 72(2016): 7620-7627.
- 84- Kenan B., Nevin T., Ahmet S. and Naki C.; *Journal of Saudi Chemical Society*, 23(2)2019: 205-214.
- 85- Nayaz A., Mohd R., Altaf A., and Madhulika B.; *International Journal of Inorganic Chemistry*, 607178(2015): 1-5.
- 86- Geary W. J.; *Coordination Chemistry Reviews*, 7(1971): 81-122.
- 87- Taghreed H.A.N. and Lekaa K. A. K.; *Chemistry and Materials Research*, 7(5)2015: 82-90.
- 88- Rehab K. R.; *Ibn Al-Haitham Journal for Pure and Applied Science*, 30(3)2017: 58-67.
- 89- Rehab K. R. Al-Shemary, Lekaa K.A.K. and Faaza H. G.; *Oriental Journal of Chemistry*, 34(2)2018:1105-1113.
- 90- Kaleda K.G.; *Ibn Al-Haitham Journal for Pure and Applied Science*, 3(2) 2018:115-136.
- 91- Ahmed T. Numan, Eman M .Atiyah, Rehab K. Al-Shemary and Sahira S.; *Journal of Physics: Conference Series*, 1003 (2018):1-12.
- 92- Ehab M. Z., Zayed M. A. and Ahmed M. M.; *Journal of Thermal Analysis and Calorimetry*, 116(1)2014: 391–400.
- 93- Lekaa K.A. K., Faaza and Rehab K. R. Al-Shemary; *Biochemical and Cellular Archives*, 8(1)2018:1437-1448.
- 94- Mohamed G., Nadia El-W., Kamal El. and Sara H.; *Journal of The Iranian Chemical Society*, 16(1)2019:169–182.

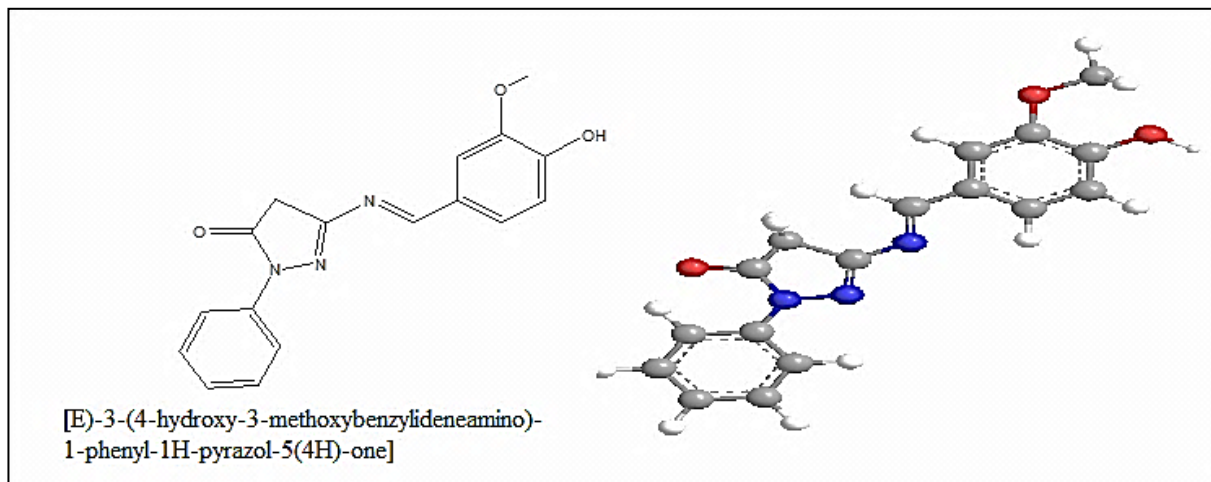
- 95- Violet V. D., Daniel T.P., Renganathan R., Elsa F. and Detlef W. B.; *Journal of Fluorescence*, 27(1)2017: 135–150.
- 96- Aurora R., Mariana C. C., Emiliaamzoiu, Nicoleta C., Irina D. and Petre R.; *Journal of Thermal Analysis and Calorimetry*, 131(3)2018: 2073–2085.
- 97- Nasser A. M., Hassan A. M., Shoeib M. A., Kmash N. El; *Journal of Bio- and Tribo-Corrosion*, 1(2015):1-19.
- 98- Walaa H. M., Reem G. D. and Gehad G. M.; *Research on Chemical Intermediates*, 42(12)2016: 7869–7907.
- 99- Taghreed.H.AL-Noor and Lekaa K. A. Karim; *Chemistry and Materials Research*, 7(3)2015:32-39.
- 100- Walaa H. M, Reem. G. D. and Gehad G. M.; *Journal of Thermal Analysis and Calorimetry*, 127(3) 2017: 2149–2171.
- 101- Devi J., Yadav M., Kumar A., and Kumar, A.; *Chemical Papers*, 72(10)2018: 2479-2502.
- 102- Manjula V. D., Chakraborty and Bhattacharya P. K., *Indian Journal of Chemistry Section A.*, 29(6)1990: 577-580.
- 103- Melnick J. and adelbrgs A.; *Sultan Qaboos University Medical Journal*, 7(3)2007: 273–275.
- 104- Swathy S. S., Joseyphus R. S., Nisha V. P., Subhadrambika N., and Mohanan K. ;*Arabian Journal of Chemistry*, 9(2) 2016:1847-1857.
- 105- Tweedy Bg; *Phytopathology* 55(1964): 910- 914.
- 106- Srivastava, K. P., Sunil Kumar Singh, And BirPrakash Mishra; *Journal Of Chemical And Pharmaceutical Research*, 7(1)2015:197-203.
- 107- Neelakantan M. A., Esakkiammal M., Mariappan S.S., Dharmaraja J., and T. Jeyakumar; *Indian Journal of Pharmaceutical Sciences*, 72 (2)2010: 216-222.



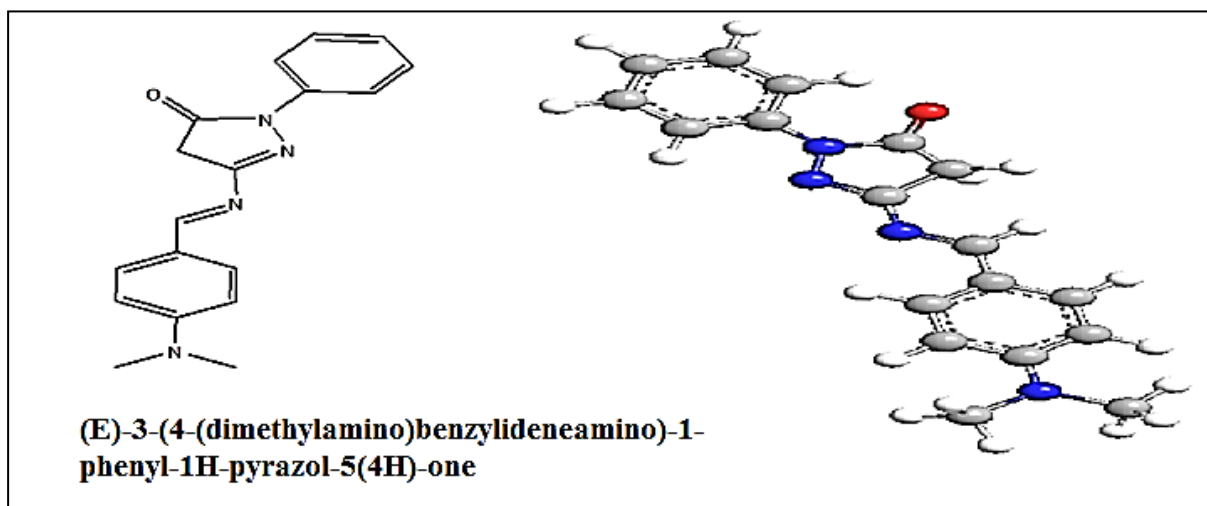
## الخلاصة

تتناول هذه الدراسة تحضير ليكاندات قواعد شف جديدة المشتقة من ( 3- امينو-1- فنيل -2- بيرزول -5- اون) مع الفانلين لتكوين ليكاند (SB1) و 4- (ثنائي مثيل امينو) بنزالديهايد لتكوين ليكاند (SB2) .

شُخصَ الليكاندين بواسطة التقنيات الطيفية مثل اطياف الاشعة تحت الحمراء وفوق البنفسجية والمرئية و الرنين النووي المغناطيسي للبروتون والتحليل الدقيق للعناصر و الكتلة .



شكل (1): التركيب والشكل الثلاثي الأبعاد لليكاند SB1



شكل (2): التركيب والشكل الثلاثي الأبعاد لليكاند SB2

تتألف معقدات مختلطة الليكاند من قواعد شف و حامض الانثرانيلك مع أيونات بعض العناصر مثل  $M(II)$ : Co و Ni و Cu و Cd و Hg ، شخّصت هذه المعقدات بواسطة التحليل الدقيق للعناصر والتوصيلية المولارية و الأشعة تحت الحمراء و فوق البنفسجية والمرئية والامتصاص الذري وقياس الحساسية المغناطيسية .

أظهرت بيانات الأطياف بان الليكاندين (SB1 و SB2) متعادل ثنائي السن و متناسق مع الايونات الفلزية من خلال ذرة النتروجين لمجموعة الازوميثين و ذرة النتروجين لحلقة البايروزول والشكل المتوقع لكل المعقدات هو الثماني السطوح .  
وأخيرا تم اختبار الفعالية البيولوجية المضادة للبكتريا تجاه *Staphylococcus aureus* و *Escherichia coli* لليكاندات ومعقداتها بتقنية قياس منطقة التثبيط (ZI) .





جمهورية العراق  
وزارة التعليم العالي والبحث العلمي  
جامعة بغداد  
كلية التربية للعلوم الصرفة / ابن الهيثم  
قسم الكيمياء

## تحضير، تشخيص ودراسة الفعالية البيولوجية لليكاندات قواعد شف جديدة ومعقداتها مع بعض الأيونات الفلزية

رسالة مقدمة إلى  
مجلس كلية التربية للعلوم الصرفة – ابن الهيثم – جامعة بغداد  
وهي جزء من متطلبات نيل درجة الماجستير في علوم الكيمياء

من قبل  
سلام كريم صاحب علي  
بكالوريوس علوم كيمياء – 2002 – جامعة بغداد

بإشراف  
ا.م.د. لقاء خالد عبد الكريم

